Queensland University of Technology

Synthesis and Characterisation of Hybrid Gold/Polymer Nanoparticles for Bioassay Application

SUBMITTED BY

TARA LOUISE SCHILLER

MASTERS APPLIED SCIENCE

PRESENTED TO THE SCHOOL OF PHYSICAL AND CHEMICAL SCIENCES

IN PARTIAL FULFILMENT OF THE REQUIREMENTS OF THE DEGREE OF

DOCTOR OF PHILOSOPHY

January 2010

KEYWORDS

Bioassay, functionalised nanoparticle, SERS, ‘click’ chemistry, RAFT polymerisation, biotin, SERS active compound

ABSTRACT

A bioassay technique, based on surface-enhanced Raman scattering (SERS) tagged gold nanoparticles encapsulated with a biotin functionalised polymer, has been demonstrated through the spectroscopic detection of a streptavidin binding event. A methodical series of steps preceded these results: synthesis of nanoparticles which were found to give a reproducible SERS signal; design and synthesis of polymers with RAFT-functional end groups able to encapsulate the gold nanoparticle. The polymer also enabled the attachment of a biotin molecule functionalised so that it could be attached to the hybrid nanoparticle through a modular process. Finally, the demonstrations of a positive bioassay for this model construct using streptavidin/biotin binding.

The synthesis of silver and gold nanoparticles was performed by using tri-sodium citrate as the reducing agent. The shape of the silver nanoparticles was quite difficult to control. Gold nanoparticles were able to be prepared in more regular shapes (spherical) and therefore gave a more consistent and reproducible SERS signal. The synthesis of gold nanoparticles with a diameter of 30 nm was the most reproducible and these were also stable over the longest periods of time.

From the SERS results the optimal size of gold nanoparticles was found to be approximately 30 nm. Obtaining a consistent SERS signal with nanoparticles smaller than this was particularly difficult. Nanoparticles more than 50 nm in diameter were too large to remain suspended for longer than a day or two and formed a precipitate, rendering the solutions useless for our desired application.

Gold nanoparticles dispersed in water were able to be stabilised by the addition of as-synthesised polymers dissolved in a water miscible solvent. Polymer stabilised AuNPs could not be formed from polymers synthesised by conventional free radical polymerization, *i.e.* polymers that did not possess a sulphur containing end-group. This indicated that the sulphur-containing functionality present within the polymers was essential for the self assembly process to occur.

Polymer stabilization of the gold colloid was evidenced by a range of techniques including, visible spectroscopy, transmission electron microscopy, Fourier transform infrared spectroscopy, thermogravimetric analysis and Raman spectroscopy. After treatment of the hybrid nanoparticles with a series of SERS tags, focussing on 2-quinolinethiol the SERS signals were found to have comparable signal intensity to the citrate stabilised gold nanoparticles. This finding illustrates that the stabilization process does not interfere with the ability of gold nanoparticles to act as substrates for the SERS effect.

Incorporation of a biotin moiety into the hybrid nanoparticles was achieved through a 'click' reaction between an alkyne-functionalised polymer and an azido-functionalised biotin analogue. This functionalized biotin was prepared through a 4-step synthesis from biotin.

Upon exposure of the surface-bound streptavidin to biotin-functionalised polymer hybrid gold nanoparticles, then washing, a SERS signal was obtained from the 2-quinolinethiol which was attached to the gold nanoparticles (positive assay). After

exposure to functionalised polymer hybrid gold nanoparticles without biotin present then washing a SERS signal was not obtained as the nanoparticles did not bind to the streptavidin (negative assay). These results illustrate the applicability of the use of SERS active functional-polymer encapsulated gold nanoparticles for bioassay application.

PUBLICATIONS ARISING FROM THIS WORK

Papers

T.L. Schiller, I. Blakey, D.J. Keddie, C.J. Hawker, P.M. Fredericks, *Surface-enhanced Raman encoded polymer stabilized gold nanoparticles: demonstration of potential for use in bioassays*, in preparation

I. Blakey, **T. L. Schiller**, Z. Merican, and P. M. Fredericks, *Interactions of Phenyldithioesters with Gold Nanoparticles (AuNPs): Implications for AuNP Functionalization and Molecular Barcoding of AuNP Assemblies,* Langmuir, 26(2):pp. 692-701, 2010

Z. Merican, **T. L. Schiller**, C. J. Hawker, P. M. Fredericks and I. Blakey, *Self Assembly and Encoding of Polymer Stabilised Gold Nanoparticles with Surface-Enhanced Raman Reporter Molecules*, Langmuir, 23(21):pp. 10539-10545, 2007

T. L. Schiller, Z. Merican, P. M. Fredericks and I. Blakey, *Characterisation of Hybrid Gold-Polymer Nanoparticles for use in Bioassays,* IEEE Proc., 626-629, 2006

Z. Merican, **T. L. Schiller**, P. M. Fredericks and I. Blakey, *Synthesis and Characterisation of Hybrid Polymer-Gold Nanoparticles: Towards Novel Biosensors*, IEEE Proc., 622-625, 2006

Conferences

T. L. Schiller, Z. Merican, C. J. Hawker, P. M. Fredericks and I. Blakey, *SERS Encoded Polymer/Gold Nanoparticles for Bioassay Application*, 7th Australian Conference on Vibrational Spectroscopy, 26-28 September 2007, Wollongong, Australia, ORAL

T. L. Schiller, Z. Merican , C. J. Hawker, P. M. Fredericks and I. Blakey, *Encoded Hybrid Gold-polymer Nanoparticles for Application in Bioassays*, 12th European Conference on the Spectroscopy of Biological Molecules, 1-6 September 2007, Paris, France, ORAL

T. L. Schiller, Z. Merican , C. J. Hawker, P. M. Fredericks and I. Blakey, *Hybrid gold/polymer nanoparticles for use in bioassays*, 234th ACS National Meeting & Exposition August 19-23, 2007 Boston, MA, USA, ORAL

T. L. Schiller, Z. Merican, I. Blakey and P. M. Fredericks, *Characterisation of hybrid gold-polymer nanoparticles for use in bioassays*, International Conference on Nanoscience and Nanotechnology, February 2008, Melbourne, Australia POSTER

T. L. Schiller, P. M. Fredericks, Z. Merican and I. Blakey *SERS barcoding of hybrid gold-polymer nanoparticles for bioassays*, International Conference on Raman Spectroscopy, 21-25 August 2006, Yokohama, Japan POSTER

T. L. Schiller, P. M. Fredericks, Z. Merican and I. Blakey *SERS barcoding of hybrid gold-polymer nanoparticles for bioassays*, International Conference on Surface Enhanced Raman Scattering (SERS2006), 28-29 August 2006, Nishinomiya, Japan POSTER

T. L. Schiller, Z. Merican, P. M. Fredericks and I. Blakey, *Characterisation of hybrid gold-polymer nanoparticles for use in bioassays*, International Conference on Nanoscience and Nanotechnology, 3-7 July 2006, Brisbane, Australia POSTER

TABLE OF CONTENTS

LIST OF FIGURES

LIST OF TABLES

ABBREVIATIONS

Ag	silver
ATR	attenuated total reflectance
Au	gold
br	broad
Bu	butyl
calc.	calculated
d	doublet
dd	doublet of doublets
DCC	dicyclohexylcarbodiimide
DCM	dichloromethane
DIPEA	N-ethyldiisopropylamine
DMF	dimethylformamide
DLS	Dynamic light scattering
DPTS	4-(Dimethylamino) pyridinium 4-toluene sulfonate
EI	electron impact
equiv	equivalent(s)
ESI	electrospray ionisation
et	ethyl
FITC	fluorescein isothiocyanate
FT	Fourier transform
GC	gas chromatography
GMA	glycidyl methacrylate
GPC	gel permeation chromatography
h	hour(s)

HATU	2-(1H-7Azabenzotriazol-1-yl)—1,3,3-tetramethyl uronium hexafluorophosphate methanaminium
HOBt	N-hydroxybenzotriazole
HPLC	high performance liquid chromatography
IR	infrared
m	multiplet
MMA	methyl methacrylate
MA	methacrylate
Me	methyl
min	minute(s)
mp	melting point
MS	mass spectrometry
NMR	nuclear magnetic resonance
Na_2S	Sodium sulfide
NHS	N-hydroxy succinimide
NP	nanoparticle
PEG	poly (ethyleneglycol)
Ph	phenyl
ppm	parts per million
RAFT	reversible addition and fragmentation chain transfer
RITC	rhodamine B isothiocyanate
RT	room temperature
s	singlet
SAC	SERS active compound
SEM	scanning electron microscopy

SERS	surface enhanced Raman spectroscopy
SPR	surface plasmon resonance
t	triplet
TBA	*tert*-butyl acrylate
TBAF	tetrabutylammonium fluoride
TEM	transmission electron microscopy
TFA	trifluoroacetic acid
THF	tetrahydrofuran
TLC	thin layer chromatography
Vis	visible

DECLARATION

The work presented in this thesis has not previously been submitted for any diploma or degree at any higher institution. To the best of my knowledge, this thesis contains no material that has previously published or written by another person, except where referenced or cited.

Tara Louise SCHILLER

January 2010

ACKNOWLEDGEMENTS

There are many people that I would like to thank including:

A/Prof Peter Fredericks, my supervisor, for his patience and willingness to let me go off but also to question things enough for me to see that I had the ability to complete this project. Your support also allowed me to gain vital funding for both of my trips to UCSB and overseas conferences.

Dr Idriss Blakey, my co-supervisor, for his input and guidance through the synthesis and for the many hours of emails discussing all aspects of my work.

Prof Craig Hawker for supporting both of my trips to your labs, and allowing me access to anything I needed there. I know was an integral part of finishing my thesis.

Dr Llew Rintoul for you amazing patience with the millions of questions regarding the spectroscopy and also having such a great knowledge base to answer 99 % of my questions.

Dr Christina Theodoropolous for helping me with my EM samples and many discussions about them. My associate supervisor Dr Eric Waclawik for his input and guidance for the nanoparticle work. Dr Zul Merican for your synthesis of some of the polymers used in this project. Dr Daniel Keddie for your assistance with the organic synthesis, as well as being able to explain from first principles the

background I needed to complete this work so that I could ask you more and more questions.

Fellow postgrads, researchers, and technical staff from UQ, QUT and UCSB for your input in my project in some way including: Dr Edeline Wentrup-Byrne, Prof Truis Smith-Palmer, Dr Kim van Berkel, Eric Pressley, Susan Given-Beck, Dr Sarah Ede, Ashley Persiarki, Pat Stevens, Nick Ryan, Dr Jerry Hu, Dr Sueng-Joon Lee, Dr Xihong Chen, Andrew Morrell, Anthony Musumeci and A/Prof Darren Martin.

1. CHAPTER 1

INTRODUCTION

1.1. Background

Bioassays for the identification and quantification of proteins are the cornerstone of biomedical research and *in vitro* diagnostic technologies. Developments in diagnostic techniques have been the focus of current research. Many research groups aim to improve existing technologies and techniques used for undertaking this type of analysis, trying to improve on detection limits.[1-4] Nanoparticles that are used for detection and are combined with fluorescence or other spectroscopic techniques have allowed detection limits to be set much lower than seen previously.[5, 6]

1.2. Bioassays

1.2.1. Conventional Bioassay Methods

Seydack[5] has provided a comprehensive review of techniques used for immunosensing related to nanoparticles. It states that there are three separate basic phenomena which might be used for the attachment of proteins to nanoparticles: attraction between the negatively charged particles and the positively charged proteins; hydrophilic interaction between the nanoparticles and the proteins; and binding between sulphur present in the proteins and the nanoparticle. Figure 1 shows a type of bioassay known as a sandwich assay. All assays have an antibody bound to a surface (usually as part of a well plate).

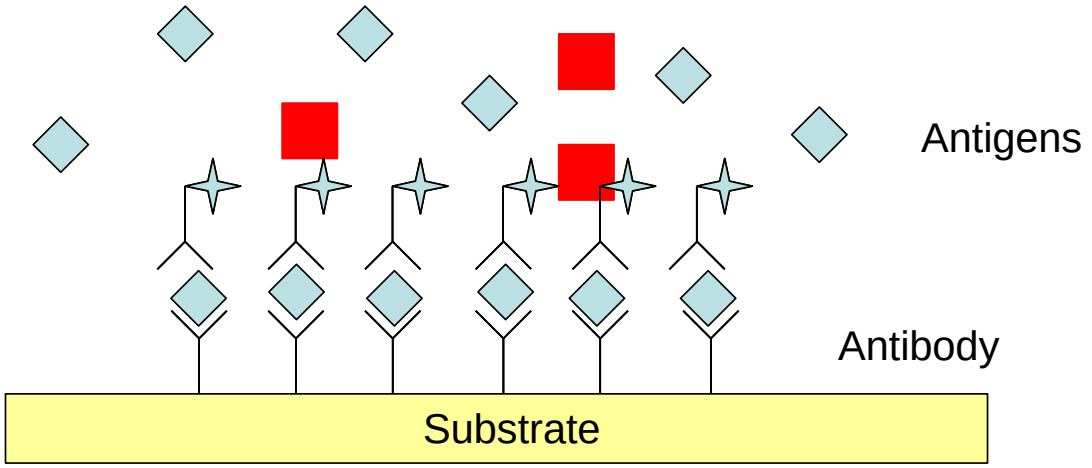

Figure 1 A typical example of antibody-antigen interaction using a 'sandwich' assay, showing antibodies bound to a substrate, with 2 types of antigens present in the solution (blue and red). The antigen pairs with the antibody on the substrate (blue), then the free tagged antibody attaches.

Protein detection and identification is one of the examples of biomedical applications of nanoparticle bioassays. Proteins regulate biochemical pathways in living cells, and as such their over or under expression can lead to various disease states. Hence, analytical bioassays for proteins are important for biomedical research and diagnosis. The huge number of proteins present in living cells and the high cost to purify or purchase small amounts of standard proteins leads to a requirement for the miniaturisation and multiplexing of experiments to provide viable assays. An emerging technology that addresses this is the protein microarray.[7, 8] Depending on the array configuration, they can be used to measure protein expression levels as well as 'protein – protein' and 'protein – small molecule' interactions.[9] For example, thousands of proteins can be arrayed on a slide and probed for interactions with a number of different ligands for the detection of diseases. A sandwich assay is one way to attach antigens (a substance that enters the body and causes the body to

produce antibodies) to antibodies (produced by the body to find and eliminate foreign bodies).[10]

1.2.2. SERS based bioassay methods

The number of binding agents that can be detected per test is dependent on the detection strategy. Fluorescence labelling is largely used for detection of protein binding events, because of its intrinsic sensitivity and ease of implementation.[7] However, due to the large bandwidth inherent to fluorescence, the numbers of ligands in an assay are usually limited to only 1 or 2. Fluorescence labelling also has other problems, which include high background counts from the substrate, photobleaching of the tags, and the need to use multiple excitation sources.[11-13] The use of surface-enhanced Raman scattering (SERS) has been flagged as a technique that has greater specificity than fluorescence labelling due to inherently narrower bandwidths and does not have the same problems as fluorescence.[11-13] The use of NPs as SERS substrates has been widely explored for use in conjunction with bioassays.[4, 13]

SERS can be used as a tool for biomedical applications by utilising a marker. This marker can then be attached to a biological material such as DNA,[14-16] proteins,[17, 18] antibodies,[19] and living cells.[6, 20-23] When the nanoparticles are immobilised onto a surface or a free antibody, a SERS spectrum of the marker is readily seen.[24] For example, indocyanine green bound to human serum albumin in a solution of gold nanoparticles produces a distinct SERS signature.[20]

1.3. Surface Enhanced Raman Scattering (SERS)

Raman spectroscopy is a form of vibrational spectroscopy where monochromatic light is scattered inelastically by a sample. The resultant spectrum is complementary, but not identical, to an infrared spectrum. Raman and infrared spectra are unique for a particular molecule. When light is incident on a molecule, it is scattered both elastically (Rayleigh) and inelastically (Raman). The Raman scattered light is of different frequency from the incident light because of interaction with the vibrational energy levels of the sample. Figure 2 shows the components of the scattered light. Only about 1 in 10^6 are Raman scattered photons amongst all scattered photons.

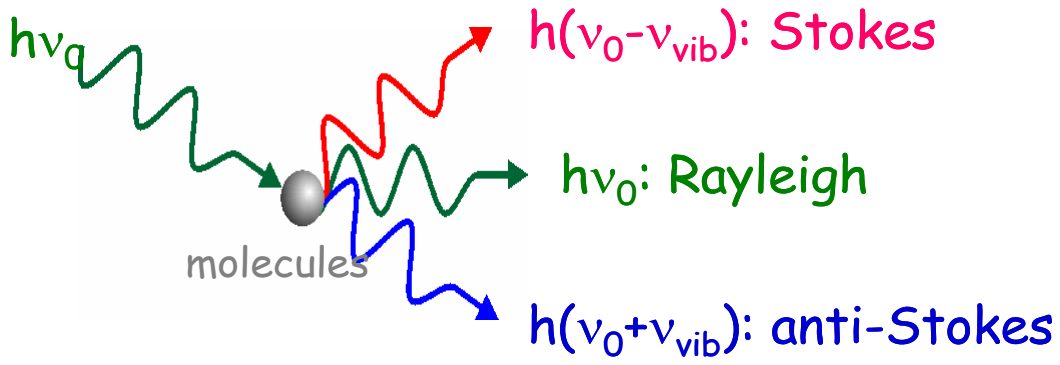

Figure 2 Monochromatic light scattered producing both Rayleigh and Raman scattering.

Typically, a Raman signal is too weak to be utilised as a detection strategy in immunoassays. However, when a Raman active molecule is brought into contact with a roughened metal surface or a metal colloid (nanoparticle) solution, the resultant signal can be enhanced by a factor of 10^6-10^{10}.[25-27] When resonant

enhancement is coupled with SERS enhancement (SERRS), reported increases in enhancements are in the 10^{10}-10^{18} range,[28] which is comparable to or greater than fluorescence sensitivity.[29] Due to the larger enhancement found with Ag, some researchers have coated Au nanoparticles with a thin film of Ag to improve SERS sensitivity and specificity.[30-32]

The SERS effect[33] was first observed for pyridine on a roughened silver electrode by Fleischmann *et al.*[34] Others soon followed with similar experimentation.[34-36] The SERS theory, in particular the enhancement mechanisms, was proposed by Moskovits soon after.[37] Aromatic nitrogen or oxygen containing compounds, such as aromatic amines (anilines or pyridines), tend to be more strongly SERS active. A molecule widely used for SERS studies is uracil as it is water soluble and gives a SERS spectrum with both silver and gold.[38-40]

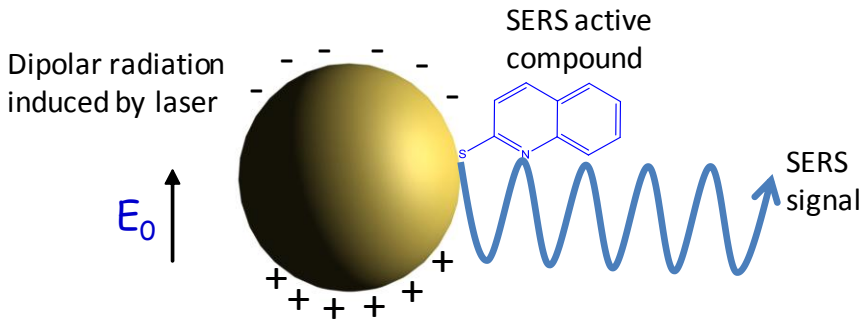

Figure 3 Enhancement of the Raman signal when a molecule is attached to a gold nanoparticle (note – figure not drawn to scale).

The initial mechanistic SERS effect was proposed by Moskovits.[35] Now, it is generally, but not universally, believed that SERS is caused by an electromagnetic enhancement and localised excitation of the surface plasmon,[41] together with a smaller chemical contribution.[42] Some researchers are not convinced that the

chemical contribution is significant and therefore disregard it totally.[41] For a SERS spectrum to be produced, the metal nanoparticles used need to be smaller than the wavelength of the exciting light. This enhancement can be seen in Figure 3 where electromagnetic field produced by is proportional to the SERS the enhancement factor. This is illustrated by a SERS active compound (SAC) shown as 2-quinolinethiol bound to a gold nanoparticle (AuNP). Typically, the nanoparticle size is in the order of 5-100 nm.[41] Conduction electrons in the metal surface are excited into an extended surface electronic state called a surface plasmon resonance.[33] Surface plasmon resonance (SPR) is an excitation of the localised surface plasmon in the metal surface resulting from shining a monochromatic light source onto the nanoparticles and is the result of the collective dipole oscillation of conduction electrons against the background of an ionic metal-core. The position of the absorption peak in the visible absorption spectrum of colloidal solutions can be related to the particle size and shape due to this resonance through SPR. From the Visible absorption spectrum, it was found that the absorbance spectra for the Au nanoparticles had a λ_{max} of around 520 nm.[43] This absorption band, also known as the plasmon mode, gives the colloidal gold its characteristic deep red-purple colour. The location of this plasmon mode is highly dependent upon the size, aggregation and shape of the particle. Figure 4 shows the shift of the SPR peak with change in particle size.

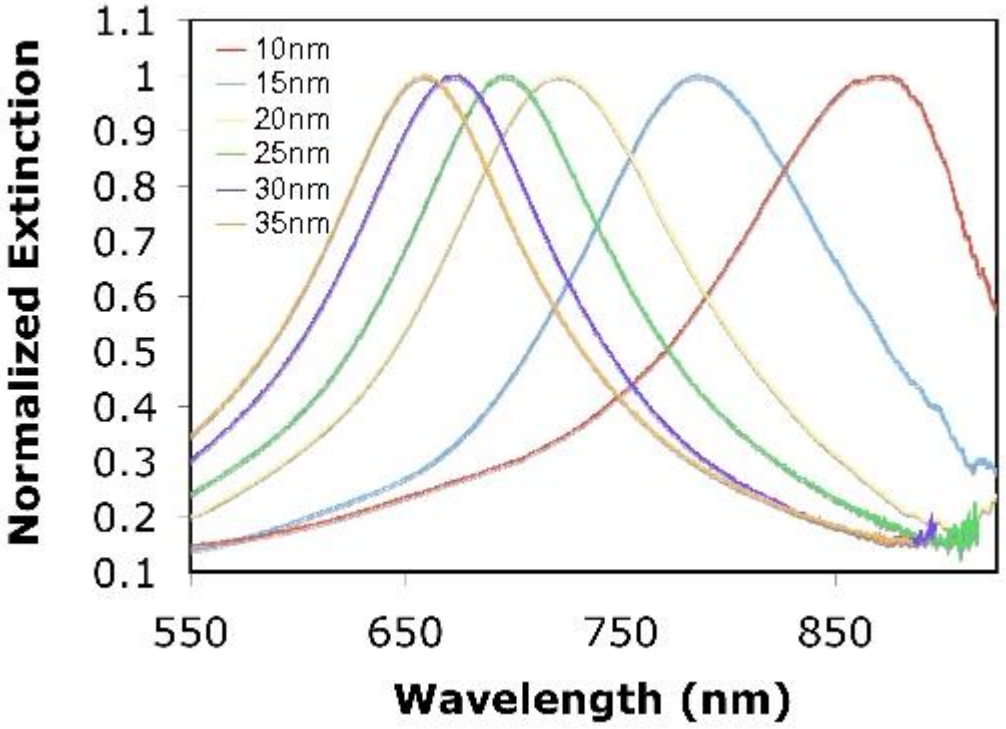

Figure 4 Surface plasmon resonance peak shift with change in particle size of NPs.[44] Image has been reproduced with the written permission from The Journal of Young Investigators.

Another contribution to the SERS effect, known as the chemical, or charge transfer, contribution, is by the formation of a charge-transfer complex between the surface and analyte molecule. The electronic transitions of many charge transfer complexes are in the visible part of the electromagnetic spectrum, so that resonance enhancement occurs between the metal (for example silver or gold) and the analyte (for example living cells).[42] Since the surface enhancement effect and the Raman scattering contribute to SERS, the intensity of the SERS signal is proportional to the fourth power of the excitation frequency and decreases with the increasing distance between the molecule used for the SERS signal and the nanoparticle. It has been shown by Tognalli *et al.*.[45] that the distance analyte molecules are from an Au nanoparticle can significantly reduce the intensity of the SERS signal. This is related

to the coupling and charge-transfer between the gold surface and the molecule. Kneipp *et al.*. stated that the SERS signal is inversely proportional to the 12^{th} power of the distance between the analyte and nanoparticle, showing that the molecule and the nanoparticle need to be in contact or very close proximity to produce a SERS signal.[6] Molecules adsorbed on or in close proximity to the surface experience an exceptionally large electromagnetic field, while molecules with lone pair electrons or π electron clouds, such as aromatic compounds or those containing nitrogen or sulphur, show the strongest SERS effect with respect to gold and silver.[42]

The very high sensitivity of SERS has led to considerable interest in the detection of single molecules by SERS and in certain instances single molecule detection has been reported.[46-48] Otto provides a summary of findings of single molecule SERS of biological molecules.[49] The narrow bandwidth of the SERS peaks (~20 cm^{-1}) provides the potential to perform multi-ligand assays on protein microarrays, which will give a huge increase in throughput compared with a single assay and conserve the amount of protein used.

Although work has been reported in areas where the sensitivity of SERS has been integral,[50] the issue of reproducibility of the SERS spectra has been questioned. The reproducibility of the SERS intensity and spectra where colloidal metal particles have been employed has been shown to be largely dependent on the concentration of the analyte and the preparation of the nanoparticles.[21, 51] The Bell research group have used nanoparticles covered with a polymer gel film to achieve a high level of reproducibility and long-term stability.[52] Raman tagged nanoparticles are commercially available with SiO_2 encapsulation[53] and the process for their synthesis

has been patented and they are now commercially available. This process has been refined but the preparation of encapsulated nanoparticles using polymers has now also been realised.[53, 54]

Unwanted fluorescence can occur in Raman,[55-57] and the use of the metal in contact with the SERS tag allows the fluorescence to be quenched via the heavy atom effect.[58]

1.4. Metal Nanoparticles

Many scientists have examined colloidal suspensions as SERS substrates and have seen that there are several factors that greatly influence their properties. These include particle size,[59] shape,[60] degree of aggregation,[61-63] monodispersity,[64] addition of anions,[29, 65] variation in surface charge, electrical potential[66, 67] and pH.[68] Studies have been conducted to determine the factors that affect size, shape and aggregation of the nanoparticles, showing that addition of salt and other destabilisation agents can significantly vary the nanoparticles.[59, 69-73] The most widely used nanoparticles for SERS are silver and gold due to their absorption characteristics and dielectric properties.[72, 74-78] Gold nanoparticles (AuNPs) exhibit an extensive range of useful properties that differ significantly from bulk gold. For example, depending on their precise size they can exhibit a strong absorption band in the visible region,[79] surface-enhanced Raman scattering (SERS) signal of adsorbed molecules,[13, 80, 81] catalytic behaviour,[82, 83] quenching of proximal fluorophores (<5 nm from surface),[84] and/or enhanced fluorescence of chromophores at a distance >10 nm.[84] These properties make AuNPs potentially useful in a broad range of applications, from photonic devices,[85] biosensors,[13, 86, 87] and nanoreactors[82] to light harvesting devices.[88] The

size, shape and degree of aggregation of AuNPs has a significant effect on the nature of the properties listed above.[79] However, if left unstabilised AuNPs readily aggregate to such an extent that these properties are lost.

There are two theories that when coupled together, explain the behaviour and characterisation of nanoparticles – the Mie Theory[43, 89] and the Drude model.[43] This combined theory uses the assumption that the nanoparticles are spherical. Whilst the synthesised particles used for the work detailed in this thesis are not completely spherical, this model gives a good approximation of their size and is in agreement with the distribution obtained from dynamic light scattering (DLS) results and LSPR absorption bands.

1.4.1. Synthesis of metal nanoparticles

The preparation method affects the degree of aggregation and the particle size, and is also dependant on the type of metal being used. For gold, particle size is largely dependent on the amount of citrate used in the reduction process when using the Lee-Meisel[75] or Frens[59] synthetic methods. Frens[59] showed that using 50 mL of 0.01 % w/w $HAuCl_4$ and varying the amount of 1 % w/w sodium citrate, can alter the size of AuNPs from 12 nm up to 150 nm. Figure 5 shows the reaction to produce the AuNPs.

$$Au^{3+}_{(aq)} + 3e^- \xrightarrow{\text{Citrate}} Au_{(ppt)}$$

Figure 5 Reaction for citrate reduction of gold ions producing gold colloids

This process was further refined by Sutherland *et al.*.[64] Other researchers have used the citrate technique with $KAuCl_4$,[27] or prepared the Au colloids at a constant temperature.[90] There are numerous variations on these methods. Other methods of producing gold colloids include modification of the citrate method by the addition of tannic acid or the use of NaCl for stabilization or controlled aggregation.[91] Other methods use Na_2S, hydroxylamine or $NaBH_4$ as the reducing agent in place of citrate ion.[62, 92] These methods are capable of producing nanoparticles between 2 and 200 nm.

1.4.2. Metal nanoparticles as SERS substrates

A range of strategies are available for attaching small molecules to gold surfaces. These include the use of thiols,[26, 93] isocyanides,[25, 27, 81] selenols,[94] xanthates[95] and isothiocyanates.[11, 71] These have been chosen because they interact with the gold surface and are commercially available. In general, groups containing the sulphur atom interact most strongly with gold surfaces, hence, thiols in particular have found extensive use in this field.[96]

While many researchers have chosen to use either silver or gold as their SERS substrate, gold core/silver shell NPs have also been examined to investigate the effects on SERS spectra. The variations in the SERS spectra with different ratios of Au to Ag were found to be quite marked, and greatly increased the intensity of the SERS spectra compared to pure Au nanoparticles.[31] Due to the larger enhancement found with Ag, some researchers have coated Au nanoparticles with a thin film of Ag to improve SERS detection, as opposed to a core/shell nanoparticle.[30] It has even been suggested that coated AuNPs can be used for calibration of SERS

instrumentation.[97] Particular attention has been given to the relationship between the excitation wavelength, metal used and the enhancement produced. Researchers have explored this relationship through using core-shell systems,[98, 99] as well as shape[100, 101] and aspect ratio.[102] All of these methods have shown that there has been an increase in the SERS signal intensity for these systems.

The discrete nature of AuNPs enables individual nanoparticles to be encoded with different SERS reporter molecules (also known as Raman tags).[11, 20] This fact has been exploited by a number of research groups, and AuNPs encoded with SERS tags have been used as a detection strategy in a variety of bioassays.[13, 14, 18, 103, 104] This strategy has a number of advantages over other more conventional detection strategies, such as fluorescence spectroscopy. Fluorophores exhibit photo-bleaching and have a limited ability to be multiplexed, due to broad fluorescence emission bandwidths. SERS is a highly sensitive technique, which can be conducted in a similar manner to fluorescence spectroscopy, and typically does not exhibit photo-bleaching. Furthermore, the spectral output can also be highly specific due to the large number of narrow bands present in a spectrum. The SERS tag can be said to constitute a "molecular barcode". Molecules which might be suitable as SERS tags should have a strong, distinctive SERS spectrum and should be able to interact strongly with the AuNPs. This implies that they should incorporate a sulphur-containing group such as thiol, thiocyanate or isothiocyanate, which will have a strong affinity for the gold surface. However, a potential problem with some SERS encoded nanoparticles is poor physiochemical stability, which results in aggregation and loss of the SERS effect. Some previously reported methods for stabilizing nanoparticles to preserve the SERS effect have been coating of AuNPs with a silica

shell,[11, 13] and stabilizing with specifically engineered polyethylene glycol polymers.[105]

1.4.3. Polymer stabilization of metal nanoparticles

Silver and gold colloids prepared using the citrate reduction method can be stable for months, with the fresh colloids exhibiting high stability due to ions adsorbed to the metal surface, which prevents aggregation of the colloidal particles.[2] If physicochemical stability is not maintained, aggregation can occur, such that the nanoparticles are no longer suspended in solution.[11, 25, 106] Synthesis of polymer coated nanoparticles has been shown to help stabilise the colloidal suspension to overcome any problems with stability.[71]

It is known that both sulphur and to a lesser extent nitrogen end-groups attach readily to Au nanoparticles.[54, 62] Hence, a polymeric compound that includes these groups will interact with the nanoparticle surface and may produce a SERS signal.[107] Luo and co-workers have successfully coated AuNPs with hydrophilic block copolymers by incorporating a thiol end group that readily attaches to the AuNPs. The polymer was then cross-linked to maintain the stability of the solution. Analysis by TEM showed that the nanoparticles were present, but were not covered with a uniform coating of polymer.[108]

Polymer beads have been used to encapsulate aggregates of nanoparticles with compounds such as sodium thiocyanate and mercaptopropionic acid attached. It was seen that, although a layer of gold colloid was found on the exterior of the polymer

bead, small nanoparticles (diameter range 2-10 nm) were also found on the interior of the bead. The nanoparticles were subsequently removed from the exterior of beads. The spectra obtained from these compounds showed that SERS of the analyte was achievable within the polymer beads.[109]

Generally, metal nanoparticles are prepared in aqueous solution. However, most polymers used in nanoparticle research are not water soluble making the encapsulation process difficult. A technique employed to overcome this problem is phase transfer of the nanoparticle solution to an organic phase by means of a phase transfer catalyst, allowing the polymer encapsulation to occur.[67] Another method for suspending the nanoparticles in organic phase is by centrifugation followed by re-suspension in an organic solution, so that the nanoparticles are present in the organic phase when the polymer is added.[110]

Typically, polymer stabilised AuNPs exhibit enhanced physicochemical stability, electrical and opto-electronic properties.[71] There are three general approaches for the generation of polymer stabilised AuNPs. The first is the "grafting to" approach, where polymers, with typically a thiol or thiolate end-group, are allowed to self-assemble at the AuNPs surface due to the specific interaction of the sulphur end-group with the gold surface.[108, 111-113] The second approach is a variation of the first, and involves the reduction of gold salts with sodium borohydride in the presence of a thiol[114-116] or dithioester[112] end-functionalised polymer to yield hybrids with a AuNP core and polymer shell. The third method is the "grafting from" approach, which involves the functionalisation of the AuNPs with an initiating species[117-120] or chain

transfer agent[121] and subsequent growth of a polymer chain from the AuNPs surface.[118, 122, 123]

A convenient method for the preparation of polymers with a sulphur containing end-group is the reversible addition-fragmentation chain transfer (RAFT) process, shown in Figure 6.[124-127]

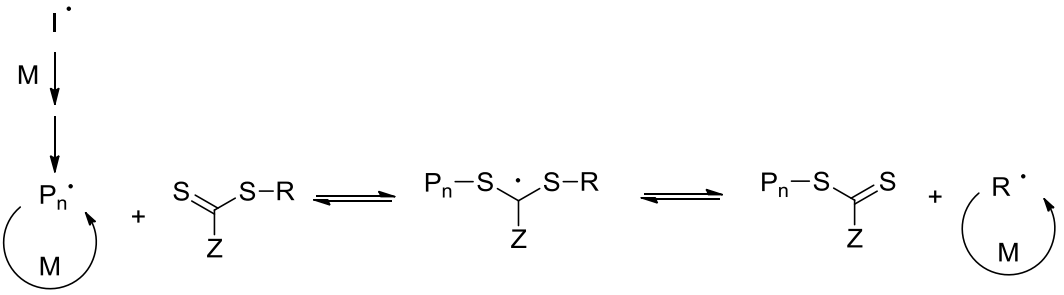

Figure 6 Mechanism of RAFT polymerisation where I = initiator, M = monomer, Pn = propagating radical, R = homolytic leaving group (early stages of polymerization) or a second propagating radical (chain equilibration)

RAFT is a living free radical polymerisation method where thiocarbonylthio compounds are used as chain transfer agents. The RAFT technique can be used to polymerise monomers with a wide variety of functional groups, to yield polymers with a thiocarbonylthio containing end-group, which can then be reduced to a thiol. Depending on the monomer – RAFT agent combination, it is also possible to control the molecular weight and to produce polymers with low polydispersity indices. Furthermore, a range of architectures are accessible, which include block copolymers,[128-131] star polymers[132-136] and branched polymers.[137, 138]

1.5. SERS for use in bioassays

Recently a number of papers have reported the use of SAC AuNPs for use in protein bioassays. Several construction strategies have been used.[11, 13, 19, 25, 103] A strategy employed by Grubisha *et al.*[12] utilises a thiol-containing SAC with a succinimidyl group. The thiol group interacts with the gold nanoparticle surface to form a self-assembled monolayer. The succinimidyl group was then available to attach an antibody or small molecule (protein ligand) to the nanoparticle (a bioassay). The assembly of these nanoparticles is depicted in Figure 7.[12] Each protein ligand is attached to a nanoparticle that is encoded with a different Raman tag. A review by Ulman discusses the investigations reported by researchers in validating self-assembled monolayers for bioassays, in particular the use of fluorescence and SERS.[96]

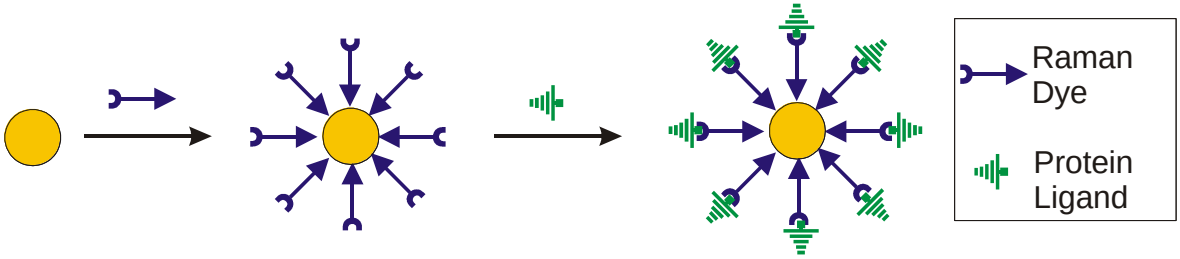

Figure 7 An assembly method to produce encoded noble metal nanoparticles for protein assays adapted from Grubisha *et al.*[12]

Screening using microarrays to detect protein-protein and protein-small molecule interactions has been performed using SERS of SAC nanoparticles (NPs).[103] The SAC is used as a specific identifier for each antibody.[139] SACs are used to make the molecules individually detectable, when there are several biological assays that need to be recognised concurrently. The possibility of using the SERS spectra of self-

assembled monolayers on AuNPs as a barcoding strategy has been postulated in a number of recent articles.[11, 13, 19, 25, 103] However, these articles did not demonstrate the potential multiplexing capabilities of the technology. Although the utility of Raman tagged nanoparticles as a detection strategy has been demonstrated, the multiplexing capabilities have been only shown with small numbers of molecules used for detection but can be deduced from the range of different SERS spectra shown in Figure 8.[140]

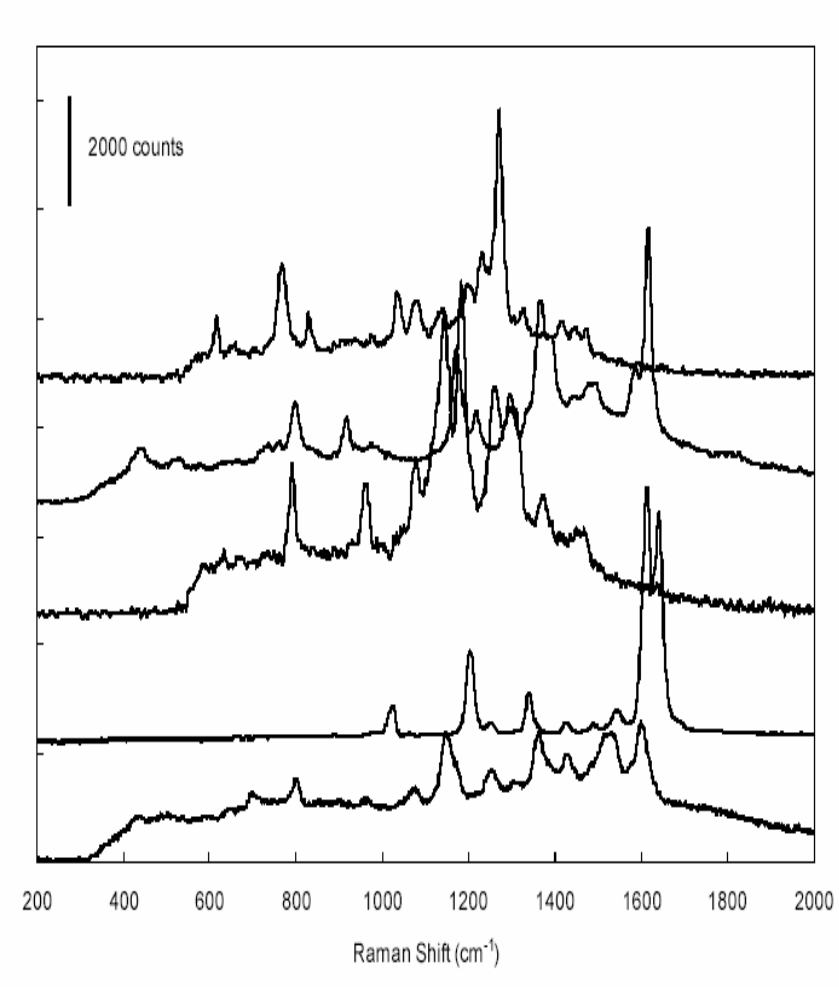

Figure 8 SERS spectra of different analytes attached to AuNPs showing the capability to use them as a bioassay detection strategy[140] This figure has been reproduced with email permission from the authors.

The method of protein microarray screening involves the printing of arrays of thiols, isocyanides and isothiocyanates on gold-coated microscope slides. Methods for producing the arrays vary. These techniques include blotting proteins onto membranes and ink-jet printing technology.[7, 8] These slides can be screened for a SERS signal using a Raman microscope with a programmable stage and imaging capabilities. This will allow the rapid screening of a large number of biological molecules to generate a library, which can then be distinguished by their SERS spectra.

It has been demonstrated that a SERS signal of Raman tagged Ag nanoparticles can be readily seen with avidin-biotin as the protein-small molecule combination. Biotin was attached to both Ag surface and also to Ag NP clusters. The nanoparticles had a Raman tag attached to them, but the surface does not. Avidin was then attached to the Ag surface by interaction with the biotin attached to it. The NP solution was then washed over the substrate and became bound to the avidin (avidin can bind four separate biotin molecules). The final complex resembled a sandwich assay.[13, 141, 142] A SERS signal of the Raman tag could be seen at those points on the surface where the nanoparticles were attached. Figure 9 shows a schematic of the points on the Ag surface where a SERS signal could be seen.[25]

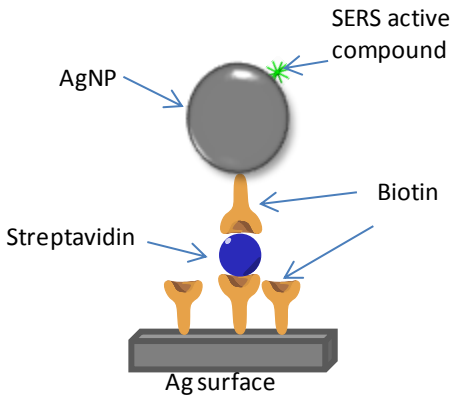

Figure 9 Diagram of the surface and nanoparticle complex adaptedfrom Kim *et al.* [25]

It has been seen that by utilizing the addition of an antibody to a Raman-tagged nanoparticle, followed by creation of an immune complex by interaction with an antigen, a SERS spectrum can be produced. The antibody concentration that was seen to be most effective for producing a SERS spectrum was 2.2×10^{-8} M.[12, 13, 143]

As explained above, there are a range of strategies available for attaching small molecules to gold surfaces. These include the use of thiols,[26, 93], isocyanides,[25, 27, 81] selenols,[94] xanthates[95] and isothiocyanates.[11, 71] For this research thiols and isothiocyanates were primarily used. These have been chosen because of the commercial availability of a diverse range of these compounds. Thiols in particular have been chosen because the chemistry of this type of system has been extensively characterised in the literature.[96]

1.6. Project rationale

The overall objective of this study was to demonstrate that polymer stabilised Raman tagged nanoparticles are an effective strategy for undertaking bioassays and allow more accurate screening compared with methods in literature. This is illustrated in Figure 10.

The aims of the study were to:

1. *Prepare and characterise AuNPs* – to determine an appropriate size and synthetic method that promotes an optimum SERS signal.

2. *Investigate Raman tags and their interaction with AuNPs* – to determine a suitable Raman tags for attachment to the nanoparticles, including determination of the most suitable tags for detection by SERS.

3. *Prepare polymer coated gold particles and determine the optimum polymer structure* – to ascertain an optimised polymer structure that attaches to the AuNPs, but also allows the Raman tags to remain attached, so that a SERS spectrum can be obtained.

4. *Test the addition of a linker and small molecule to hybrid nanoparticles* - determination of most suitable polymer structure for the chosen linkers (ligands) and proteins.

5. *Demonstrate the potential for protein arrays by showing that a binding event can be detected by SERS* – evaluate that multiplexing using SERS is a useful tool for protein detection, shown in Figure 10.

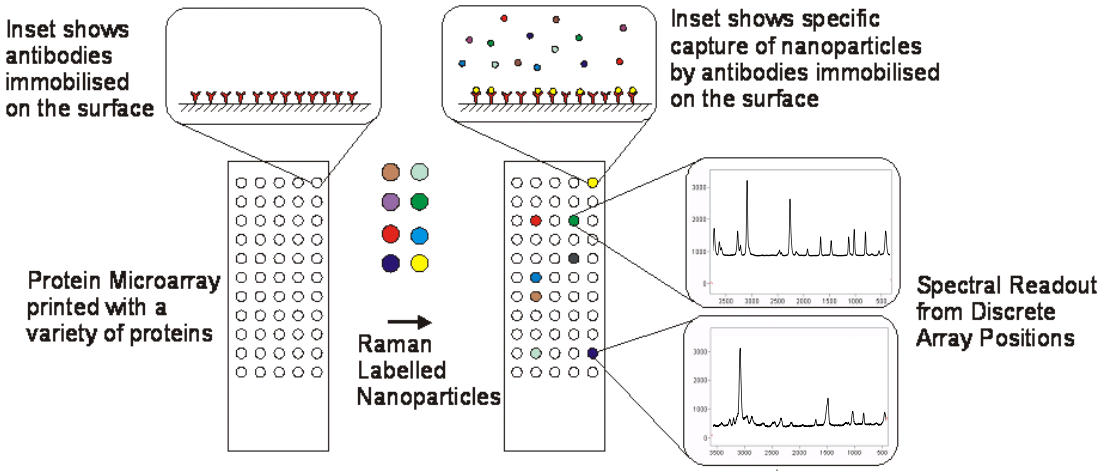

Figure 10 Pictorial representation of anticipated project outcome.

2. CHAPTER 2

METHODS AND MATERIALS

2.1. Experimental Methods

2.1.1. Polymer synthesis

2.1.2. Nuclear Magnetic Resonance (NMR)

^{1}H Nuclear Magnetic Resonance (NMR) spectra were collected using a 5 mm BBOz gradient probe at 298 K on the Bruker Avance 300 or 400 MHz and ^{13}C spectra were collected using a 5 mm SEIz probe at 298 K on the Bruker Avance 500 MHz. Deuterated solvents for NMR spectroscopy were commercially obtained (Cambridge Isotopes) and were of 99.8 atom % D. Chemical shifts (δ) are reported in parts per million (ppm) relative to residual solvents. Samples were dried then dissolved in an appropriate deuterated solvent. Samples were typically 5 mg for ^{1}H NMR and 20 mg for ^{13}C NMR.

2.1.3. Gel Permeation Chromatography (GPC)

Gel permeation chromatography (GPC) measurements of the polymers were performed using a Waters Alliance 2690 Separations Module equipped with an auto sampler, column heater, differential refractive index detector and a photo diode array (PDA) connected in series. HPLC grade tetrahydrofuran was used as the eluent at a flow rate of 1 mL min^{-1}. The columns consisted of three 7.8 x 300 mm Waters Styragel SEC columns connected in series, comprising of two linear Ultrastyragel and one Styragel HR3 columns. Polystyrene standards ranging from 2000000 - 517 g mol^{-1} were used for calibration.

GPC was used to determine the molecular weight averages (M_n) and molecular weight distributions (PDI = M_w/M_n) of the polymers synthesised in this work.

2.2. Raman and surface-enhanced Raman spectroscopy measurements

Raman spectra were recorded with a Renishaw inVia micro Raman spectrometer (Renishaw plc, Wotton-under-Edge, UK) equipped with a 785 nm as the excitation source from a diode laser, a single diffraction grating and a thermo-electrically cooled CCD detector. A 10 % neutral density filter was used, which resulted in a laser power at the sample of about 1 mW. A single accumulation in the spectral range 2000 – 200 cm^{-1} was collected for each sample. Confocal mode with a pinhole inserted was used for measurements taken on the streptavidin well plate detailed in Chapter 6.

FT Raman spectral measurements were undertaken on a Perkin Elmer 2000 spectrometer with a Nd:YAG laser emitting at 1064 nm.

For solid state measurements, approximately 200 μL of solution was dropped onto a low fluorescence glass slide and allowed to dry. This was then mounted under the microscope and the surface nanoparticles were focussed on using the 50X long working distance lens objective. For liquid solutions a series of low fluorescence glass miniature vials were made and mounted in an aluminium tray. These vials held approximately 200 μL. Once under the microscope the top meniscus of the solution

was found then the laser was focussed into the middle of the solution. Typically a single ten second scan was taken.

2.2.1. SERS active compounds used in this work

The following is a list of compounds used for the SERS component of work:

- Uracil
- 2-Quinolinethiol
- Naphthalenethiol
- Rhodamine B isothiocyanate
- Fluorescein isothiocyanate
- 1,2,4-Triazole
- 2,5-Mercapto-1,3,4-thiadiazole
- 2-Mercapto-1,3,4-thiadiazole
- 2-Mercaptothiazoline
- 4-Mercaptopyridine

2.3. Determination of Gold/Polymer Composition

The relative composition of the stabilised nanoparticles with respect to gold and polymer was determined using thermogravimetic analysis (TGA) to degrade the polymer portion. To ensure removal of any free polymer, solutions of the AuNP stabilised with polymer were centrifuged (14000 rpm, 9400 g, 10 min) at least four times, with the supernatant solution being removed and replaced after each run. TGA was performed in a TA® Instruments, series Q500, high-resolution TGA where the flow rate of oxygen over the samples was set to 60 cm^3 min^{-1}. The runs were

performed in triplicate and between 10-20 mg of sample were used in each analysis. A heating rate of 5 °C min^{-1} to 800 °C was utilised. With the quasi-isothermal, quasi-isobaric heating program of the instrument the furnace temperature was regulated precisely to provide a uniform rate of decomposition in the main decomposition stage.

2.3.1. Determination of gold nanoparticle size

Transmission Electron Microscopy (TEM) micrographs were imaged on a JEOL 1200 TEM, where the energy was set to 80 kV and spot size 3. Solutions of citrate-stabilised AuNPs in water and solutions of polymer stabilised AuNPs in chloroform were dropped onto carbon-celloidin coated 200-mesh copper TEM grids and allowed to dry before placing in TEM sample holder.

Citrate stabilised AuNPs that were dispersed in water, were synthesised using the citrate method.[144, 145] Size of the nanoparticles was initially confirmed on TEM, imaging was also attempted on a SEM but the resolution was not adequate. TEM micrographs of AuNPs synthesised by the citrate-stabilised method were analysed and average size was taken. It should be noted that the NPs aggregated on the carbon coated TEM grids during sample preparation.

AuNPs are known to exhibit a surface plasmon resonance (SPR) in the visible region, which is caused by incoming electromagnetic radiation inducing the formation of a dipole in the nanoparticle. The restorative force, which compensates for the dipole results in electron oscillations that correspond to a specific frequency

of light. Mie theory has been applied to model this phenomenon for dilute solutions of spherical AuNPs and nanorods.[146]

Dynamic Light Scattering (Nanosizer Nano ZS, MALVERN Instruments) was used to analyse the particle size distribution of polymer and polymer/Au hybrid suspensions from 0.6 to 6000 nm, in which the peak position and the width at the half-maximum were automatically calculated with the Malvern Instruments software. Chloroform was used as a dispersant. Measurements were performed at 25 ºC.

2.3.2. FTIR-ATR analysis

Attenuated Total Reflectance - Fourier Transform Infrared (ATR-FTIR) spectra were obtained on a Nicolet Nexus 5700 FTIR spectrometer equipped with a Nicolet Smart Orbit single bounce, diamond ATR accessory (Thermo Electron Corp., Waltham, MA). Spectra were recorded at 4 cm^{-1} resolution for at least 32 scans with an optical path difference velocity of 0.6289 cm s^{-1}. Solids were pressed directly onto the diamond internal reflection element of the ATR accessory without further sample preparation. Spectra were manipulated using the OMNIC 7 software package (Thermo Electron Corp., Waltham, MA).

The FTIR-ATR spectra were obtained using a Diamond ATR crystal for all analysis except work conducted in Chapter 5 where a Ge crystal was used due to the azide band appearing where the diamond crystal absorbs.

2.3.3. Visible analysis

Ultraviolet-Visible spectra, with a spectral range of 450 – 650 nm were acquired using a Varian Cary 3000 Visible absorption spectrophotometer. The reference cell was filled with solvent corresponding to that in the sample cell.

2.4. Materials

Unless otherwise stated, all reagents and solvents were used as received. All water used was MilliQ Ultrapure 18 MΩ cm. All samples were purchased through Sigma Aldrich with the exception of streptavidin and biotin that were purchased from Anaspec (CA, USA).

Polymers synthesised as part of this research are detailed in chapter 4. Note that the initial polymers were supplied by Dr. Zul Merican as detailed in Table 1.

3. CHAPTER 3

SYNTHESIS AND

CHARACTERISATION

OF

NANOPARTICLES

FOR

SERS

3.1. Introduction

Colloidal gold has been used for several hundred years for many applications, including medical and artistic. Gold has many unique properties, which have been well documented, including the ability to maintain brilliant colour for artistic purposes and possess an excellent biocompatibility.[4, 71] A review on AuNPs was published in 2006,[71, 84] this details many applications including diagnostics. An application of AuNPs is as a substrate for SERS spectroscopic analysis of small molecules adsorbed at the nanoparticle surface.[147] The discrete nature of AuNPs enables individual nanoparticles to be encoded with different SERS tags.[11, 148] This piece of evidence has been taken advantage of by a number of research groups, and AuNPs encoded with SERS tags have been used as a detection strategy in a variety of bioassays.[13, 14, 103, 149, 150]

The aim of this work was to determine an appropriate synthetic method that produces a nanoparticle size that gives an optimal and reproducible SERS signal. A SERS signal is optimally obtained from nanoparticles with a size between 15 and 100 nm.[41] Anything outside these parameters either doesn't produce the dipole oscillation or also produces multiple oscillations which hamper the intensity of the SERS signal.

As part of determining an optimal SERS signal, appropriate Sacs need to be determined. For this, several factors need to be taken into account including compound size and resonance possibilities.[151] Several compounds were tested and

selection from these compounds was determined from the consistency of spectral results.

3.2. Experimental methods

This work has been performed to determine the optimal colloid size, concentration, aggregation and method to produce the most intense SERS signal from the SERS-active Raman tag. An option explored was to purchase the AuNPs from several different companies with an almost monodisperse size range for comparison with the particles synthesised in this section. This was ultimately not pursued since the commercially available citrate reduced gold contained stabilizing agents such as tannic acid. It was thought that the stabilizing agents may interfere with the polymer encapsulation process detailed in later chapters.

3.2.1. Synthesis of nanoparticles by citrate reduction

When the nanoparticles were first synthesised, both silver (AgNP) and gold were prepared. The AgNPs were synthesised following the method detailed by Sutherland.[64]

For AuNP preparation, all glassware was washed with aqua regia due to its ability to remove any residual AuNPs and oven dried. A typical preparation method was as follows: 30 μL of Auric Acid ($HAuCl_4$) was added to 100 mL 18 MΩ cm ultrapure water and brought to boil, after which approximately 40 mg of tri-sodium citrate was added to the boiling solution. The solution could be seen to change from pale yellow to clear, then dark purple then to a reddish colour.

AuNPs have been prepared by several variations of the citrate reduction method. The method used initially in this project was adapted from Grabar *et al.*;[152] 100 mL 1.0 mM aqueous $HAuCl_4$ was heated to boiling, then 3.5 mL 38.8 mM sodium citrate was added. To ensure complete reduction, the solution was boiled for a further 15 min. The amount of citrate added was varied from between 2 mL to 10.5 mL to vary the size of the colloids between approximately 15 nm and 90 nm.

To prepare colloids with a target diameter of 60 nm the following procedure was used. Glassware was cleaned with aqua regia (3 parts HCl to 1 part HNO_3) then rinsed with ultrapure water (18 MΩ cm). In a 50 mL conical flask, 30 mL of 0.01 % aqueous solution of $HAuCl_4$ was brought to boil with magnetic stirring. 180 µL of 1 % sodium citrate rapidly injected. Solution turned from pale yellow to purple then red within min. The solution was boiled for approximately 15 min to ensure complete reduction, cooled to room temperature, then reconstituted to 30 mL before use.[11]

To prepare colloids with a diameter of approximately 40 nm the following procedure was used. Glassware cleaned aqua regia (3 parts HCl to 1 part HNO_3) then rinsed with ultrapure water (18 MΩ cm). Aqueous $HAuCl_4$ (500 mL 1.0 mM) was brought to boil while stirring. Aqueous trisodium citrate (17.5 mL,38.8 mM) was added. Boiling was continued for 10 min.[61]

3.2.2. Synthesis of gold nanoparticles by other synthetic methods

AuNPs or colloidal gold can be produced by many different methods including the addition of glucose and starch to the $HAuCl_4$ during the nanoparticle synthesis. Although other methods were tested as part of this research, only the citrate reduction method produced nanoparticles within the required size range. This included the Na_2S method[62] which is reported to allow a larger range of molecules to bind to the gold for nanoassembly, as well as greater control of aggregation. The nanoparticles produced using this method were not stable in solution for extended periods of time and thus the citrate method was favoured.

3.2.3. Results and Discussion

During initial synthesis, there was great variation in the size and in turn the colour and surface plasmon resonance (SPR) peak due to the variation in growth of the nanoparticles. Figure 11 shows the variation resulting from the different batches of gold synthesised. The discrepancy appeared to be related to an inconsistency with heating related to the cessation of boiling of the gold chloride solution when the citrate was added. In the larger batch lots this was seen to occur for several min before boiling started again. It was observed that the longer the batch took to start boiling again, the longer the nanoparticles took to form and in turn the greater the variability in the size of the nanoparticles in the solution. The variation in the batch vessel seemed to also make a difference. Since a conical flask was used, if the size

and in turn the surface area of the conical flask in contact with the hot plate was varied, then variation also occurred in the size and shape of the nanoparticles. Also, in initial experiments the $HAuCl_4$ purchased was a solid, since the $HAuCl_4$ is highly hygroscopic, and proved difficult to weigh accurately. The $HAuCl_4$ was then purchased as a solution, eliminating another variable in producing the AuNPs. These observations were further verified by TEM image shown in Figure 12, showing the large variation in the initial batches of AuNPs.

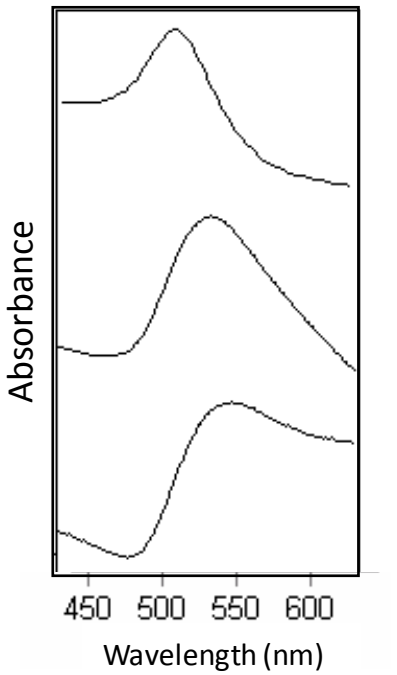

Figure 11 Visible absorption spectra showing the variation in initial gold batches produced in initial work before a refinement of the synthetic procedure was undertaken

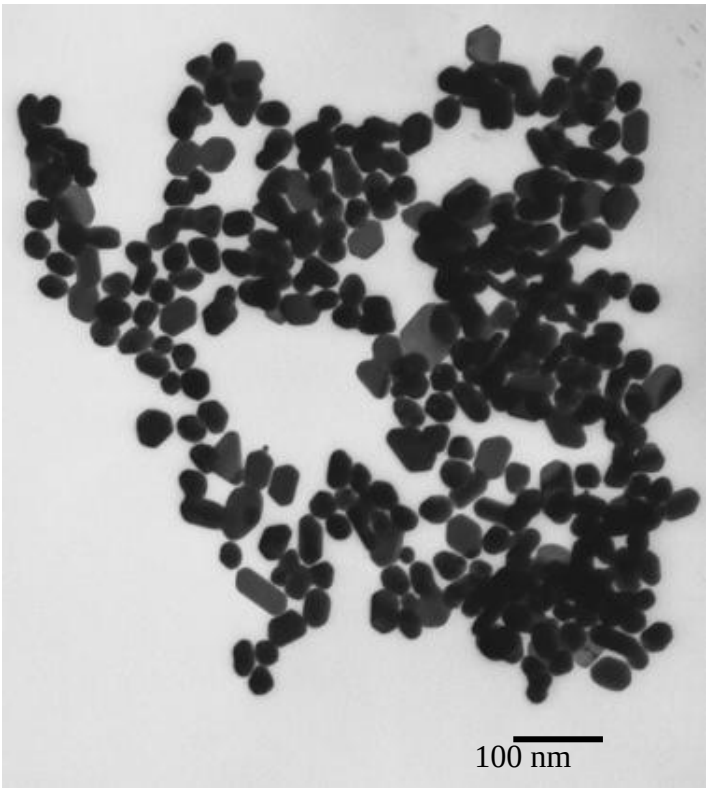

Figure 12 TEM image of representative batch of AuNPs produced initially by the citrate reduction method with large batch

It was found that the optimal size for the AuNPs was approximately 40 nm, taking into account size with respect to SERS. The optimal size of the gold needed to be such that a dipole oscillation of the surface photons occurred and therefore giving rise to the SERS signal. Also, the long-term stability in solution over several months to years must also be considered. Sizes between 10 and 150 nm were tested and it was seen that the smaller nanoparticles were very stable but SERS intensity improved with size, while larger nanoparticles were not stable in solution for any prolonged period due to their size and the intrinsic mass of the nanoparticles. The samples were examined using TEM and visible spectroscopy. This initial testing was used to determine that an adapted version of a method published by Olson[61] was used for synthesizing AuNPs throughout this work from this point forward.

AuNPs were prepared in sizes ranging from 15 nm to 100 nm. The larger particles were found not to be stable over prolonged time periods (sediment appeared). Particles approximately 40 nm produce a SERS signal and remain stable over periods of at least 6 to 12 months.

The method results in a colour change of the solution with AuNP size, following the variation in the amount of citrate added to the $HAuCl_4$ adapted by Olson *et al.*[61] from the method of Frens (see Figure 13).[59]

Figure 13 Observed colour change of AuNPs produced by citrate reduction. From left to right the size of the particles shown by TEM are approximately 100 nm, 40 nm and 15 nm respectively.

3.3. Observation of aggregation of gold nanoparticles

It is known that AuNPs are physicochemically unstable in the absence of stabilizing agents.[31, 153] It was seen that the addition of salts, altering the pH and the addition of solvents, such as THF, greatly reduced the usable lifetime of the AuNPs.[154] The addition of the SACS also produced significant irreversible aggregation in the AuNPs on every occasion when no stabilising agent was present.

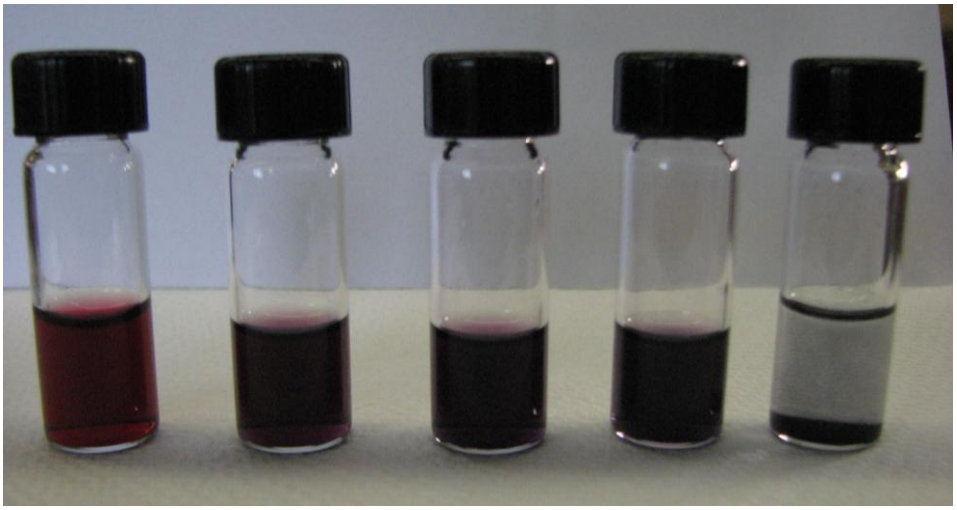

Figure 14 Progression from as-made AuNPs (left), AuNPs with limited aggregation (centre), AuNPs with irreversible aggregation (right), AuNPs with irreversible aggregation after about an hour. These nanoparticles were produced by the citrate reduction method and were approximately 40 nm in size.

3.4. Characterisation

AuNPs are known to exhibit a surface plasmon resonance (SPR) in the visible region, which is caused by incoming electromagnetic radiation inducing the formation of a dipole in the nanoparticle. The restorative force, which compensates for the dipole, results in electron oscillations that correspond to a specific frequency

of light. Mie theory has been successfully applied to model this phenomenon for dilute solutions of spherical AuNPs and nanorods.[146] Figure 15 shows a typical visible spectrum achieved with citrate-stabilised AuNPs in aqueous solution. This exhibited a surface plasmon resonance (SPR) maximum at approximately 529 nm, which according to calculations using Mie theory is typical of spherical AuNPs of approximately 40 nm in diameter.[155,43] This is representative of the AuNPs used in this work and of visible spectra obtained when the procedure outlined in this chapter was followed.

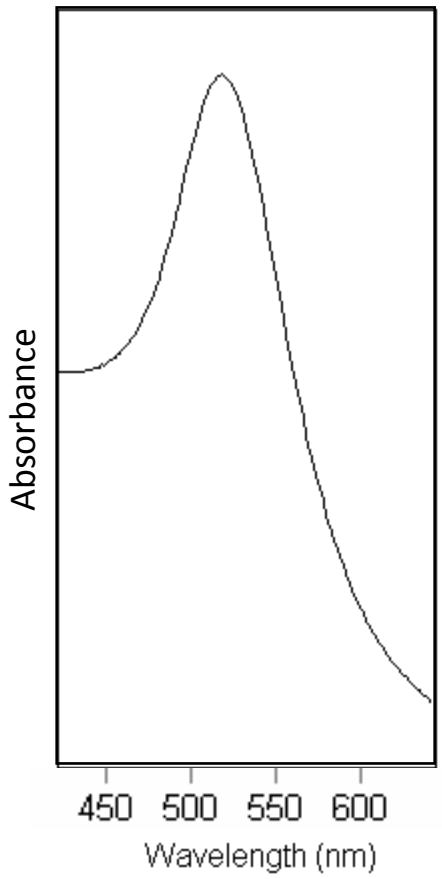

Figure 15 Visible spectrum obtained from a typical batch of gold colloids

TEM and DLS were also used to determine an average size of the nanoparticles. DLS measurements were taken for citrate-stabilised AuNPs. Analysis of the DLS results indicated the citrate-stabilised nanoparticles had a diameter of 56 ± 10 nm, this value is expected to be higher than the TEM result as the method of measuring by DLS biases towards the larger particles. Figure 16 shows TEM and SEM images of the typical size and distribution of the nanoparticles made using the citrate reduction method. It can be seen that the particles are varying in both shape and size. It was found that the smaller sized nanoparticles were less polydisperse than the ones that were chosen for this project. They were not chosen for this work as the SERS signal produced was harder to achieve than from the larger particles.

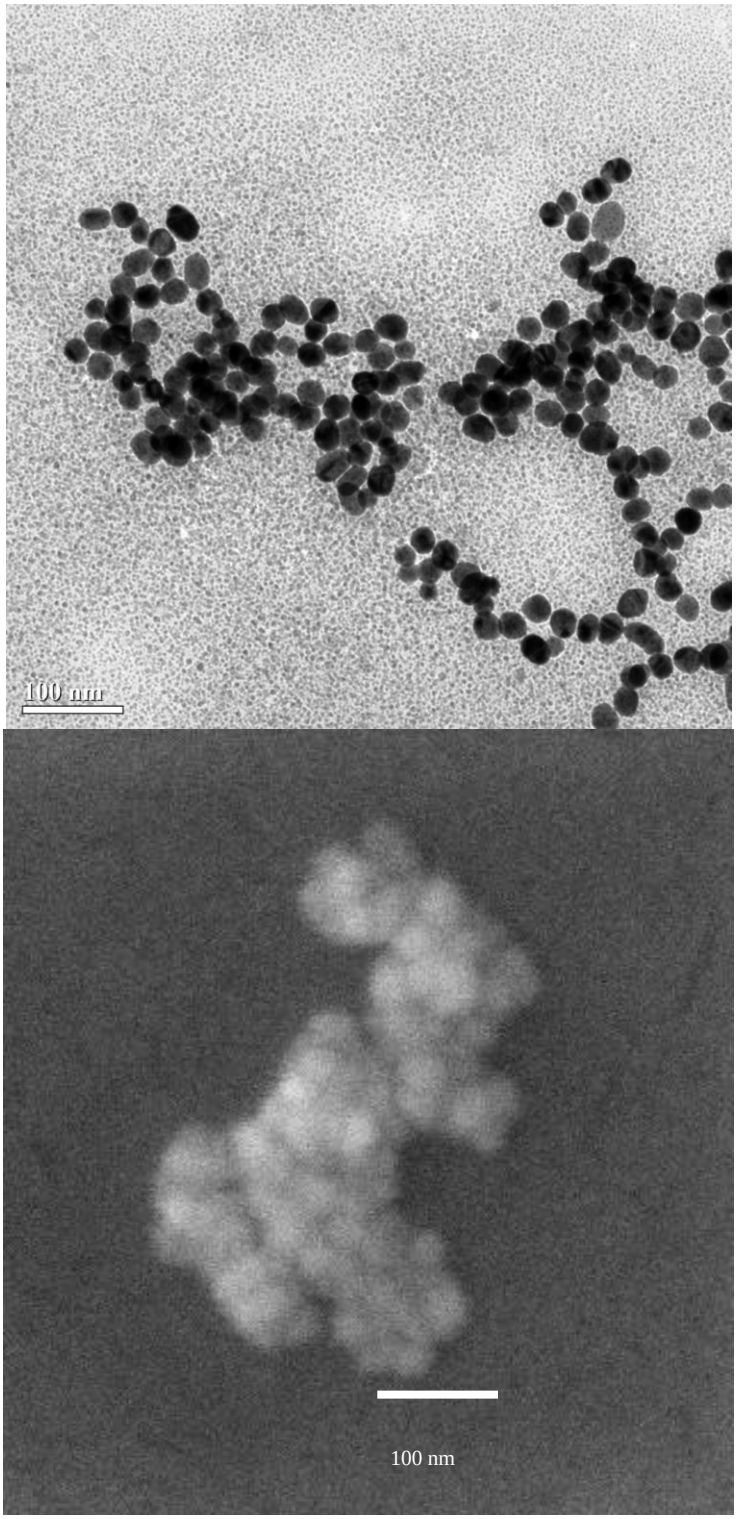

Figure 16 Typical TEM image (top) and SEM image (bottom) of citrate reduced AuNPs used in the latter part of this work

3.4.1. SERS and AuNPs

Compounds containing either nitrogen or sulphur end groups have been commonly used for obtaining a strong SERS signal. In this work sulphur containing end group compounds were found to perform more consistently with the AuNPs. In Chapter 2 a list of the Sacs investigated throughout this work can be found.

Initially, uracil was used as it was found to give a signal for both AgNPs and AuNPs. Typically, a solution of 5 mM of the SERS compound was made, and then 4-40 μl was taken and added to a 1 mL AuNP solution. It was found that a concentration of between 5 and 50 nM was able to generate a SERS signal. This result shows that the SERS signal is not only dependant on the analyte being attached to but is also strongly concentration dependant agreeing with the literature.[51] If the concentration of the SERS compound was too high a Raman spectrum could be observed, if the concentration was too low then no signal was seen at all. Studies showed that the optimal signal for SERS comes from 'hot spots' created between the AuNPs, this is also supported by the use of the 785 nm laser.[156] If the signal was achieved by single molecule SERS (single AuNPs), then the optimal SERS signal would be achieved by a laser at a shorter wavelength closer to the SPR absorption peak of the AuNPs.[157]

It was observed that there was a variation in the signal, in terms of reproducibility of the spectrum, of some SACs used, especially with the larger compounds, such as fluorescein isothiocyanate and rhodamine B isothiocyanate (data not shown). This may be attributed to either different positioning of the tag on the surface of the AuNP or a resonant effect.[158, 159] It may be possible through calculations to identify

what exactly the cause of this change is, but since the purpose of this work was to determine SACs with a strong and consistent SERS signal, this was not explored. There has been evidence of this type of anomalous banding in SERS spectra before, theories postulated by Sanchez-Cortes and Garcia-Ramos can explain these.[160]

After examining the intensity of the signals of the compounds listed in Chapter 2, it was found that although most gave an enhanced Raman signal, 2-quinolinethiol gave the largest enhancement and overall the most reproducible signal. Most of the other compounds, although used in the literature, were found not to be optimal for this system.

Figure 17 shows a comparison of the Raman spectrum of 2-quinolinethiol with the SERS spectrum of 2-quinolinethiol adsorbed to the AuNPs. It can be seen that there are shifts in the intensity of peaks in different regions of the spectrum. The variation of the spectrum, plus the marked reduction in concentration to 10^{-9} M illustrates that this is a SERS spectrum.[161]

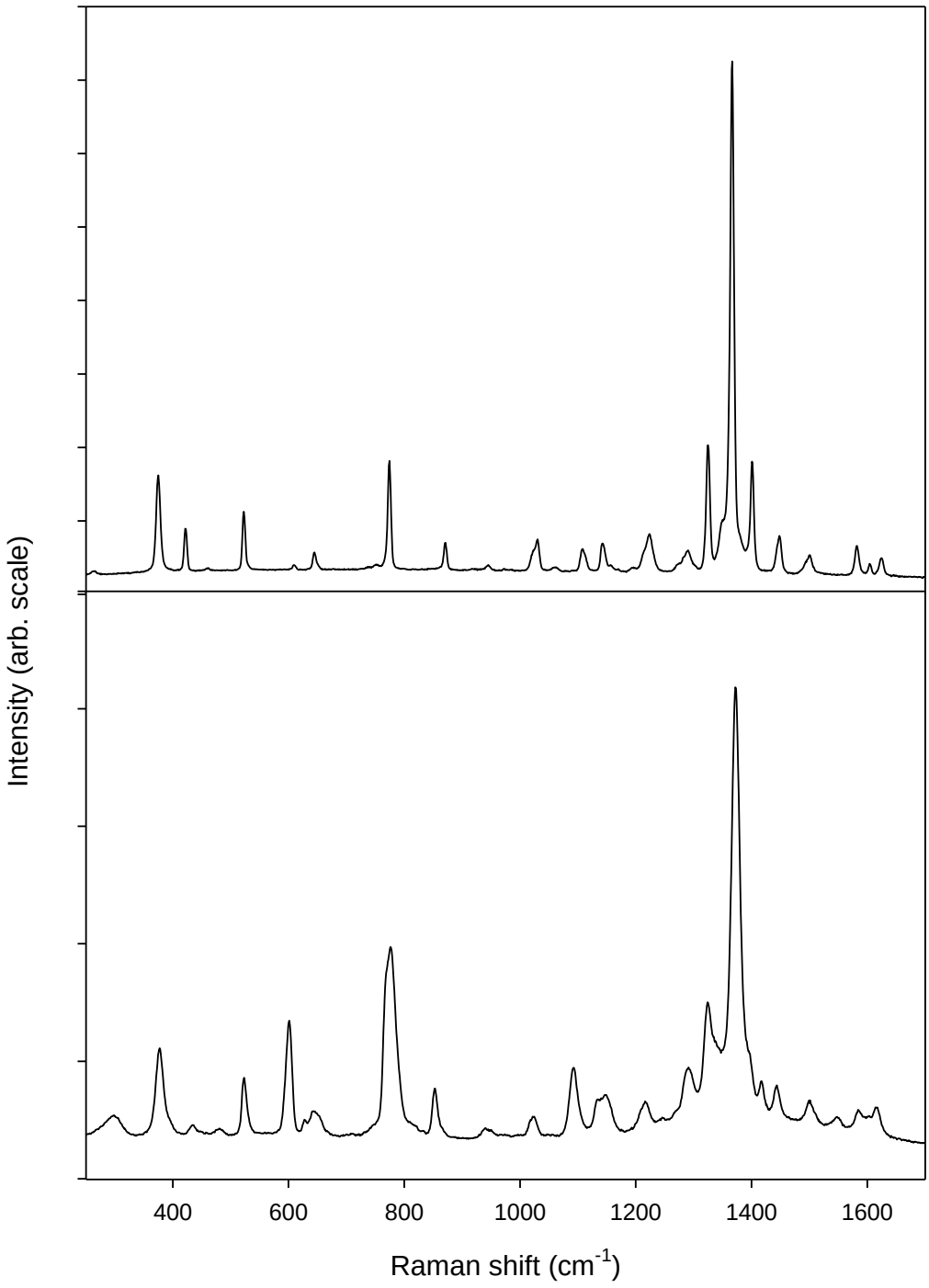

Figure 17 Raman spectrum of solid 2-quinolinethiol (top) with the SERS spectrum (bottom) of the analyte adsorbed to the AuNPs

This compound was selected for incorporation into the hybrid polymer AuNPs due to its strong SERS signal.

3.5. Summary

Initially both silver and AuNPs were synthesised following literature procedures using tri-sodium citrate as the reducing agent. The size of the silver was not as dependant on the amount of citrate added to the $AgNO_3$, as was seen with the Au. The shape of the AgNPs was found to be quite difficult to control. Although AgNPs gave a more intense SERS signal, the citrate reduced AuNPs formed more regular shapes and therefore gave a more visually consistent SERS signal with respect to peak ratios, broadness and intensity.

Once it was determined that the AuNPs were to be used, several different methods were tested to establish if there were any better techniques than the citrate reduction method to use for their preparation. Although the literature methods were followed with rigour, it was found that it was quite difficult or impossible to reproduce all methods in various ways.[162] Nanoparticles were sometimes produced, but not to the specifications stated in the methods followed. It was found that when the literature procedures were not able to be reproduced, the experiments producing particles larger than 150 nm when the literature stated a size that could be used for SERS i.e. 10 to 100 nm.[41, 162] These larger particles would not remain suspended in solution and are too large to use for SERS studies: they would aggregate. Otherwise they would aggregate during the synthetic procedure rendering the nanoparticles useless.

The optimal size of nanoparticles of approximately 40 nm was consistently achieved via the citrate method, by preparing each batch in 100 mL amounts based upon previous methods. It was seen that if the nanoparticles were much smaller than this it was more difficult to obtain a consistent SERS signal, rendering them useless for

our desired application. If the nanoparticles were much larger than 50 nm then they became too heavy to remain suspended for longer than a day or two and a precipitate formed. The nanoparticle size was able to be determined by using TEM, DLS and visible absorption. The surface plasmon resonance peak was shown to be around 525 nm, with the shift and broadness of this peak shown through TEM to relate to the shape and size distribution of particles in each batch. The particles that were used for these experiments have been found to have a shelf life of over 6 months in our laboratory. It was shown that particle sizes of 12-100 nm could be synthesised by using the citrate reduction method. It was found for this work using 30 μL of $HAuCl_4$ to 100 mL of Ultrapure (18 MΩ cm) yielded the best reproducibility batch to batch, with a shelf life of over 6 months. This also yielded the most consistent SERS signal over the batches. This method was found to produce significant aggregation if carried out with the literature procedure amount of 500 mL. The size and shape of the particles was also found to be more variable in the larger batch preparation. It is thought that the heat distribution through the larger volume affected the nucleation of the gold particles.

4. CHAPTER 4

DESIGNER POLYMERS FOR GOLD NANOPARTICLE ENCAPSULATION

4.1. Introduction

AuNPs need to be stabilised to minimise aggregation and to aid in surface functionalisation so that further binding can occur. Polymers are widely used for this purpose and to ensure that the AuNPs are stable for prolonged periods in suspension.[118, 122, 163, 164] Furthermore, polymers offer a convenient method to functionalise nanoparticles to allow the attachment of additional species, especially biomolecules.

The polymer needs to bind strongly to the gold surface, to stabilise the nanoparticles and have them remain as a suspension. Functionalisation for bioconjugation is also required, and therefore the polymer must contain a group which would easily allow the chemical attachment of additional molecules. As well as these constraints, it also requires a group that hinders non-specific binding so that only binding from the desired molecules is obtained. Together with these functionality requirements, the polymer must allow attachment of a SERS tag molecule to the AuNP surface so that a SERS signal can be obtained from the particle.

There are several approaches used for the attachment of polymers to gold surfaces or nanoparticles, which can be grouped into "grafting-to" or "grafting-from" methods. The grafting-to approach allows the pre-synthesised polymer to self assemble onto the gold, whilst the grafting-from approach involves firstly functionalizing the gold surface, usually by thiol capping, then synthesizing the polymer from the surface using a technique such as emulsion polymerisation. In this work we have chosen to

use the grafting-to approach to encapsulate the AuNPs as this allows us to synthesise and characterise a range of tailored polymers separately from the NPs. Since the polymer requires a particular structure and functionality, reversible addition, fragmentation chain transfer (RAFT) polymerisation is the synthetic method of choice.[125-127] RAFT is a living free radical polymerisation method where thiocarbonylthio compounds are used as chain transfer agents, shown in Figure 6. The technique can be used to polymerise monomers with a wide variety of functional groups, to yield polymers incorporating a thiocarbonylthio containing end-group, which can be reduced to a thiol. Depending on the monomer – RAFT agent combination, it is also possible to control the molecular weight of the resulting polymer. This control allows the production of polymers with low polydispersity indices (PDI). Furthermore, using RAFT polymerisation, a range of architectures are accessible, including block copolymers,[128, 130, 131, 165] star polymers[132-136] and branched polymers. [125, 137, 138, 166-170] In addition to this, the RAFT agent can also be tailored to provide an end group for the final polymer which contains a useful chemical group for further reaction, such as an acetylene group which can take part in 'click' reactions.

This chapter details the design and synthesis of polymers containing the most favourable functionality. The development of different polymers and RAFT agents has allowed the testing of the hybrid nanoparticles in aqueous and organic environments.

4.2. Polymer synthesis

The following materials were used in this work: Pyrrole was obtained from Sigma and was purified by distillation. Azobisisobutyronitrile (AIBN) was recrystallised from methanol before use. Sodium citrate, chloroauric acid, carbon disulfide (CS_2), toluene, dichloromethane (DCM), dimethylsulfoxide (DMSO), diethyl ether, *n*-hexane, α-methylstyrene, sodium hydride, *p*-toluenesulfonic acid, carbon tetrachloride, concentrated hydrochloric acid, concentrated nitric acid, fluorescein isothiocyanate, rhodamine B isothiocyanate, 2-quinolinethiol and 2-naphthalenethiol were obtained commercially and were used without further purification. Diethyleneglycol monomethyl ether methacrylate, *t*-butyl methacrylate, glycidyl methacrylate and styrene were passed through a basic alumina column to remove polymerisation inhibitor immediately prior to use. MilliQ water (18 MΩ cm) was used for AuNP synthesis. The polymers outlined in Table 1 were obtained from Dr Zul Merican (UQ) and were used as supplied for preliminary studies as part of this work.

Label	Polymer structure	M_n	M_w	PDI
Z1	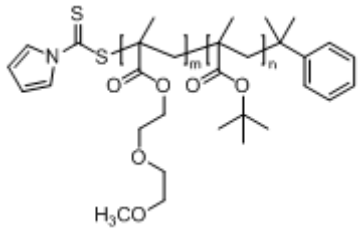	16000	23500	1.5
Z2	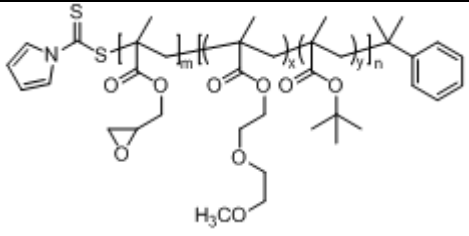	34300	60800	1.8

Z3	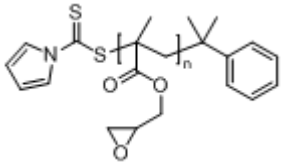	34100	81900	2.4
Z4	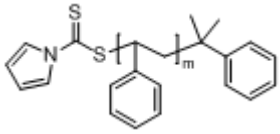	7900	8800	1.1
Z5	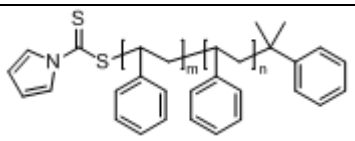	19200	24000	1.2

Table 1 Polymers supplied and characterised by Z. Merican. Values for number average molecular weight (M_n) and weight average molecular weight (M_w) and polydispersity index (PDI) were calculated from GPC calibrated using polystyrene

4.2.1. Synthesis of prop-2-ynyl 2-phenyl-2-(phenylcarbonothioylthio)acetate (acetylene RAFT)

Note: All reactions were conducted at room temperature unless otherwise stated.

For the later RAFT polymerisation work in this thesis, we required a RAFT agent with an acetylene end group, so that click chemistry could be used to attach additional molecules to the encapsulated AuNPs. A suitable RAFT agent was chosen (shown in Figure 18).

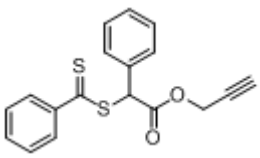

Figure 18 Structure of prop-2-ynyl 2-phenyl-2-(phenylcarbonothioylthio)acetate

This RAFT agent was synthesised starting from α-bromophenylacetic acid and propargyl alcohol. To ensure this reaction ran efficiently, the first (esterification) step involved preparing a salt, 4-(dimethylamino) pyridinium 4-toluene sulfonate (DPTS), that was used with this reaction.

4.2.2. Part I: esterification reaction (prop-2-ynyl 2-bromo-2-phenylacetate)

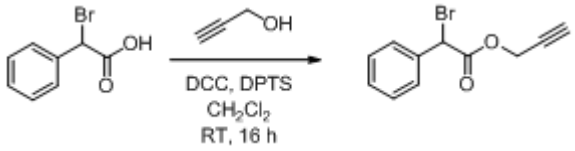

Figure 19 Reaction scheme of the first step of the procedure for making the acetylene RAFT

DPTS was prepared by mixing saturated THF solutions of 4-(dimethylamino) pyridine (DMAP) (1 equiv) and *p*-toluenesulfonic acid monohydrate (1 equiv). Upon mixing, a white precipitate was produced and isolated by vacuum filtration. The DPTS was then washed in a small amount of THF and dried under high vacuum and used without further purification. ^{1}H and ^{13}C NMR spectra were collected to show purity, and were found to match those reported in the literature.[171]

The esterification reaction was carried out by dissolving propargyl alcohol (1.21 g, 21.62 mmol, 1 equiv) in DCM (12.5 mL), then adding α-Bromophenylacetic acid (5.58 g, 25.93 mmol, 1.2 equiv) and DPTS (1.27 g, 4.32 mmol, and 0.2 equiv) to the solution. Dicyclohexylcarbodiimide (DCC) (6.69 g, 32.40 mmol, 1.5 equiv) was

dissolved in a separate flask in DCM (12.5 mL) and then transferred slowly into the reaction vessel. Upon addition of the DCC, the reaction mixture became cloudy, as DCC urea, the expected solid product, was produced as a precipitate. The reaction was stirred overnight at room temperature under Ar to ensure that the reaction went to completion, after which the reaction mixture was filtered to remove the precipitate. The DCM solvent was removed under vacuum leaving an oily yellow residue. This was purified by column chromatography (SiO_2, eluent *n*-hexane) to give the desired propargyl ester as a clear, colourless oil (1.97 g, 8.0 mmol, 37 %). Further product was isolated then analysed by ^{1}H and ^{13}C NMR and found to contain impurities and as such was not included in the product yield. The purified product was analysed using ^{1}H and ^{13}C NMR spectroscopy before completing the second part of the synthesis.

^{1}H NMR (400 MHz, $CDCl_3$) δ ppm 2.54 (1H, t, *J* = 2.3 Hz, C≡C*H*), 4.76 (1 H, dd, *J* = 2.3 and 15.3 Hz, HC*H*C≡CH), 4.82 (1 H, dd, *J* = 2.3 and 15.3 Hz, *H*CHC≡CH), 5.42 (1H, s, CBr*H*), 7.34-7.44 (3H, m, Ar*H*), 7.54-7.61 (2H, m, Ar*H*); ^{13}C NMR (100 MHz, $CDCl_3$) δ ppm 45.9 (alkyl C), 53.7 (alkyl C), 75.8 (*C*≡C), 76.5 (C≡*C*), 128.6 (Ar*C*), 128.8 (Ar*C*), 129.4 (Ar*C*), 135.1 (Ar*C*), 167.5 (C=O).

4.2.3. Part IIa - Synthesizing Grignard reagent PhMgBr

A Grignard reaction was used as an intermediate step to produce a dithioester, which is required for the second reaction step. A Grignard reagent was reacted with CS_2 for its preparation.

Pre-dried magnesium (0.561 g, 23.38 mmol, 3 equiv) and two small crystals of iodine were placed in a 50 mL oven-dried two-neck round-bottomed flask (RBF). The flask was then attached to a Schlenk manifold via a reflux condenser. The flask was flame-dried under high vacuum, resulting in a fine coating of iodine on the magnesium. The vessel was then placed under argon for the remainder of the reaction.

Et_2O (dried over Na wire) (10 mL) was added to the reaction vessel. Subsequently, bromobenzene (0.99 mL, 1.47 g 9.35 mmol, 1.2 equiv) was added dropwise ensuring the reaction occurred at a constant rate. When the addition was complete, the reaction was stirred until all activity subsided. The solution of Grignard reagent, PhMgBr was then transferred in a dry, gas-tight syringe to a clean oven-dried 3-neck RBF, attached to a reflux condenser. This was placed in a silicone oil bath for part IIb. All Grignard residues that remained in the preparation vessel were deactivated with isopropanol, as was all contaminated glassware.

4.2.4. Part IIb – synthesis of acetylene RAFT (prop-2-ynyl 2-phenyl-2-(phenylcarbonothioylthio)acetate) [R1]

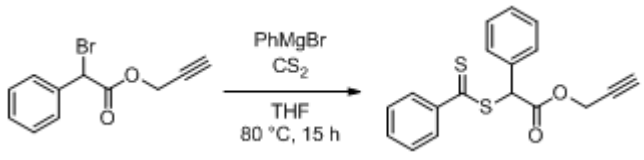

Figure 20 Reaction scheme of the second step of the procedure for making the acetylene RAFT

Dry THF (20 mL) was added to the RBF containing the PhMgBr solution. CS_2 was added drop wise to the RBF using a dry glass syringe and needle, and the solution became dark red-brown. After the addition was complete, the reaction was heated to 50 °C for 30 min to ensure full conversion. A solution of the propargyl ester (prop-2-ynyl 2-bromo-2-phenylacetate) (1.98 g, 7.79 mmol, 1 equiv) in dry THF (20 mL) was then added to the reaction vessel. The flask was covered with Al foil to minimise degradation of the compound by light and stirred at 80 °C for 15 hours. The THF was removed under high vacuum. TLC was used to determine that *n*-hexane was the appropriate eluent for removal of the impurities from the compound by column chromatography. It was seen that there were two dominant spots on the TLC. The slower fraction was found to be the desired compound and this was characterised by ^{1}H and ^{13}C NMR. This still showed a high level of impurities and the sample was further purified by additional column chromatography. Purification by elution with 50% $CHCl_3$/ 50% *n*-hexane gave the acetylene RAFT agent **R1** as a red oil (0.92 g, 2.81 mmol, 38 %). This was analysed using ^{1}H and ^{13}C NMR, and FTIR.

FT-IR ATR (cm^{-1}): 2920, 1691, 1588, 1463, 1443; ^{1}H NMR (400 MHz, $CDCl_3$) δ ppm 2.52 (1H, t, *J* = 2.3 Hz, C≡C*H*), 4.73 (1 H, dd, *J* = 2.3 and 15.3 Hz, HC*H*C≡CH), 4.84 (1 H, dd, *J* = 2.3 and 15.3 Hz, *H*CHC≡CH), 5.77 (1H, s, SC*H*Ph), 7.36-7.61 (8H, m, Ar*H*), 8.00-8.06 (2H, m, Ar*H*); ^{13}C NMR (100 MHz, $CDCl_3$) δ ppm 53.6 (alkyl C), 58.6 (alkyl C), 75.7 (*C*≡C), 76.9 (C≡*C*), 127.0 (Ar*C*), 128.5 (Ar*C*), 128.9 (Ar*C*), 129.1 (Ar*C*), 129.2 (Ar*C*), 132.6 (Ar*C*), 132.9 (Ar*C*), 143.8 (Ar*C*), 168.2 (C=O), 225.7 (C=S).

Figure 21 shows the ^{1}H NMR for the acetylene RAFT agent after the second chromatography column. The shift of the H at ~5.77 shows the addition at the bromo site, this shift is consistent with the desired compound. There are now 10 aromatic H's rather than 5 which shows the addition of the second benzyl ring and shows the dithioester and ester shifts.

4.2.1. Synthetic Procedures

For polymers shown in Table 1, which were prepared at UQ, the preparation procedure is detailed in Merican *et al.*.[172] The PEGMA polymers in Table 2 and Table 3 were synthesised by RAFT polymerisation as follows: RAFT agent R1 was weighed and set aside. The monomer (poly(ethyleneglycol)methacrylate (M_n=475) was weighed into a Schlenk flask, then solvent was added. AIBN was added to the flask, along with the RAFT agent and a stirring bar. The mixture was purged under argon for approximately 10 min to remove any oxygen present. The argon line was removed after the flask was sealed. The flask was then placed in an oil bath at 70 °C for 15 h. Afterwards, crude samples were taken from the mixture for NMR and GPC analysis to ascertain whether the polymerisation gave the desired product. Once this was confirmed, the polymer was dissolved in a small amount of DCM and purified by precipitation by adding it dropwise to cold diethyl ether. The ether was then removed by decantation to give the polymer as a pink gum. The glassware was rinsed with a small amount of DCM, dissolving the polymer and the resulting solution was placed into a small round bottom flask. The DCM was removed under reduced pressure. NMR and GPC analysis of the now purified polymer were undertaken to confirm the removal of the starting materials. The synthesis was

modified from the methods reported by Schilli *et al*.,[173] and Barner-Kowollik *et al*..[174]

The acetylene RAFT agent **R1** was used to synthesise a series of homopolymers, random copolymers and block copolymers, which are listed in Table 2; most of this work was completed in Professor Craig Hawker's laboratory at the Materials Research Laboratory, University of California Santa Barbara (UCSB). These polymers, with a range of pendant groups, were selected to determine what effects variations in polymer structure had on the self assembly of the hybrid nanoparticles. During this visit to UCSB several polymers were synthesised. Structures are shown in Table 2, with the RAFT agent used for the synthesis of **P4**, **P5** and **P6** was not synthesised by the author. These polymers (i.e. P4, P5 and P6) were not used in further work as after initial studies were conducted it was found that the binding site for the bioattachment was difficult to functionalise.

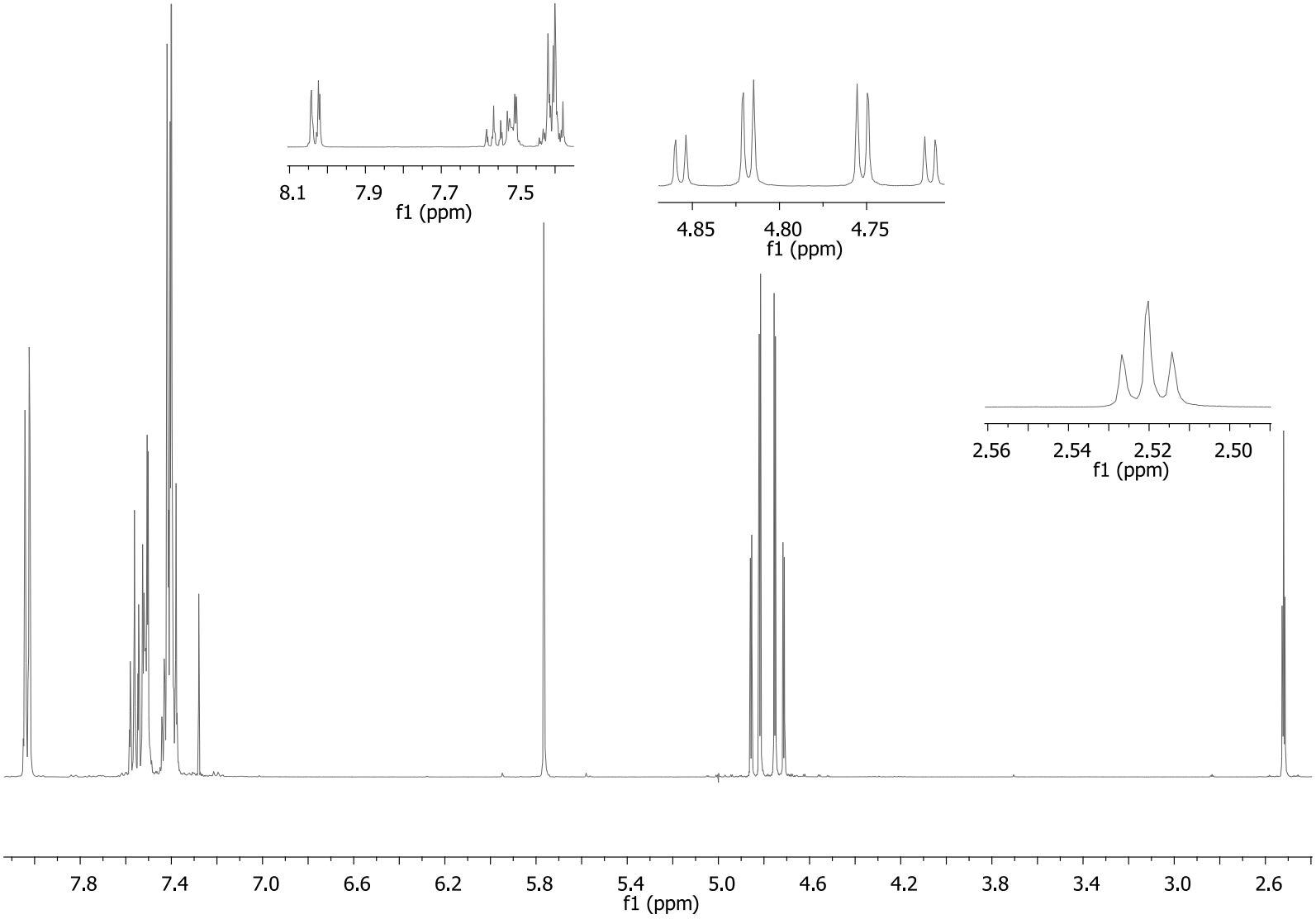

Figure 21 ^{1}H NMR of RAFT agent R1

Label	Polymer structure
P1	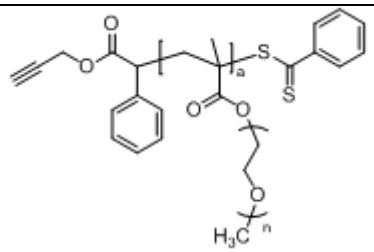
P2	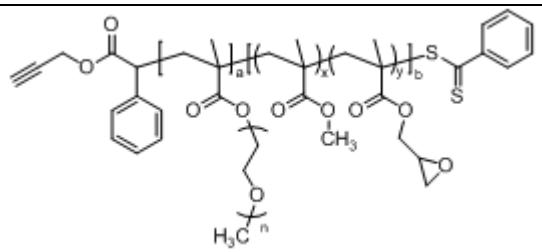
P3	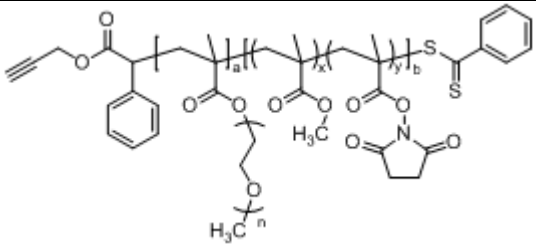
P4	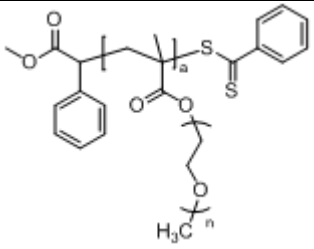
P5	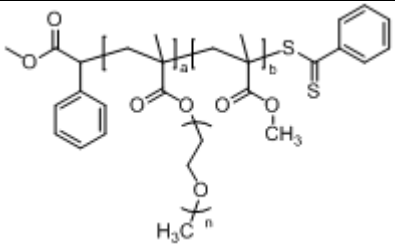
P6	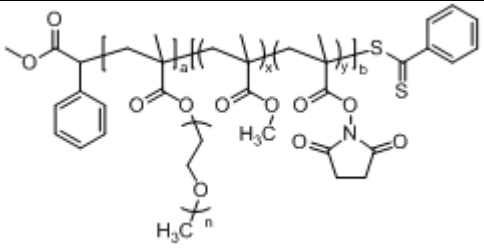

Table 2 Structures of polymers synthesised

4.2.2. Rationale for polymer structure

The aim of this work was to produce a polymer that would result in a stable encapsulation for an AuNP and be able to be further functionalised with a biomolecule with no non-specific binding. The synthesis and application of the first RAFT agent and polymer (see Table 1) has been detailed in Merican *et al.*.[172] The polymer used in this section of work contained the following: a RAFT agent with a dithiocarbamate, and a block copolymer with *tert*-butyl acrylate (TBA), methyl methacrylate (MMA) and glycidyl methacrylate (GMA) chains, the structure of which can be seen in Figure 22. The RAFT agent was chosen so that it would attach readily to the AuNP. The polymer chain functionalities bring different properties to the diblock copolymer. For example, the MMA moiety is used to ensure that non-specific binding does not occur and is also important for biocompatibility. The TBA moiety was incorporated to be a potential attachment site for the antigen or protein, while the GMA moiety was incorporated for its crosslinking capabilities, so that the polymer could be stabilised once it had encapsulated the nanoparticle. The ring opening of the GMA and the hydrolysis of the TBA were proposed to be achieved using TFA. This was found to be too harsh a process and although the polymer could be phase transferred and the AuNPs stabilised in organic solvent, the addition of the TFA caused a gel like polymer, possibly caused by ring opening of the GMA moiety. This rendered the polymer unusable as there was no longer a stable suspension. This is explained in more detail in Chapter 5.

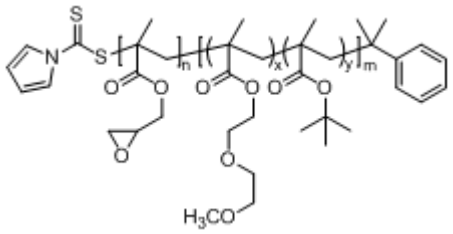

Figure 22 The first generation of polymers explored in this work with GMA, MMA and TBA polymer groups

Since this first series of polymers was unsuccessful in forming a useful encapsulation of the AuNPs, it was decided that the next generation of polymers should include either a polymer chain that could be functionalised with an acetylene or azide group, or have a RAFT end group incorporating an acetylene group, so that 'click' chemistry could be used to bind the antigen or protein to the polymer. Azide-alkyne 'click' chemistry was expected to be a relatively simple approach for the functionalisation step. The term 'click' chemistry is given due to a reaction's simplicity, giving typically high yields and having wide scope of application.[175] The first diblock copolymer explored used PEG, MMA then either a n-hydroxysuccinimide (NHS) or trimethylsilylacetylene functionality, as shown in Figure 23. The proposed approach for the NHS-containing polymers was to use an amino compound to turn the NHS into an azide, whereas tetrabutylammonium fluoride (TBAF) would be added to the trimethylsilylacetylene-based polymer to furnish the acetylene. Both of the above mentioned polymers were unable to be synthesised so another approach was explored.

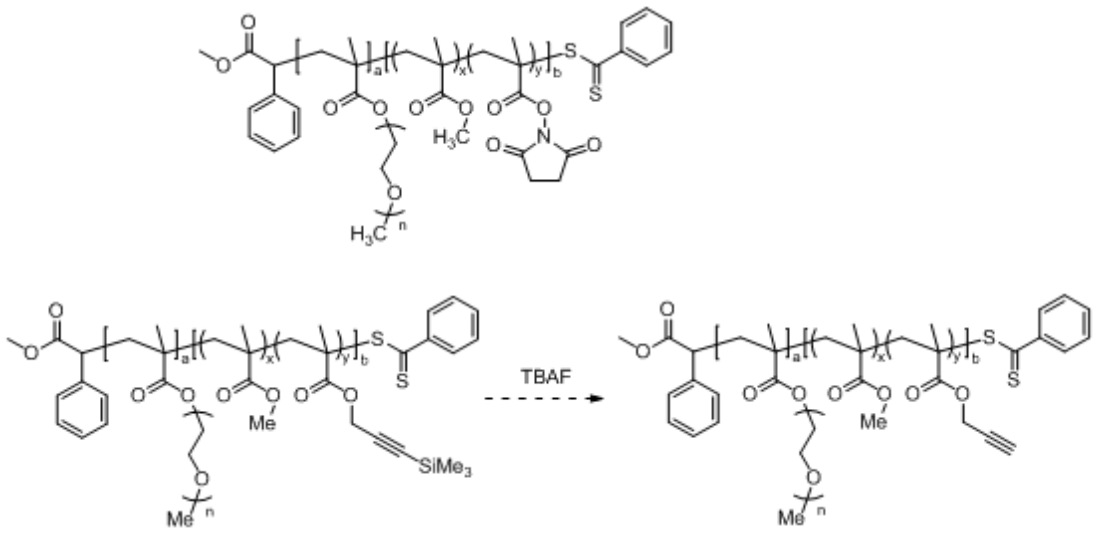

Figure 23 The initial exploration of incorporating groups that could incorporate an acetylene group as part of a polymer chain

A RAFT agent with an acetylene end group was synthesised and used for the remainder of the work described in this thesis. It was thought that the alkynyl end group would provide enough binding sites, one per polymer molecule, to attach the antigen or protein to the polymer. This approach allowed polymer groups with various architectures to be explored, including diblock, random copolymers and homopolymers, to elucidate which system was best for this work. Chapter 5 details some of the binding to AuNP work conducted in this area. For most of this work **Q1** from Table 3 below has been used to illustrate the significant points of the approach.

Table 3 Polymers synthesised using an acetylene RAFT agent (data from GPC relative to polystyrene)

Label	Polymer structure	M_n	M_w	PDI
Q1	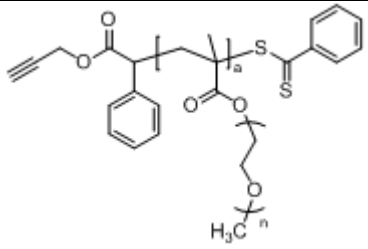	7800	8600	1.10
Q2	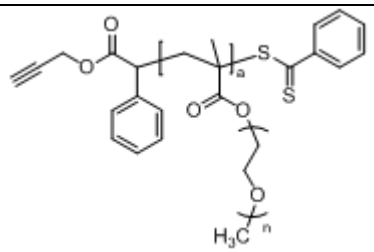	8300	9300	1.11
Q3	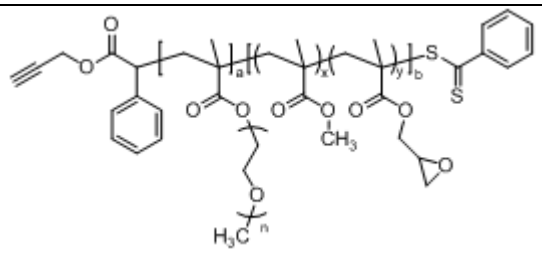	51,800	59,500	1.15
Q4	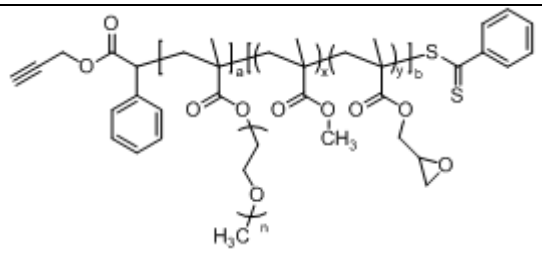	51,500	60,500	1.17
Q5	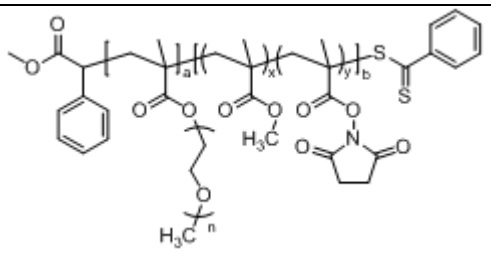	96,400	162,500	1.68

Q6	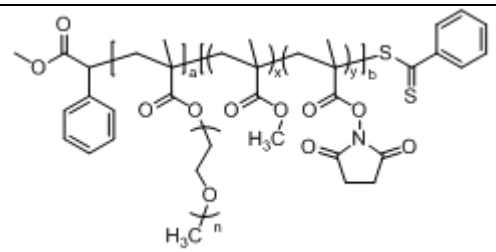	24,300	30,300	1.25

4.3. Summary

The optimum approach to the attachment of antigen molecules to the encapsulated AuNPs was determined to be via 'click' chemistry. To this end a novel RAFT agent containing an acetylene group was successfully synthesised and characterised. This RAFT agent was used to prepare a suite of polymers having various structures, by the use of copolymer synthesis.

These polymers were designed both to encapsulate the AuNP and to provide an anchor point for the attachment of the antibody/antigen. Through change in design in the polymers it was decided that an acetylene end-group RAFT agent was best for this work. It was found that the polymerisations were successful with benzene as solvent except for **P3** which was successful when DMF was used. The PDI of the azide PEG and the block copolymer were found to be 1.11 and 1.15 respectively in THF as compared to a polystyrene standard. Determination of which polymers were best suited for use in encapsulation of AuNPs is discussed in further detail in Chapter 5.

5. CHAPTER 5

COATED NANOPARTICLES FOR BIOASSAYS

5.1. Introduction

Since AuNPs do not possess robust physicochemical properties, researchers have investigated ways of improving their stability. The addition of a stabilising agent has been successful to ensure that precipitation of the AuNPs does not occur.[176] Further to this, it has been shown that thiol groups provide excellent binding to AuNPs, which is essentially covalent.[177] Sulfur-containing molecules have an affinity with Au and have been studied in-depth both experimentally and theoretically.[178] Dithioester binding is particularly relevant to this branch of polymer science as it is a component of the RAFT end-group used in living free radical polymerisation.[108] RAFT polymers with dithioester end groups have been shown to bind to AuNPs.[120] Polymer encapsulation of the AuNPs can be used in a range of applications including bioassays and *in-vivo* detection of tumour cells.[111, 179] However, evidence for the mode of binding is limited to techniques such as XPS of small molecules or monitoring the disappearance of the S-H bond.[180] The binding of the RAFT polymer to the AuNPs has not been directly observed for this type of system, only indirectly using techniques such as a solubility change of AuNPs[111] as well as size techniques such as dynamic light scattering.[181]

Whilst the signal of a SERS tag can be observed inside a hybrid system,[163] SERS may also be a potential way to study the interaction of polymers with AuNPs. In this chapter the attachment and stability of the different polymers, prepared in Chapter 4 to AuNPs are examined. The SERS signal achieved from small polymers (M_n<10,000) is also presented.

5.2. Experimental

AuNP synthesis is discussed in Chapter 3. Detailed RAFT agent synthesis and polymerisation is discussed in Chapter 4.

5.2.1. Hybrids (polymer stabilised AuNPs)

Initially, the polymer stabilised AuNPs, or hybrids, were generated by drop-wise addition of the polymer dissolved in tetrahydrofuran (THF) (2 mg/mL, 3mL) to citrate stabilised AuNPs dispersed in water (10 mL), which yielded a red-purple precipitate. The precipitate could be resuspended in solvents in which the polymer was soluble such as chloroform and acetonitrile. For water soluble polymers, aqueous solutions of the polymer were added to the AuNPs in similar concentrations but no precipitate was produced.

5.3. Characterisation of hybrid gold/polymer nanoparticles

Hybrids were prepared using a range of AuNP to polymer ratios. The SERS signal of the SACs rhodamine B isothiocyanate, 2-quinolinethiol, 2-naphthalenethiol was collected from either a solution or solid state. The SACs were prepared by making a 2 mM solution, of which 5 μL was added to 1 mL of AuNPs. The solution samples were placed in 200 μL low fluorescence glass vessels and left uncovered. The laser was then focussed below the meniscus of the solution and the Raman spectrum

collected. Solid state measurements were taken after drying the solution onto a low fluorescence glass slide.

5.4. AuNP Synthesis and Characterisation

Citrate-stabilised AuNPs that were dispersed in water, were synthesised using the citrate method, as discussed in Chapter 3.[144, 145]

Figure 24 shows a typical TEM micrograph of the product AuNPs which had an average particle diameter of 40 ± 10 nm. As discussed in Chapter 3, it was found that the size of the AuNPs was dependant on the amount of citrate added during synthesis, which has been previously reported by others. It should be noted that the AuNPs aggregated on the carbon coated TEM grids during sample preparation.

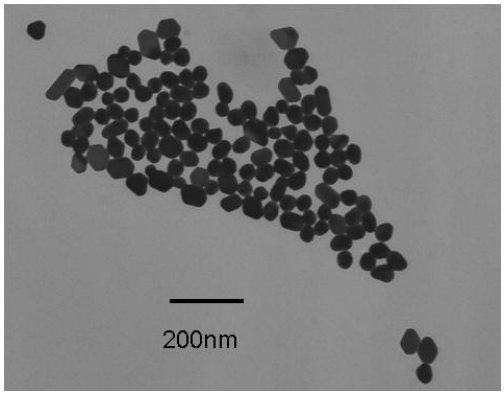

Figure 24 A typical TEM micrograph of citrate stabilised AuNPs that have been cast from an aqueous dispersion onto a carbon-celloidin coated TEM grid.

As detailed in Chapter 3, AuNPs are known to exhibit a surface plasmon resonance (SPR) in the visible region, which is caused by incoming electromagnetic radiation inducing the formation of a dipole in the nanoparticle. This restorative force, which

compensates for the dipole results in electron oscillations that correspond to a specific frequency of light. Mie theory has been applied to model this phenomenon for dilute solutions of spherical AuNPs and nanorods.[146]

5.5. Polymer Synthesis and Characterisation

Polymers synthesised by the RAFT process will have dithioester or dithiocarbamate end-groups depending on the nature of the RAFT agent.[125-127] A RAFT agent synthesised by Dr Zul Merican at UQ was chosen because it contained a heterocyclic group, rather than for its ability to produce polymers with narrow molecular weight distributions. The work in this chapter with organic solvent phase transfer (resuspension) was conducted with polymers detailed in Table 1. This study was to generate polymers that have end-groups that strongly interact with gold surfaces. It is known that sulphur containing groups tend to exhibit a high affinity for gold surfaces.

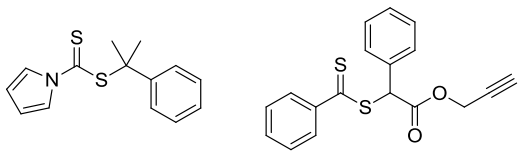

Figure 25 Structure of RAFT agent synthesised by Dr Zul Merican used in the initial stages of this work (left) and RAFT agent R1 used to complete the proof of concept

RAFT agent **R1** was used to synthesise a series of homopolymers, random copolymers and block copolymers, which are listed in Table 2 in Chapter 4. These polymers were synthesised with a range of pendant groups in order to determine if the polymer pendant group had any effect on the self assembly process. This second

group of polymers were either completely or partially water soluble. One of these polymers, **P1,** was used to complete the work in Chapter 6.

5.6. Self Assembly and Characterisation of Polymer Gold Hybrids

Self assembly of the polymer stabilised AuNPs was achieved by the drop-wise addition of a solution of RAFT polymer in THF to a solution of citrate stabilised AuNPs dispersed in water. Figure 27 (a) is a photograph of a solution of the citrate stabilised AuNPs dispersed in water. After addition of **P2** to this solution, a reddish coloured precipitate was observed to form, and the aqueous phase became essentially colourless (Figure 27 (b)). The colour of the precipitate indicated that the AuNPs had co-precipitated with the polymer, which was not soluble in water. The polymer stabilised AuNPs could either be isolated by centrifugation or phase transferred to an organic solvent in which the polymer was soluble. For example, when chloroform was added, a two phase system was generated where the bottom chloroform layer was coloured red. The colour of the chloroform layer indicated that AuNPs had become dispersed in the organic layer. The fact that the AuNPs were now soluble in an organic solvent suggests that the polymer was coating and stabilizing the AuNPs. An example of this is shown in the photograph presented in Figure 27 (c), where chloroform has been added to the precipitate of AuNPs and **P2**. Similar behaviour was observed for all the RAFT polymers, **P1-P5**, listed in Table 1, Chapter 4. These polymers covered a range of molecular weights and pendant functional groups. This indicated that the self assembly process was independent of the nature of the pendant side chains of the polymer except where these groups control solubility. As controls,

solutions of either polystyrene or poly(methyl methacrylate), synthesised by standard free radical polymerisation, so that they did not contain a RAFT end-group, were added to the citrate stabilised AuNPs. Formation of a co-precipitate was not observed. This indicated that the self assembly of the RAFT polymers on the AuNPs was facilitated by the interaction of the sulphur-containing RAFT end-groups with the AuNP surface. The polymer stabilised AuNPs formed using **P2** were selected for more detailed characterisation of the hybrid structure.

Figure 26 shows the visible spectra of citrate stabilised AuNPs dispersed in water and chloroform. Figure The AuNPs in water exhibited an (SPR) maximum at approximately 529 nm, which according to calculations using Mie theory is typical of spherical AuNPs of approximately 40 nm in diameter.[155]

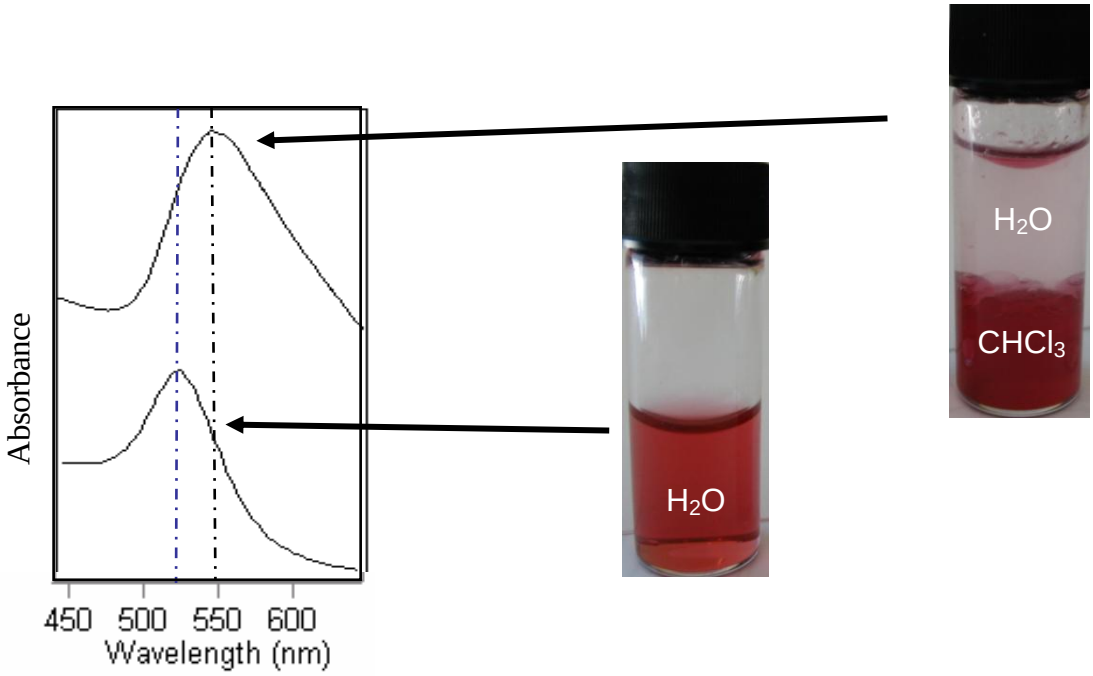

Figure 26 Visible spectra of (bottom) citrate stabilised AuNPs dispersed in water and (top) polymer stabilised AuNPs dispersed in chloroform after the precipitation and phase transfer of the AuNPs once polymer binding was complete.

The visible absorption peaks were at 534 nm in the spectrum of PEGMA **P1** without AuNPs, and an SPR peak of 535 nm were found in the spectrum for PEGMA P1 AuNP and SAC and no aggregation peak around 650 nm. When the SAC is present at the same time as the polymer there is an aggregation as the peaks appear now at 536 nm with a shoulder at 645 nm (i.e. peak no longer Gaussian). The SPR peak position for the AuNPs is 529 nm indicating a particle size distribution in the range 15-80 nm, with an average of approximately 40 nm.

Mie theory predicts that if the refractive index of the medium surrounding the AuNPs increases then a red shift of the SPR band is expected.[88] The visible absorption spectrum in Figure 26 (top) is of the polymer-stabilised AuNPs dispersed in chloroform. The SPR band at 539 nm exhibited a red shift of approximately 10 nm relative to the SPR band in the absorption spectrum of citrate stabilised AuNPs dispersed in water. Mie theory predicts that a red shift of 9.5 nm would occur in the SPR band when the AuNPs are transferred from water (refractive index (n) = 1.33) to chloroform (n = 1.446). The refractive index of the polymer is similar to that of chloroform, so it is not expected that an additional shift (greater than experimental error) will be observed due to the presence of swollen polymer at the surface of the AuNPs. Nonetheless, the observation of a red shift consistent with Mie theory suggests that the polymer coated AuNPs were transferred to the chloroform layer.

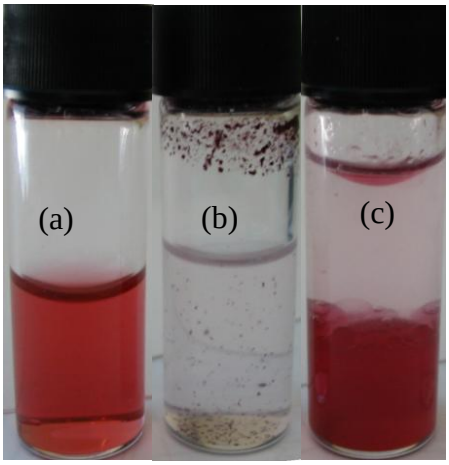

Figure 27 (a) As synthesised AuNPs, (b) after precipitation and coating of AuNPs by addition of a THF solution of polymer P2 with a RAFT end-group, and (c) after resuspension of polymer stabilised AuNPs in chloroform.

Layers of polymer-stabilised AuNPs were cast from chloroform suspension onto a carbon-celloidin coated TEM grid. A typical TEM micrograph of such a layer of sample is presented in Figure 28(b) that the micrograph shows that the polymer stabilised AuNPs form semi-regular arrays of AuNPs during the casting process. The separation of the AuNP cores ranges from 30-70 nm. The polymer cannot be directly observed in the TEM micrograph, due to the lack of contrast between the carbon coated grid and the polymer as well as the relatively large contrast compared to the AuNP. However, it can be inferred that the polymer causes the AuNPs to take up such an arrangement, compared to the aggregated citrate stabilised particles observed in Figure 28(a) Ohno *et al.*[119] observed similar arrangements for films of polymer stabilised AuNPs prepared in a Langmuir trough.

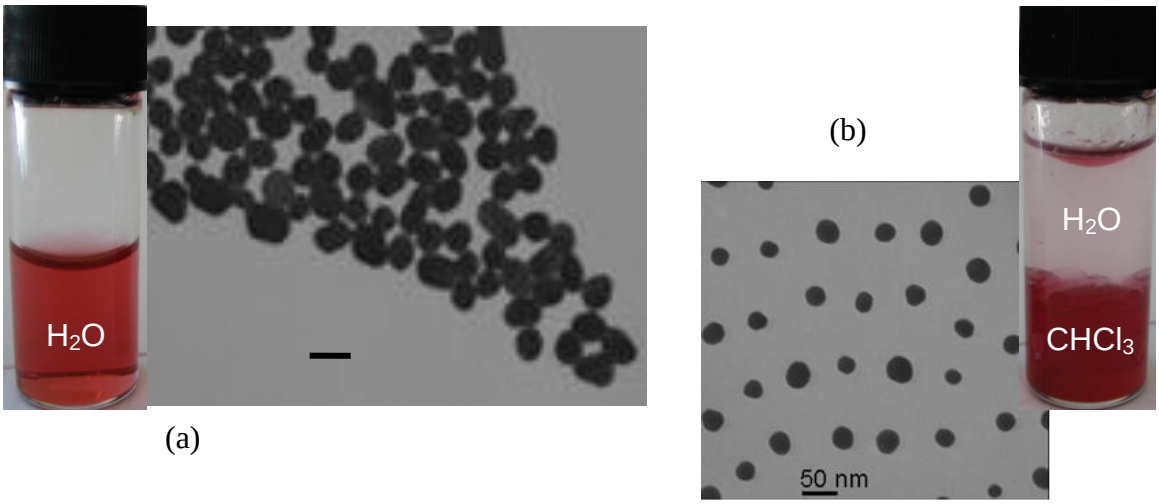

Figure 28 TEM micrographs of (a) citrate-stabilised AuNPs and of (b) polymer stabilised AuNPs. The AuNPs have been cast onto a carbon / celloidin coated TEM grid, scale bar is 50nm of both images.

However, in our case it is likely that the separation observed is accentuated by the presence of a small amount of 'free' or excess polymer that is not bound to the nanoparticles. Interestingly, when the AuNPs were bound to the water soluble PEGMA **P1,** the polymer could be easily observed in the TEM. This was enhanced by using a negative stain (uranyl acetate). The resultant image can be seen in Figure 29.

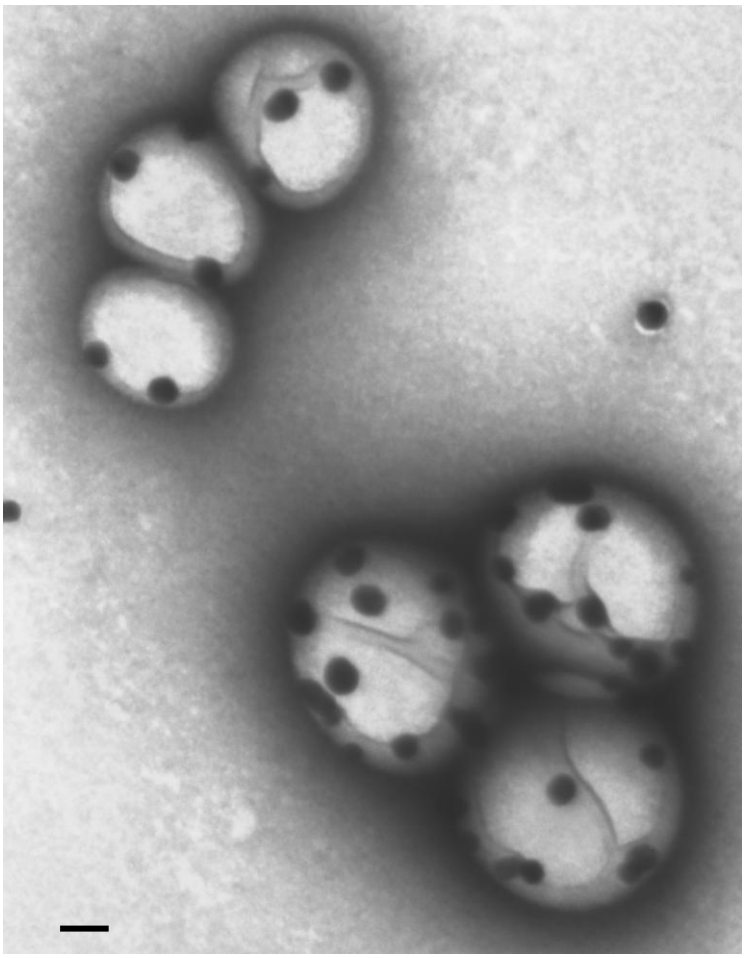

Figure 29 AuNPs coated with PEGMA P1, showing the formation of inverse micelles (vescicles). The scale bar is 50 nm.

5.7. Thermogravimetric analysis (TGA)

To determine the gold content of the polymer-stabilised AuNPs, a sample of AuNPs stabilised with **P2** was subjected to heating controlled by a temperature program to degrade the stabilizing polymer. Following the degradation cycle, 89 ± 1% of the total mass was found to remain. Based on a polymer molecular weight of 34 kDa and an AuNP radius of 22.5 nm for this sample, polymer coverage of 0.3 chains nm^{-2} was calculated, which is an area of 3.2 nm^2 per chain. This result indicates that the graft has brush-like characteristics, but the chains are much less dense than reported

for polymer-stabilised AuNPs prepared by other methods. Densities in the order of 3-4 chains nm^{-2} have been reported.[182, 183]

5.8. Dynamic Light Scattering (DLS)

DLS measurements were taken for a batch of AuNPs before and after stabilization with **P2**. Analysis of the DLS results indicated that the citrate-stabilised AuNPs had a diameter of 26 ± 10 nm, while the same AuNPs stabilised with **P2** had an average diameter of 110 ± 20 nm in chloroform. The increase in size indicates that the AuNPs were stabilised by polymer. The discrepancy between the DLS results and those from TEM of over 10 nm, is due to DLS being inherently biased towards larger particles in particle distributions. Valentini *et al.*.[184] observed similar discrepancies for DLS results for polypropylene sulfide nanoparticles.

5.9. Encoding of Polymer Stabilised AuNPs with SERS Tags

To demonstrate that the properties of AuNPs can be preserved after their stabilization with polymers, the ability to encode the polymer stabilised AuNPs (P-AuNPs) with SERS tags was tested. To this end a variety of molecules known to give SERS signals in the presence of AuNPs were added to **P2**. As a comparison the same SERS tags were added to solutions of citrate-stabilised AuNPs dispersed in water. The SERS tags that were utilised were 2-naphthalenethiol, 2-quinolinethiol, and rhodamine B isothiocyanate (RITC). As well as their ability to produce a SERS signal these tags were also chosen because they had sulfur containing functional

groups that allow the SERS tags to self assemble to the surface of the AuNPs. SERS spectra of these samples were collected and the results for the citrate stabilised AuNPs are shown in Figure 30 and those for the polymer stabilised AuNPs are shown in Figure 31. The major bands that can be observed in Figure 30 for the reporter tags on citrate stabilised AuNPs are also observed in Figure 31 for the polymer stabilised AuNPs. However, minor differences in the spectra were observed, including additional weak bands and changes in band shape.

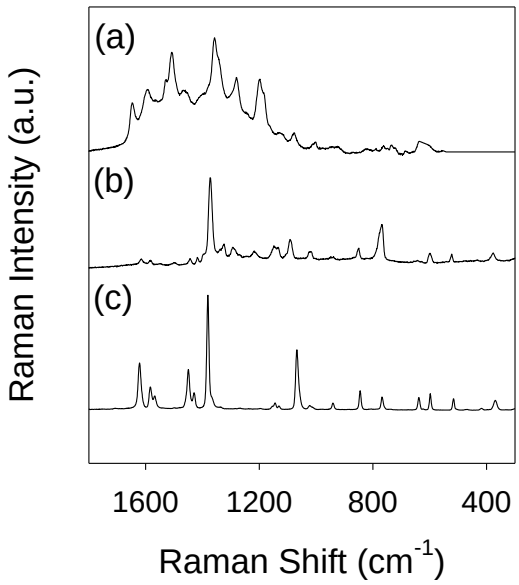

Figure 30 SERS spectra of citrate stabilised AuNPs that have been labelled with (a) rhodamine B isothiocyanate (b) 2-quinolinethiol, (c) 2-naphthalenethiol.

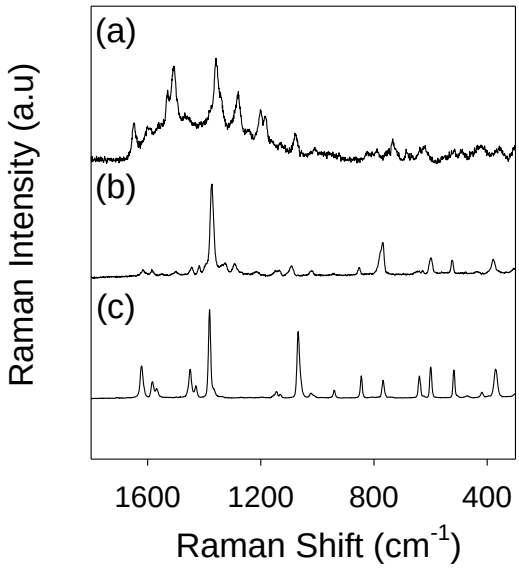

Figure 31 SERS spectra of polymer stabilised AuNPs that have been labelled with (a) rhodamine B isothiocyanate (b) 2-quinolinethiol, (c) 2-naphthalenethiol.

SERS spectra are by definition surface sensitive, and the fact that SERS spectra were observed for the polymer stabilised AuNPs indicates that the presence of the polymer chains at the surface of the gold does not prevent SERS tags from self assembling at the gold surface. This is not unexpected because the method of grafting used in this work utilises the 'grafting to' approach, and as discussed above the graft density was demonstrated to be brush-like, but sparse compared to other literature reports.[182, 183] This less dense packing of polymer chains compared to a 'grafting from' approach has allowed sufficient space for the SERS tags to reach the AuNP and bind to the surface, or even allowed space for a tag to displace a polymer chain. However, the fact that a more defined SERS signal was observed for the smaller tags, such as 2-naphthalenethiol and 2-quinolinethiol compared to RITC indicates that there may be some steric effects that inhibit the self assembly of larger tags at the gold surface. It was also observed that small additional bands appeared in

spectra of the polymer stabilised AuNPs encoded with the RITC tag. A possible explanation for this, given by Aroca *et al*.[2] is that the presence of the polymer may distort the conformation of the larger RITC molecules at the surface to the extent that a change in the SERS spectrum occurs. The fact that a change in the SERS spectrum occurs for polymer stabilised AuNPs does not detract from the usefulness of an encoder molecule, provided that the spectrum is consistent and sufficiently intense to be easily measured.

5.10. Analysis of SERS signal from stabilised AuNPs

To demonstrate the reproducibility of the SERS data a series of tests was conducted with the same SERS tag. Quinolinethiol was chosen as the appropriate SERS tag due to its intense yet simple SERS spectrum as shown in Figure 30 and Figure 31. The procedure detailed in Chapter 2 was used to create the labelled hybrid nanoparticles. These particles were then dried onto a low fluorescence glass slide and imaged accordingly.

The SERS of the samples were measured at 633 and 780 nm to examine the difference in relative intensities of the peaks. The changes in the spectra are probably a result of the surface plasmon of the AuNP enhancing the bands at different wavelengths for different lasers and suggest that this is not a molecular resonance effect. Figure 32 below shows the 633 nm and 785 nm spectra for the solid state and aqueous samples. The peak ratios in these spectra are similar.

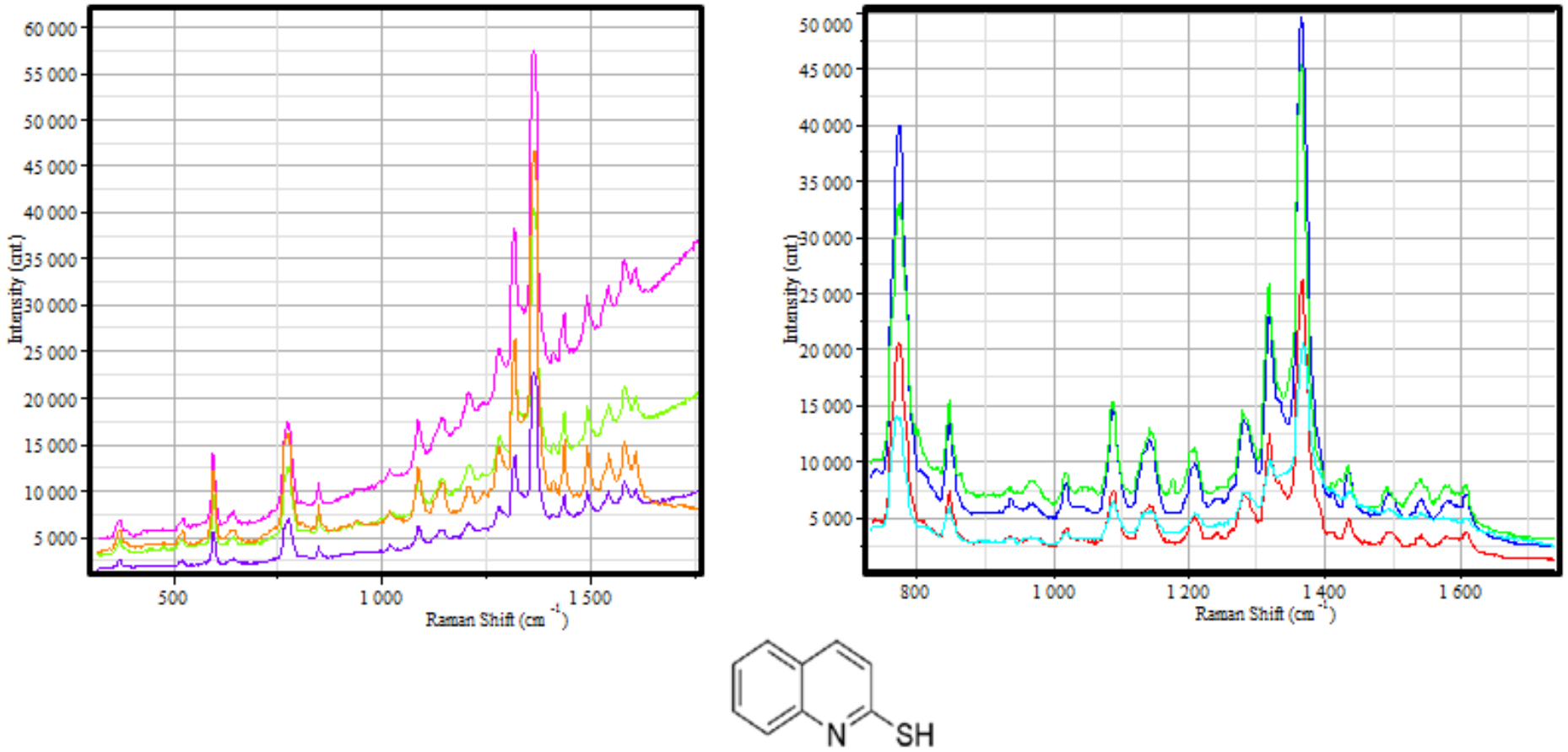

Figure 32 Experiments conducted on a Horiba µRaman to check signal intensity over a range of locations on dried encapsulated AuNPs with quinolinethiol used as the SERS tag. These samples were taken over 32 scans without baseline correction.

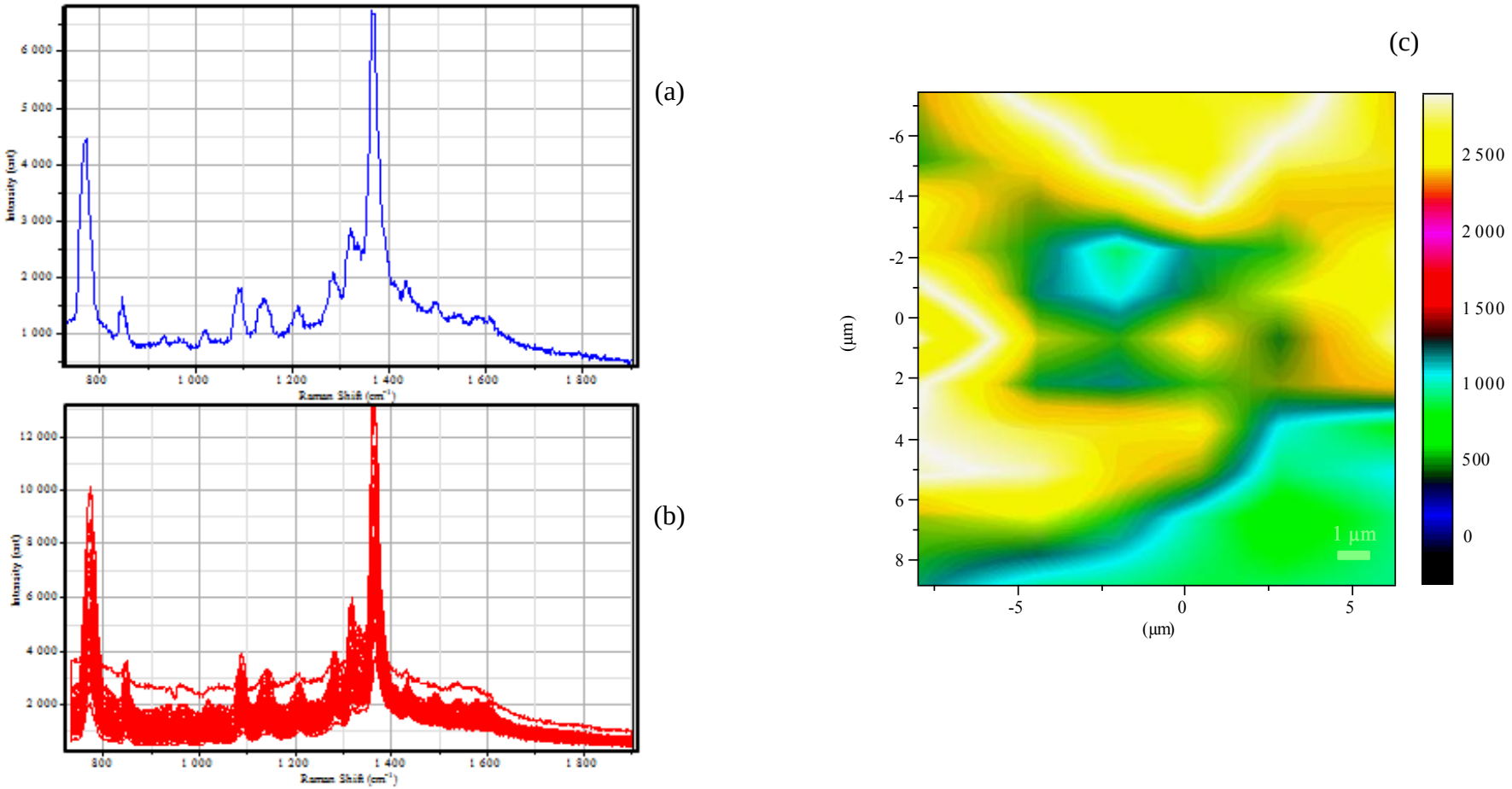

Figure 33 Raman spectra of Q-P_2-AuNPs; (a) shows the single SERS spectrum from one point, (b) is an overlay of the spectral data from the area scanned and (c) is the mapped area, showing the variation in intensity of the 1386 cm^{-1} peak

One complication of using smaller molecular weight polymers (M_n<10,000) was that the polymer exhibited a SERS signal from the RAFT agent, due to the binding of the dithio group to the gold nanoparticle. As the molecular weight of the polymer decreases the number of molecules which can attach to an NP increases and hence the number of RAFT end groups at the surface increases. When the concentration is sufficient these RAFT end groups will generate a SERS spectrum. This can be seen in Figure 34 by representation of the SERS of the RAFT agent R1 in polymer P1 and SERS of the 2-quinolinethiol as compared with the SERS of the hybrid nanoparticle. For the use of these nanoparticles as part of a bioassay the polymer signal could be removed by spectral subtraction, or the use of higher molecular weight polymer.

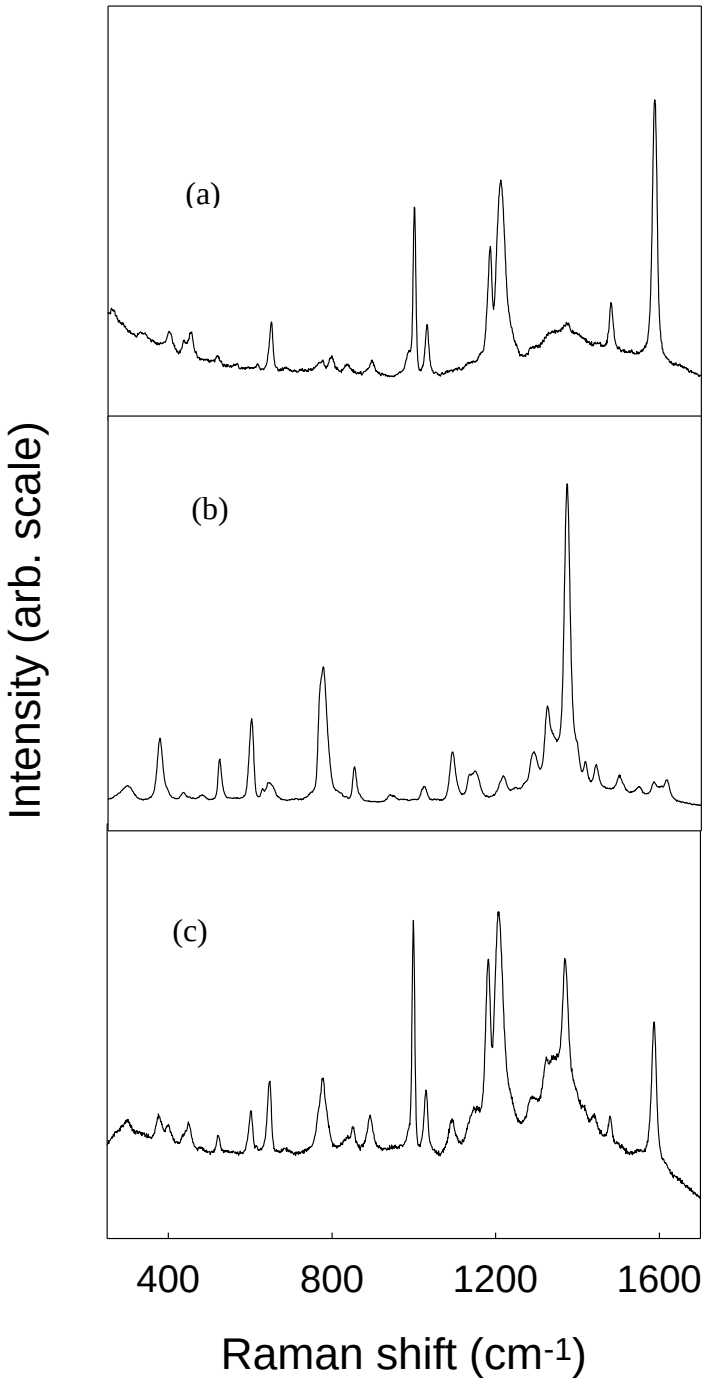

Figure 34 Raman spectra of (a) RAFT agent R1 in polymer P1, (b) 2-quinolinethiol compared to (c) the combination of both on the stabilised AuNPs

5.11. Investigation of the stability of hybrid polymer AuNPs

Since aggregation of the AuNPs occurred so readily, the polymer encapsulated AuNPs appeared to be stable but to ensure this was correct, several strategies were employed to try and destabilise the P-AuNPs. The techniques used included addition of isopropanol to the water as well as varying amounts and the size of the polymer to be added. It was thought that AuNPs may not have been stable at elevated temperatures (~80 °C). The hybrid AuNPs were suspended in DMSO and then heated to 100 °C for approximately 16 h. After this period the solution was analysed by visible absorption for any aggregation effects. No observed signs of aggregation were noted, such as colour change or a SPR peak above 600 nm. Another method for examining stability examined was the addition of known destabilising agents. Salt, ethanol and acid were each added dropwise to separate vials. Only the acid was able to cause irreversible aggregation in the P-AuNPs at low pH due to the cleaving the polymer from the AuNPs.

5.12. Discussion

Figure 35 depicts a schematic representation of the generation of RAFT polymer stabilised AuNPs and their subsequent encoding with SERS tags.

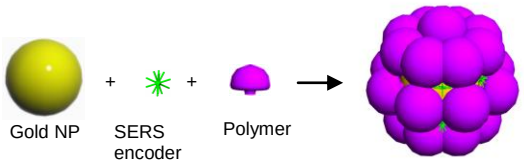

Figure 35 Schematic representation of the generation of RAFT polymer stabilised AuNPs encoded with SERS tags. This product is represented as SAC-P-AuNP

It has been demonstrated that water soluble polymers with thiol end-group functionality are able to self assemble via a "grafting to" approach at the surface of AuNPs that are dispersed in water.[108, 185, 186] Duwez *et al.*[113] have shown that thiocarbonylthio thiol groups specifically interact with gold surfaces, and Hotchkiss *et al.*[111] have reported the surface modification of gold nanorods with water soluble polymers that had RAFT end-groups, *i.e.* they were not reduced to the thiol. They also presented an example of the self assembly of polystyrene that had RAFT end-groups, at the surface of gold nanorods, which were dispersed in dimethylformamide (DMF). However, the method developed in this work has the advantage of being able to use AuNPs dispersed in water, without having to transfer them to an organic based solvent, such as DMF. Furthermore, during the preparation process the polymer stabilised nanoparticles precipitate from the aqueous solution, which means they can be easily recovered by filtration or by addition of a water immiscible solvent in which the polymer is soluble. This represents a significant simplification in the processing and preparation of polymer stabilised AuNPs where the polymer is insoluble in water. This allows the polymer stabilised AuNPs to be easily cast into thin films or incorporated into polymers. Most other reports of AuNPs stabilised with water insoluble polymers have involved the reduction of gold salts with sodium borohydride in the presence of polymers with a thiol[115, 116, 187] or dithioester[112] end-

group. However, a feature of those systems was that the size of the nanoparticle cores was typically 2 – 6 nm in diameter.

This method provides an alternative way to prepare physico-chemically stable SERS-encoded nanoparticles, with advantages over previous methods such as coating with silica[188, 189] or stabilization with specifically engineered polymers which have been modified with a tag at the chain end.[190] The stabilised nanoparticles that have been prepared should be compatible with the range of SERS tags described previously by others.[103, 191, 192] The fact that polymers prepared using RAFT polymerisation can be used directly to stabilise AuNPs allows significant flexibility in the choice of functional groups that can be incorporated into the stabilizing polymer.

5.13. Summary

A simplified method for the preparation of polymer stabilised AuNPs has been shown. AuNPs that have been synthesised by the citrate method, *and hence* dispersed in water, can be stabilised by the addition of as-synthesised RAFT polymers dissolved in a water miscible solvent. Polymer stabilised AuNPs were not observed for polymers synthesised by conventional free radical polymerisation, *i.e.* polymers that did not possess a RAFT or sulphur containing end-group. This indicated that the sulphur-containing RAFT end-groups were essential for the self assembly process. The stabilised AuNPs were further characterised using a range of techniques including, Visible absorption spectrometry, TEM and TGA. In addition SERS was used to analyse the binding of dithioester polymer endgroups to AuNPs. These techniques all provided evidence for the gold colloid being stabilised by the

polymer. These hybrid nanoparticles were also encoded with a series of Raman tags. It was demonstrated that SERS signals with the exact signature to that found using citrate-stabilised AuNPs and SACS could be obtained. This indicated that the stabilization process did not significantly interfere with the ability of AuNPs to act as substrates for the SERS effect. The method of stabilization and encoding provides an alternative method for generating stable SERS-encoded-AuNPs. Unfortunately, a complication of this approach is that an additional SERS signal can be seen from the RAFT agent if the polymer is of lower molecular weight (M_n<10,000). This signal can contaminate the signal from the Raman tag but can be removed by spectral subtraction techniques. Analysis of the hybrid NPs in various solvents and at various temperatures were undertaken and successfully illustrated the hybrids were intrinsically stable.

6. CHAPTER 6

BIOCONJUGATION AND DETECTION

6.1. Introduction

Applications of hybrid nanoparticles are largely biomedical[104] and electronic.[193] Throughout this research there have been avenues explored to create nanoparticles that can be used in bioassay applications.[172] After the addition of a bio-molecule to the AuNP, it is essential to test that the attachment process works for its desired application – a bioassay. This chapter outlines the methods used to illustrate that hybrid P-AuNPs functionalised with biotin will bind to the protein streptavidin, with which it is known to have a strong affinity. These investigations show that biotin-Q-P_2-AuNP does in fact bind to streptavidin and that a SERS signal from the Raman tag can be subsequently obtained. We also show that the particles bind specifically to streptavidin and that non-specific binding is not observed.

6.2. Synthesis of Biotin Azide

Since biotin is commercially available as biotin cadaverine (Figure 36 left) containing an amine end group, polymers were initially synthesised containing a *tert*-butyl group which could in turn be converted to a carboxylic acid (Figure 36 right) to facilitate the attachment via an amide linkage.

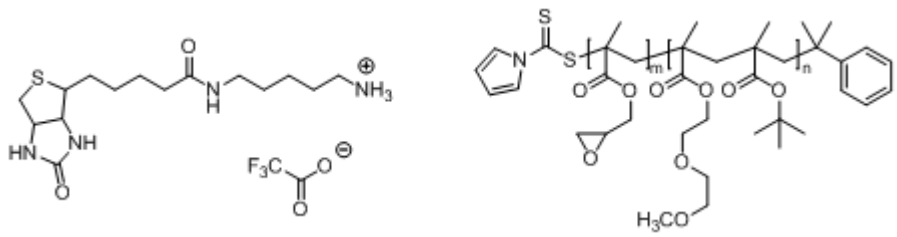

Figure 36 (left) Initial modified biotin purchased from Anaspec for use with (right) the initial design of the diblock copolymer

The results obtained from the addition of TFA (as outlined in Chapter 4) to both crosslink the polymer around the nanoparticle for stabilization and provide carboxylate functionalisation were inconclusive and did not seem to produce the desired result of P-AuNP. The procedure seemed too ambitious to try and ensure stabilization and functionality in one step. From these reactions it was difficult to identify whether a carboxyl group had been produced, and if so what yield had been obtained. Over the course of this project it was discovered that more hydrophilic polymers were better suited for potential bioassay application.[172] To ensure that binding took place, the AuNPs and polymer would have to be phase transferred to organic solvent to allow the polymer to bind. Although this P-AuNP system showed promise, other designs of polymers with RAFT end groups were investigated that would be more water soluble. A RAFT agent containing an acetylene end-group that can undergo triazole 'click' chemistry was employed as it would be more versatile than other designs previously investigated as well as being a facile approach to binding. This reaction, known as the Huisgen 1,3 dipolar cycloaddition, has become synonymous with the philosophy of 'click' chemistry due to its simple reaction conditions, typically high yields and wide scope of application. For this reason the synthesis of a biotin molecule bearing azide functionality was undertaken. The synthetic procedure, adapted from Meier *et al.*,[194] used peptide coupling reagents and a commercially available azide as indicated below (see Figure 37).

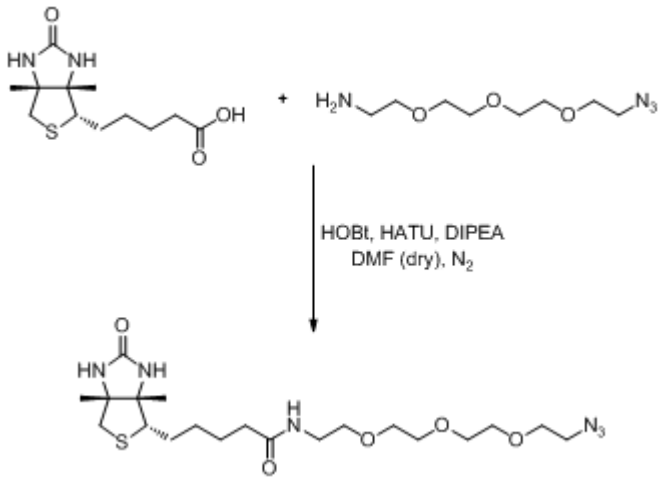

Figure 37 Synthetic route adapted from Meier *et al.* using peptide coupling reagents and a commercially available azide.[194]

6.2.1. Attempted Synthesis of Biotin Azide

Biotin (100 mg, 0.41 mmol), 11-azido-3,6,9-trioxaundecan-1-amine (197 µl, 0.82 mmol, 2 equiv.), 2-(1H-7-azabenzotriazol-1-yl)-1,3,3-tetramethyl uronium hexafluorophosphate methanaminium (HATU) (171 mg, 0.45 mmol, 1.1 equiv.), N-hydroxybenzotriazole (HOBt) (61mg, 0.45 mmol, 1.1 equiv.) were dissolved in dry DMF (2 mL). N-ethyldiisoproylamine (DIPEA) (350 µl, 2.05 mmol, 5 equiv.) was then added. The reaction was allowed to stir for 4 hours under argon. The DMF was removed under vacuum and the solid was taken up in DCM and subsequently purified by column chromatography (SiO_2, eluent 100 % DCM with gradient to 10 % MeOH/DCM).

On the first occasion this purification technique the product band only moved once the 10 % MeOH/DCM was added. This resulted in a poor separation, resulting in an isolated yield of approximately 1 %. It was found that the best separation could be obtained using 5 % MeOH/DCM. The biotin azide eluted as an oily solid. Whilst the NMR of this product had many spurious peaks indicating a high level of

impurities, the molecular ion for the desired compound was present in the high resolution mass spectrum (HRMS calculated for $C_{18}H_{33}N_6O_5S$: 444.2233 experimental EI $[M]^+$: 444.2155).

Further purification was attempted by various techniques including additional columns utilizing different solvent mixtures, acid and base washes as well as HPLC but none of these further techniques yielded a pure product.

Other coupling reactions using EDC, DCC and thionyl chloride were also attempted but none of these yielded the desired product. Due to these reasons another synthetic scheme needed to be devised.

After searching the relevant literature for the devised synthetic route (Figure 38), it was found that the only novel (and crucial) step was synthesizing the azide functionality. The acid group of the D-biotin was converted to the corresponding ethyl ester.[195] The biotin ethyl ester was then reduced to biotinol[196] and subsequently converted to the tosylate.[197] The azide can then be produced by heating in the presence of sodium azide.[198]

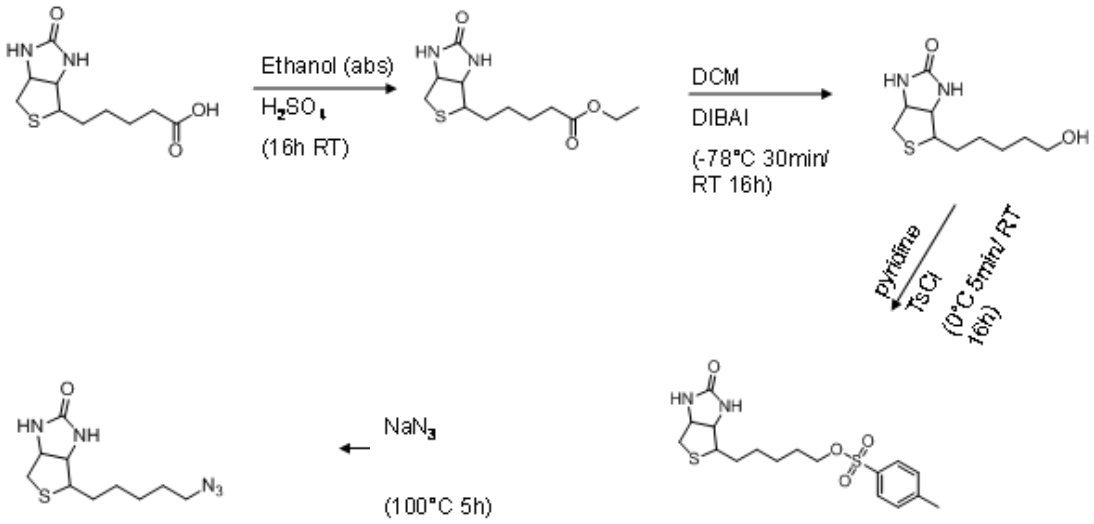

Figure 38 Synthetic route for the desired biotin azide by firstly esterification of the acid, reduction to an alcohol, tosylating the alcohol and exchanging this for the azide.

6.2.2. Synthesis of Ethyl[(3aS,4S,6aR)-2-oxo-hexahydro-thieno[3,4-*d*]imidazol-4-yl]pentanone (1)

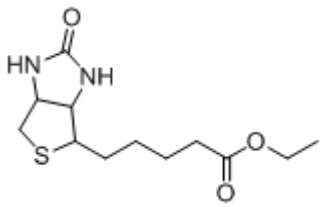

Figure 39 Biotin ethyl ester produced in the first step of the biotin azide reaction

Biotin (1.0 g, 4.09 mmol) was dissolved in absolute ethanol (25 mL) and the resulting solution was acidified by adding several drops of conc. H_2SO_4. The reaction mixture was stirred at room temperature for 16 h, after which the volatiles were removed under reduced pressure. The crude product was taken up in DCM (50 mL), and washed with saturated $NaHCO_3$ (3 × 30 mL) and H_2O (2 × 30 mL). The organic layer was dried (Na_2SO_4) and the solvent was removed under reduced

pressure to give a white solid. Recrystallisation from cold acetone gave ethyl [(3aS,4S,6aR)-hexahydro-thieno[3,4-*d*]imidazol-4-yl]pentanoate (**1**) as a white crystalline solid (0.82 g, 3.01 mmol, 74 %).

FT-IR ATR: 3227, 2937, 2861, 1729, 1693, 1478, 1258 cm^{-1}; ^{1}H NMR (400 MHz, *CDCl*$_3$) δ ppm 6.00 (s, 1H), 5.61 (s, 1H), 4.53-4.43 (m, 1H), 4.32-4.24 (m, 1H), 4.09 (q, *J* = 7.13 Hz, 2H), 3.25-3.03 (m, 1H), 2.88 (dd, *J* = 12.80, 4.96 Hz, 1H), 2.71 (d, *J* = 12.78 Hz, 1H), 2.30 (t, *J* = 7.50 Hz, 2H), 1.77-1.54 (m, 4H), 1.52-1.33 (m, 2H), 1.23 (t, *J* = 7.13 Hz, 3H); ^{13}C NMR (100 MHz, *CDCl*$_3$) δ ppm 173.686, 163.744, 61.931, 60.284, 60.101, 55.443, 40.530, 33.933, 28.328, 28.220, 24.781, 14.232; HRMS mass calculated for $C_{13}H_{23}N_2O_3S^+$: 273.1195 experimental ESI $[M+H]^+$: 273.1273.

6.2.3. Synthesis of 4S-[(3aS,6aR)-5-Hydroxy-pentyl]-tetrahydro-thieno[3,4-*d*]imidazol-2-one (2)

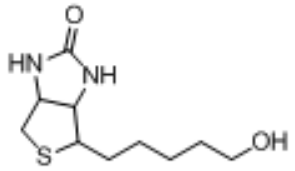

Figure 40 Biotinol produced in the second step of the biotin azide reaction

Biotin ethyl ester **1** (200 mg, 0.733 mmol) was dissolved in DCM (0.7 mL) and placed under argon and cooled to -78 °C (dry ice/acetone). Diisobutylaluminium hydride (1.72 mL, 2.5 mmol, 1.5 M in toluene) was added dropwise over 10 min. The mixture was stirred at -78 °C for a further 20 min then allowed to warm to room temperature and stirred for 16 h. The mixture was again cooled to -78 °C and

quenched by dropwise addition of methanol, a mixture of methanol and water and finally water. The solvents were removed under reduced pressure and the product was extracted with ethanol using a Soxhlet apparatus. Subsequently the EtOH was removed under reduced pressure to give an off white solid. Purification by column chromatography (50% EtOAc/50% EtOH) gave 4S-[(3aS,6aR)-5-hydroxy-pentyl]-tetrahydro-thieno[3,4-d]imidazol-2-one (**2**) as a white solid (119 mg, 0.517 mmol, 71 %).

FT-IR ATR: 3237, 2929, 2385, 1680, 1461 cm^{-1}; ^{1}H NMR (400 MHz, MeOH-d_4 6.62 (s, 1H), 6.58 (s, 1H), 4.56-4.46 (m, 1H), 4.35-4.29 (m, 1H), 3.57 (t, J = 6.50, 6.50 Hz, 2H), 3.27-3.19 (m, 1H), 2.95 (dd, J = 12.76, 4.98 Hz, 1H), 2.72 (d, J = 12.72 Hz, 1H), 1.91 (s, 1H), 1.83-1.35 (m, 1H); ^{13}C NMR (100 MHz), MeOH-d_4 δ ppm 161.7, 62.0, 61.5, 55.8, 39.6, 33.5, 32.0, 28.8, 28.4, 25.5. HRMS mass calculated for $C_{10}H_{19}N_2O_2S^+$: 231.1089 experimental ESI $[M+H]^+$: 231.1167. These data were found to have some discrepancies compared with those reported in the literature.[196, 197] As the product reported in the literature was not purified after the Soxhlet extraction it is suggested that some of the NMR data may have been misreported or incorrect as there were additional peaks beyond those that could be accounted for by the biotinol.

6.2.4. Synthesis of 4S-[(3aS,6aR)-5-(4-toluenesulfonyl)pentyl]-tetrahydro-thieno[3,4-d]imidazol-2-one (3) (4S-[(3aS,6aR)-5-chloropentyl]-tetrahydro-thieno[3,4-d]imidazol-2-one (4)

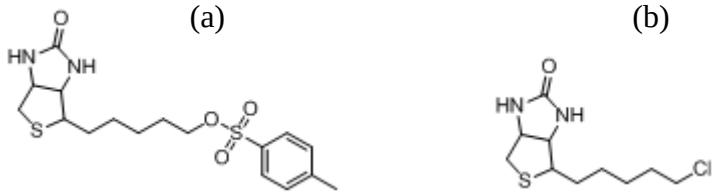

Figure 41 Biotintosylate (a) produced in the third step of the biotin azide synthesis, together with chloro- functionalised biotin byproduct (b)

Biotinol **2** (119 mg 0.57 mmol) was dissolved in warm anhydrous pyridine (2.5 mL) under argon. This solution was cooled in an ice bath for 30 min after which p-toluenesulfonyl chloride (120 mg, 0.63 mmol, 1.1 equiv.) was added. After stirring at 0°C for 5 min the reaction mixture was allowed to warm to RT and was stirred for a further 16 h. The mixture was poured into cold water (~50 mL) and extracted with DCM (3 × 50 mL). The DCM solutions were then washed with 1.8 M H_2SO_4 (3 × 50 mL). The aqueous layers were extracted with additional DCM (2 × 150 mL). The DCM layers were combined and subsequently washed with brine (3 × 100 mL) and dried over Na_2SO_4. The solvent was removed and the obtained solid was purified by column chromatography (1:20 MeOH:DCM). NMR and MS characterisation of the obtained product indicated the presence of both tosyl- and chloro- functionalised biotin[199] (see structures above) in an approximately a 1:1 ratio (54 % tosylate, 46 % chloride from NMR). This appearance of the chloro species in the reaction of biotinol with sulfonyl chlorides has literature precedent. In the case of

Islam et al.[199] treatment of biotinol with $MeSO_2Cl$ gave both the mesylate and chloride.

This step was repeated several times in an attempt to produce a higher purity product and it was found that the conversion to the azide proceeded with a much higher yield when the all biotinol had been removed from the system (i.e. biotinol had been had all been converted to both tosylate and chloride rather than having starting material remaining). The mass isolated from this was 60 mg corresponding to a yield of 35 % (calculated by mole ratio of both the –Cl and –OTs).

Tosylate **10** ^{1}H NMR (400 MHz, $CDCl_3$) δ ppm 7.79 (d, 2H, J=8.1 Hz), 7.36 (d, J=8.1 Hz, 2H), 6.34 (s, 1H), 5.65 (s, 1H), 4.56-4.50 (m, 1H), 4.03 (t, J = 6.4 Hz, 2H), 3.22-3.07 (m, 1H), 2.94-2.87 (m, 1H), 2.76 (d, J = 5.7 Hz, 1H), 2.46 (s, 3H), 1.83-1.30 (m, 8H); ^{13}C NMR (100 MHz, $CDCl_3$) δ ppm 163.9, 144.7, 133.0, 129.8, 127.8, 77.2, 70.6, 60.0, 55.6, 28.5, 28.3, 28.3, 25.3, 21.6; HRMS calculated for tosylate $C1_7H_{24}N_2O_4S_2$: 384.12 experimental ESI [M+H]+: 385.1256;

Chloride 11 ^{1}H NMR (400 MHz, $CDCl_3$) δ ppm 6.05 (s, 1H), 5.73 (s, 1H), 4.36-4.30 (m, 1H), 3.54 (t, J = 6.7 Hz, 2H), 3.22-3.07 (m, 1H), 2.96-2.87 (m, 1H), 2.73 (d, J = 5.7 Hz, 1H), 1.54-1.31 (m, 8H); ^{13}C NMR (100 MHz, $CDCl_3$) δ ppm 163.8, 61.9, 60.0, 55.5, 45.0, 40.5, 32.2, 28.4, 28.2, 26.7); HRMS calculated for chloride $C_{10}H_{17}ClN_2OS$: 248.0750 experimental ESI [M+H]+: 249.0828. These data agree with both biotin tosylate and biotin chloride.[199]

6.2.5. Synthesis of 4-(5-Azidopentyl)tetrahydro-1*H*-thieno[3,4-*d*]imidazole-2(3*H*)-one (5)

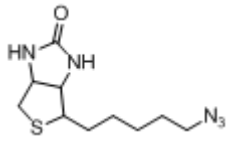

Figure 42 Structure of the biotin azide

To the biotin tosylate (chloride) **3, 4** (60 mg, 0.2 mmol) and sodium azide (32 mg, 0.6 mmol, 3.2 equiv.) was added to DMF (0.5 mL). The resultant solution was heated at 100 °C for 5 hours. The reaction mixture was cooled and water was added forming a white precipitate. Filtration of the precipitate gave 4-(5-azidopentyl)tetrahydro-1H-thieno[3,4-d]imidazole-2(3H)-one (30 mg, 0.117 mmol, 62 %). The ^{1}H NMR spectrum for this compound is shown in Figure 43.

FT-IR ATR, 3201, 2925, 2088, 1706 cm^{-1}; ^{1}H NMR (400 MHz, $CDCl_3$) δ ppm 1.55-1.36 (m, 4H), 1.85-1.57 (m, 8H), 2.76 (d, J = 12.81 Hz, 1H), 2.95 (dd, J = 12.84, 5.05 Hz, 1H), 3.22-3.15 (m, 1H), 3.29 (t, J = 6.83, 6.83 Hz, 2H), 4.38-4.29 (m, 1H), 4.57-4.50 (m, 1H), 5.21 (s, 1H), 5.47 (s, 1H); ^{13}C NMR (100 MHz, $CDCl_3$) δ ppm 163.3, 62.1, 60.1, 55.5, 51.4, 40.6, 28.6, 28.6, 26.7; HRMS mass calculated for $C_{10}H_{18}N_5OS^+$: 256.1154 experimental ESI $[M+H]^+$: 256.1232; mp : 85 °C

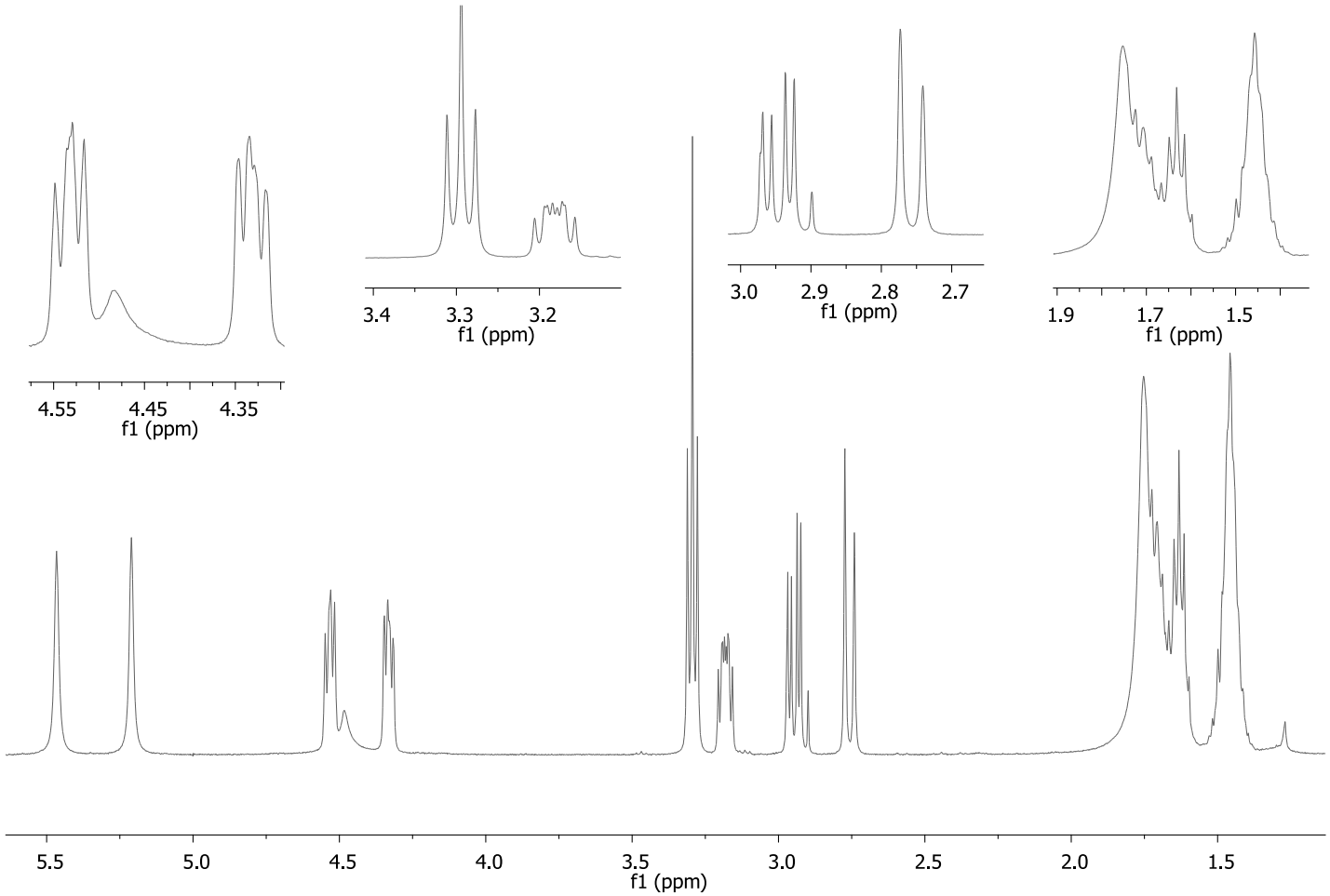

Figure 43 ^{1}H NMR spectrum of the biotin azide

6.3. 'Click' Chemistry on Gold Nanoparticles

1,3-Dipolar cycloaddition reactions to form 1,2,3 triazoles were first performed by Huisgen[200] in the early 1960s and were further refined by Sharpless,[175] who focussed on Cu-catalysed reactions as well as coining the term 'click' chemistry. For polymer chemistry in particular this technique has been exploited for many aspects of attachment. Furthermore, polymer coated NPs can be bound to ligands and linker molecules through this useful technique, whilst maintaining structural integrity. [165,169, 175, 201-208]

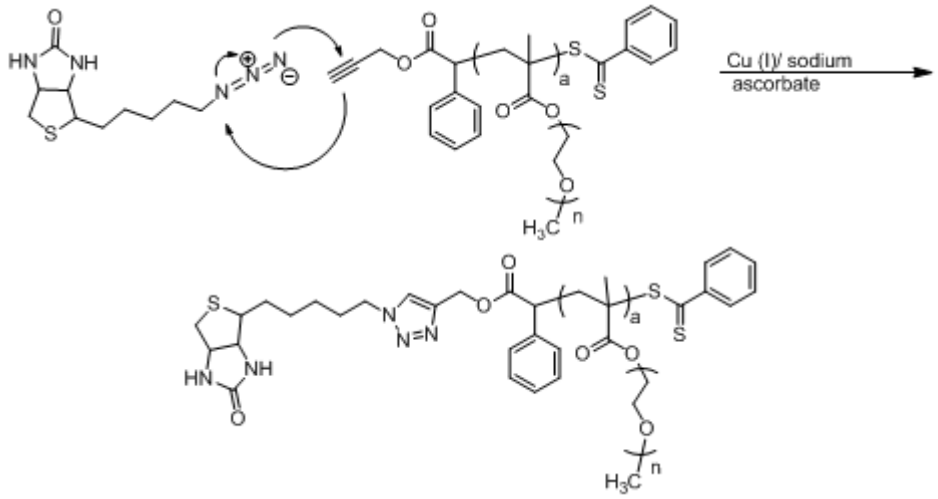

Figure 44 Reaction scheme for attachment of biotin azide to the PEGMA P1 through 'click' chemistry

Whilst AuNPs have been bound to molecules using click chemistry,[209-214] to date the ideas involved in the current investigation have not been previously reported. The synthetic route that was followed is shown in Figure 44. A model system was tested initially using PEGMA **P1** (refer to Chapter 4 for synthetic detail). As this polymer is soluble in water it was postulated that if the reaction worked successfully using a water soluble azide then the efficacy of the reaction in the most desirable conditions

would be seen. Both the acetylene and the azide compound initially used were both water soluble, just to ensure that the reaction occurred with the polymer (note – biotin azide prepared in this work is not water soluble). 3,6,9-Trioxy-1,10-diazidooctane (Figure 45) was supplied by Z. Merican and used for initial investigation of this reaction both with free polymer and polymer bound to AuNPs.

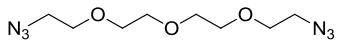

Figure 45 Structure of 3,6,9-trioxy-1,10-diazidooctane used for preliminary tests to determine the viability of this type of reaction with both the AuNPs and polymers produced throughout this work

Table 4 Stoichiometry used for 'click' reactions where M_w is the molecular weight, m is the mass required in mg and n the number of moles.

Compound	**Stoichiometry (equiv.)**	**M_w**	**m (mg)**	**n (x 10^{-3})**
3,6,9-trioxy-1,10-diazidooctane	1	244.45	1	4.09
PEGMA P1	2.2	8200	74	9.01
Sodium ascorbate	2	198.11	1.6	8.19
$CuSO_4.5H_2O$	2	159.61	1.3	8.19

Compound	**Stoichiometry (equiv.)**	**M_w**	**m (mg)**	**n (x 10^{-3})**
Biotin Azide	1	255.12	1.1	4.09
PEGMA P1	2.2	8200	74	9.01

Sodium ascorbate	2	198.11	1.6	8.19
$CuSO_4.5H_2O$	2	159.61	1.3	8.19

Compound	**Stoichiometry (equiv.)**	**M_w**	**m (mg)**	**n (x 10^{-3})**
PEG Azide	1	435.258	1.78	4.09
PEGMA P1	2.2	8200	74	9.01
Sodium ascorbate	2	198.11	1.6	8.19
$CuSO_4.5H_2O$	2	159.61	1.3	8.19

The 'click' reaction was first performed in water to test the reaction, since it is reported to proceed more readily in aqueous media. The polymers may curl up and not have the end groups available for binding, so using the most accessible system would demonstrate that this would not hinder the binding. Both ^{1}H NMR and FTIR-ATR were used to monitor the disappearance of the azide functionality. These reactions were performed with an excess of the acetylene coupling partner (in this case the PEG homopolymer) to ensure complete conversion of the azide.

6.4. Preparation of biotin functionalised AuNPs

6.4.1. Click reaction of hybrid gold polymer nanoparticle with biotin azide

Table 5 Stoichiometry used for 'click' reactions between PEGMA P1 and biotin azide

Compound	Stoichiometry (equiv.)	M_w	m (mg)	n (moles)
PEGMA P1	2.3	8200	74	0.0090
Sodium Ascorbate	2	198.11	1.6	0.0082
$CuSO_4.5H_2O$	2	159.61	1.3	0.0082
Biotin Azide	1	255.12	1.1	0.0041

The polymer PEGMA **P1** (74 mg) was dissolved in 1 mL water. Biotin azide (1.1 mg) was added to the vial, from an 11 mg/ mL solution shown in Table 5. The click reagents were made up to 1 mL in water. 100 µL of each was added to the reaction vials stirred for 24 hours. The solution changed colour from a pale pink (the colour of the RAFT polymer) to a dark brown, showing the change in oxidation state of the Cu (I) to Cu (II) and progress of the desired reaction. Purification was obtained by centrifugation, to remove any of the Cu solid.

AuNPs were made as previously stated in Chapter 3 (section 3.2.1). Approximately 1 mL AuNP solution was placed in a clean vial. One hundred µL of the biotin polymer product was added to the AuNPs and followed approximately 60 seconds

later by 5, 10 or 200 µL of a 54 µM solution of quinolinethiol (QSH) and the resultant mixture was stirred overnight, to allow the QSH to penetrate into the polymer. The reaction was monitored for completion using ATR-IR with a Ge crystal. It was found that the ^{1}H NMR was not as sensitive as FTIR for observing the click reaction between the polymer and azide compound, due to other peaks obstructing the region where the alkyne would be.

Figure 46 shows a comparison between the FTIR spectra of commercially available D-biotin, the biotin azide, and the polymer used for these reactions, PEGMA **P1**. After the 'click' reaction, the azide peak disappears due to the formation of the triazole, as shown in Figure 45 (d).

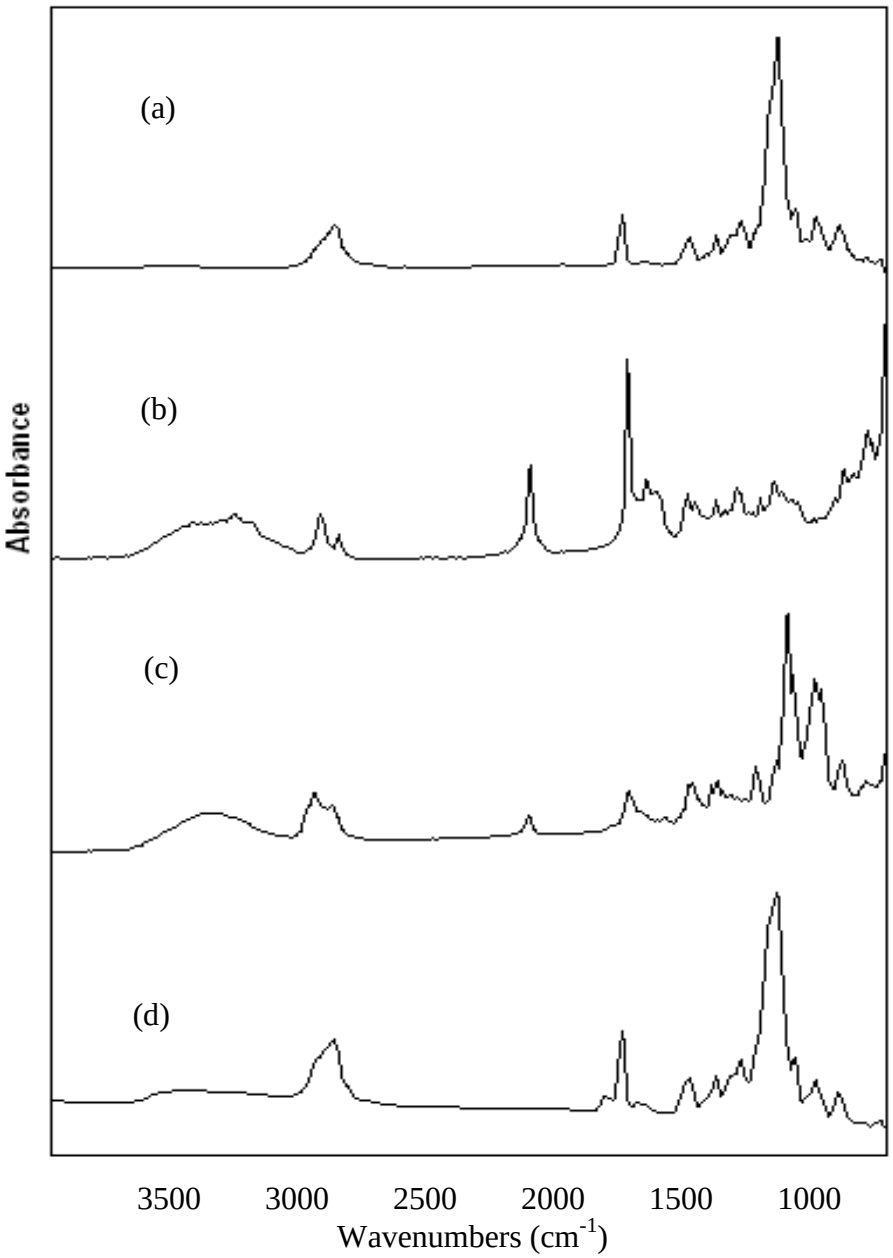

Figure 46 ATR-IR spectra of (a) PEGMA P1 (b) biotin azide (4) (c) product of the addition of (a) and (b) and (d) product after biotin azide is reacted with PEGMA P1 after approximately 2h. The disappearance of the azide peak at 2089 cm^{-1} is noted.

Approximately 1 mL of AuNP solution was placed in 10 separate vials, so that reproducibility of the binding could be checked. PEGMA **P1** (35 mg) was dissolved in 10 mL water. Subsequently, 0.5 mL of the polymer solution was added to the AuNP vial. They were shaken and then set aside for an hour to allow attachment of

the polymer to the NP surface. Stability of the AuNPs was assessed by the addition of NaCl to a vial of the hybrid AuNPs and to a vial of citrate stabilised AuNPs. The citrate stabilised AuNPs showed complete destabilization on addition of salt. The AuNPs went from being bright pink/purple suspension to black (a sign of aggregation) immediately after the salt was added. Within a few minutes the aggregated AuNPs fell out of suspension leaving a black film on the bottom of the vial and a clear colourless supernatant indicating that there are no NPs left in suspension. When the NaCl was added to the N_3-P_1-AuNPs, there was no observed colour change and no change in the SPR, which verified that the AuNPs were then stable in solution. Once this enhanced stability of the particles had been confirmed, the 'click reaction' was undertaken. During this process some destabilization from the azide was observed through a slight darkening of the solution. This did not seem to vary the maximum SPR peak, but the appearance of an additional peak at approximately 750nm indicated that there was a degree of aggregation in the suspension.

6.4.2. Demonstration of binding to streptavidin

A standard test of bioconjugation is the binding between biotin and streptavidin, demonstrating an antibody-antigen pair.[104] This binding is reported as one of the most favoured binding mechanisms. To examine whether the biotin has attached to the P_1-AuNP, it was thought that streptavidin should be added to the AuNP suspension. Since the streptavidin has several binding sites, the AuNPs should fall out of solution after the addition of the streptavidin. Although this was observed, it

was not clear how to analyse unequivocally that the binding had occurred through analytical techniques since there were no significant markers that could be shown on the AuNPs that would separate the B-P_1-AuNPs from the Strep- B-P_1-AuNPs since the concentration of the streptavidin was much less than that of the AuNPs.

To confirm this binding event had occurred an assay test was employed, where the streptavidin is bound to a surface (well plate) and the nanoparticles are washed over the top. The well plate is washed to remove any unbound media. If after cleaning the NPs remain, then binding has occurred. Binding was checked by using the presence of SERS signal. When the P_1-AuNPs were not conjugated to biotin a SERS signal could not be obtained.

Originally it was planned to make functionalised glass surfaces to bind the streptavidin then wash over the surface. After further research it was found that Sigma Aldrich sold a streptavidin functionalised well plate that could be used for this work.

6.4.3. Preparation of assay well plates

The biotin was added to a well plate that had been pre-treated with streptavidin. Instructions supplied by Sigma with the well plate meant that approximately 200 µL of the AuNP/biotin solution needed to be added to individual wells on the well plate. This was left at RT for at least 2 hours then washed vigorously with PBS (phosphate buffered saline) and 5 % tween 20 (mild surfactant). The streptavidin solutions for this study were prepared at a concentration of 5×10^{-6} M in 0.5 M aqueous NaCl.

The SERS signal of solution and plate was examined before and after washing. Control samples were also analysed, using AuNPs with a SERS tag but no biotin attached. Wells were prepared using the above procedure except without any biotin present.

Figure 47 shows the binding event that has occurred on the streptavidin well plate. The signal from the well plate incorporates both SERS from the RAFT end group discussed in Chapter 5 (Figure 47 (a)) and the SERS signal obtained from 2-quinolinethiol (Figure 47 (b)). The peaks denoted with a (*) are from the SAC. The remaining peaks are from the RAFT contribution. These results cannot be obtained if there is no biotin attached to the hybrid AuNPs and there is only a background from the well plate.[215]

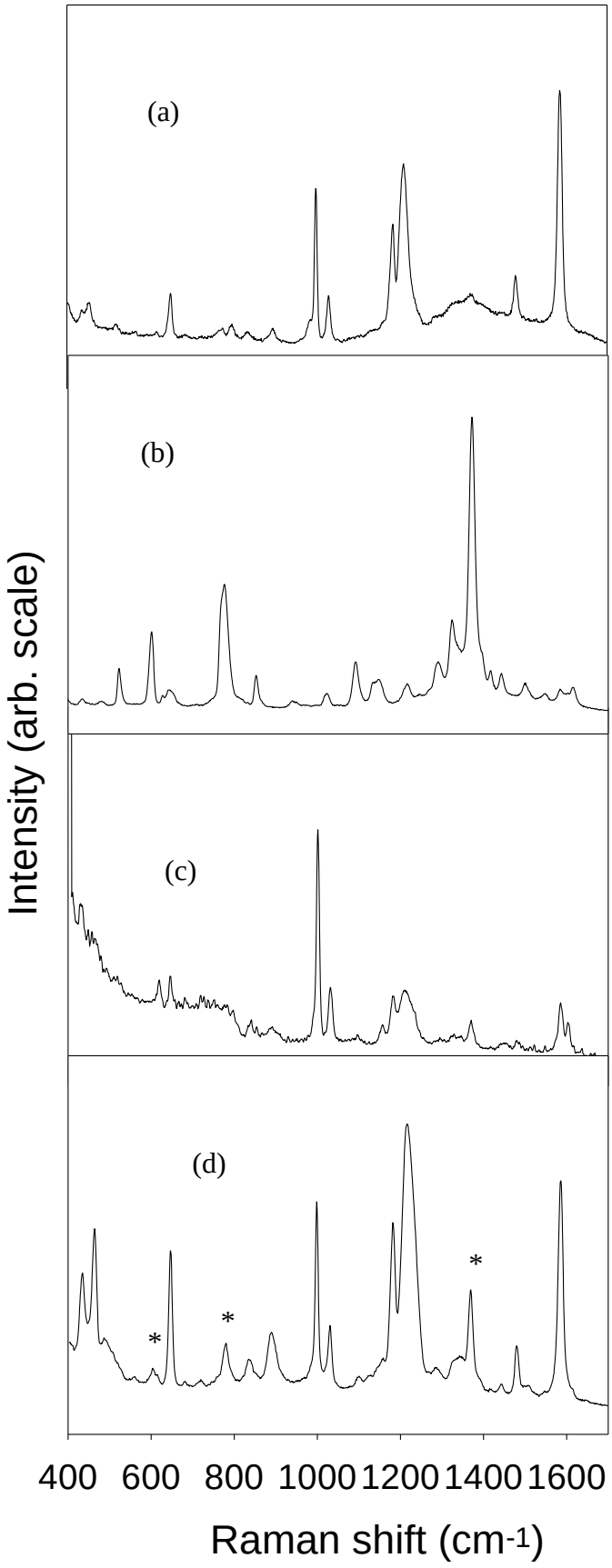
(a)
(b)
(c)
(d)
*
*
*
Intensity (arb. scale)
400
600
800
1000
1200
1400
1600
Raman shift (cm-1)

Figure 47 SERS Spectra of (a) RAFT end group (b) 2-quinolinethiol, (c) the well plate's polystyrene substrate and (d) after the binding event.

There have been different approaches for this work in the literature,[25, 104] none of which have controlled both the polymerisation and synthesised a novel biotin. This proof of concept has shown that the use of a SAC as a bioassay marker molecule is achievable.

6.5. Summary

The hybrid Au nanoparticles were tested for potential use in bioassays by attaching a biotin molecule to the polymer and demonstrating binding to the protein streptavidin. The original plan to use a commercially available biotin molecule containing an amine group to attach to a designed polymer containing a carboxylic acid group proved to be unsuccessful. An alternative approach was undertaken utilizing 'click' chemistry, which required a biotin molecule containing an azido group as well as a polymer incorporating an acetylene group.

A simple synthetic route for making the biotin azide compound to attach to the polymer was devised which used an amide linkage to attach an aliphatic azido compound to the carboxylic acid group of biotin. This proved unsuccessful as the product could not be purified. A 4-step synthesis of the biotin azide utilizing displacement of a tosylate group by azide ion proved to be successful. The biotin azide was successfully attached to the polymer coated NPs through 'click' chemistry.

It was then successfully shown that this novel hybrid AuNP binds to streptavidin. This binding was confirmed by the use of a SAC incorporated in the hybrid AuNP that was carrying the biotin moiety. This constitutes a "proof-of-concept" that polymer coated hybrid nanoparticles have the potential to be used successfully in bioassays and that a SAC can be used to detect and identify the NP in the manner of a "molecular barcode".

7. CHAPTER 7

CONCLUSIONS AND SUGGESTED FURTHER WORK

7.1. Conclusions

The aim of the current investigation was to illustrate the applicability of a bioassay technique, based on a SAC tagged AuNP encapsulated within a biotin functionalised polymer. This has been successfully demonstrated through the spectroscopic detection of the B-P_1-Q-AuNPs bound to streptavidin using SERS to verify this binding event.

Reproducible synthesis of AuNPs of consistent size was essential to the success of this project. It was found that the optimal size of AuNPs of approximately 40 nm was consistently achieved by making up each batch in 100 mL amounts based upon previous methods. If the AuNPs were much smaller than this it was more difficult to obtain a consistent SERS signal rendering them useless for our application. NPs much larger than 50 nm were found to be too heavy to remain suspended for longer than a day or two and a precipitate would form.

Synthesis of AuNPs with a mean size of 12-100 nm was possible by using the citrate reduction method. It was found for this work that adding 30 μL of $HAuCl_4$ to 100 mL of ultrapure water (18 MΩ cm) yielded the best reproducibility batch to batch, as well as a shelf life of over 6 months. NPs produced using this method also yielded the most consistent SERS signal across various the batches. A modification of the literature procedure of Olson *et al.*[61] reduced the variability in the size and shape of the particles.

AuNPs synthesized by the citrate method and dispersed in water were able to be stabilized by the addition of as-synthesized RAFT polymers dissolved in a water

miscible solvent. This stabilization of the AuNPs was not observed when using polymers synthesized by conventional free radical polymerisation, indicating that sulphur-containing RAFT end-groups were essential for the self assembly process. The AuNPs stabilized with polymer were further characterised using a range of techniques including Visible absorption spectrophotometry, TEM, ATR-FTIR, TGA and NMR. These techniques all provided strong evidence for the gold colloid being stabilized by the polymer. These hybrid nanoparticles were also encoded with a series of SACS. It was demonstrated that signals with comparable intensity to the citrate stabilized AuNPs could be obtained. This indicated that the stabilization process does not significantly interfere with the ability of AuNPs to produce a SERS signal. This method of stabilization and encoding provides an alternative method for generating stable SERS-encoded-AuNPs.

The original plan to use a commercially available amine functionalised biotin molecule to attach to a designed polymer containing a carboxylic acid group proved to be unsuccessful. An alternative approach, utilizing 'click' chemistry, required the synthesis of a functional biotin containing an azido group as well as a polymer incorporating an acetylene group. A synthetic route for making the biotin azide compound to attach to the polymer was devised which used an amide linkage to attach an aliphatic azido compound to the carboxylic acid group of biotin. This route had limited success and was eventually abandoned due to an inability to purify the product using conventional techniques. A 4-step synthesis of the biotin azide via a tosylate functional precursor proved to be successful. The biotin azide was

successfully attached to the polymer coated AuNPs through Cu catalysed 'click' chemistry.

Upon exposure of the hybrid B-P-Q-AuNPs to streptavidin assay-style well plate a SERS signal was able to be obtained from the Raman tag attached to the NPs (positive assay). AuNPs without biotin attachment gave no SERS signal (negative assay). These results illustrate the utility of SERS active functional-polymer encapsulated P-Q-AuNPs for bioassay application. The summary of this work is represented schematically in Figure 48.

7.2. Further Work

Due to the multi-dimensional nature of this project it was only possible to demonstrate a single "proof of concept" binding of the biotin functionalized NPs to the streptavidin. The use of the NPs in SERS based assays needs to be investigated further. A quantitative study of the sensitivity and reproducibility of these P-AuNPs could also be undertaken in the future.

Further to this, once the bioassay has been multiplexed, the design of an assay protocol that would allow an end-user to simply add the hybrid AuNPs to a well plate, perform a wash and then take a spectrum. This assay could then be analysed quickly using specifically tailored software such that the main peaks belonging to the SERS tag could be used to identify the antibody present, shown in Figure 10.

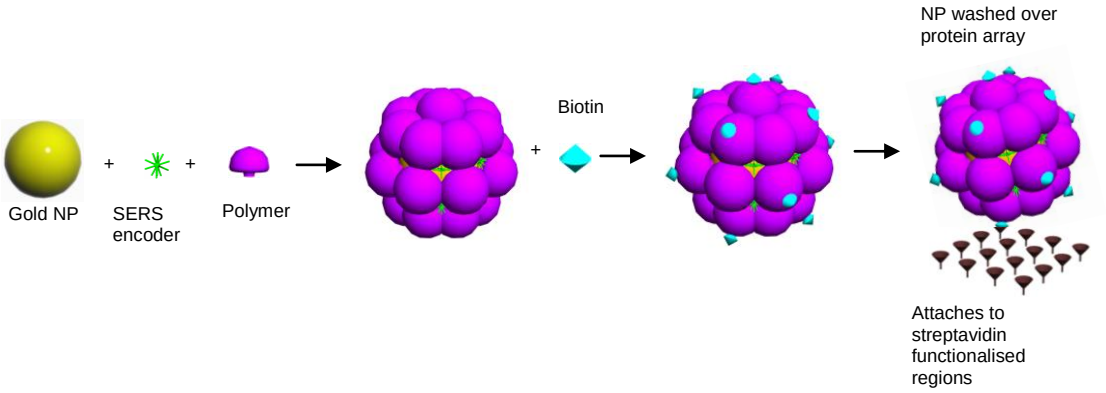

Figure 48 schematic summary of this work

8. CHAPTER 8

REFERENCES

1. J. D. Driskell, K. M. Kwarta, R. J. Lipert, M. D. Porter, J. D. Neill and J. F. Ridpath, *Analytical Chemistry*, 2005, **77**, 6147-6154.
2. R. F. Aroca, R. A. Alvarez-Puebla, N. Pieczonka, S. Sanchez-Cortez and J. V. Garcia-Ramos, *Advances in Colloid and Interface Science*, 2005, **116**, 45-61.
3. Anshup, J. S. Venkataraman, C. Subramaniam, R. R. Kumar, S. Priya, T. R. S. Kumar, R. V. Omkumar, A. John and T. Pradeep, *Langmuir*, 2005, **21**, 11562-11567.
4. S. G. Penn, L. He and M. J. Natan, *Current Opinion in Chemical Biology*, 2003, **7**, 609-615.
5. M. Seydack, *Biosensors & Bioelectronics*, 2005, **20**, 2454-2469.
6. K. Kneipp, H. Kneipp, I. Itzkan, R. R. Dasari and M. S. Feld, *Current Science*, 1999, **77**, 915-924.
7. K. D. Kumble, *Analytical Bioanal Chem*, 2003, **377**, 812-819.
8. M. F. Lopez and M. G. Pluskal, *Journal of Chromatography, B*, 2003, **787**, 19-27.
9. D. A. Vignali, *Immunological Methods*, 2000, **243**, 243-255.
10. T. Zhu, Z. H. Zhu, J. Wang, Y. C. Wang and Z. F. Liu, *Molecular Crystals and Liquid Crystals Science and Technology, Section A: Molecular Crystals and Liquid Crystals*, 1999, **337**, 237-240.
11. W. E. Doering and S. Nie, *Analytical Chemistry*, 2003, **75**, 6171-6176.
12. D. S. Grubisha, R. J. Lipert, H.-Y. Park, J. Driskell and M. D. Porter, *Analytical Chemistry*, 2003, **75**, 5936-5943.

13. S. P. Mulvaney, M. D. Musick, C. D. Keating and M. Natan, *Langmuir*, 2003, **19**, 4784-4790.

14. Y. C. Cao, R. Jin and C. A. Mirkin, *Science*, 2002, **297**, 1536-1540.

15. K. Kneipp, H. Kneipp, V. B. Kartha, R. Manoharan, G. Deinum, I. Itzkan, R. R. Dasari and M. S. Feld, *Physical Review E: Statistical Physics, Plasmas, Fluids, and Related Interdisciplinary Topics*, 1998, **57**, R6281-R6284.

16. M. Oestblom, B. Liedberg, L. M. Demers and C. A. Mirkin, *Journal of Physical Chemistry B*, 2005, **109**, 15150-15160.

17. S. Habuchi, M. Cotlet, R. Gronheid, G. Dirix, J. Michiels, J. Vanderleyden, F. C. De Schryver and J. Hofkens, *Journal of the American Chemical Society*, 2003, **125**, 8446-8447.

18. J.-M. Nam, C. S. Thaxton and C. A. Mirkin, *Science*, 2003, **301**, 1884-1886.

19. S. Xu, X. Ji, W. Xu, X. Li, L. Wang, Y. Bai, B. Zhao and Y. Ozaki, *Analyst* 2004, **129**, 63-68.

20. J. Kneipp, H. Kneipp, W. L. Rice and K. Kneipp, *Analytical Chemistry*, 2005, **77**, 2381-2385.

21. A. Sengupta, M. L. Laucks and E. J. Davis, *Applied Spectroscopy*, 2005, **59**, 1016-1023.

22. C. R. Yonzon, D. A. Stuart, X. Zhang, A. D. McFarland, C. L. Haynes and R. P. Van Duyne, *Talanta*, 2005, **67**, 438-448.

23. C. Otto, C. J. de Grauw, J. J. Duindam, N. M. Sijtsema and J. Greve, *Journal of Raman Spectroscopy*, 1997, **28**, 143-150.

24. K. C. Grabar, P. C. Smith, M. D. Musick, J. A. Davis, D. G. Walter, M. A. Jackson, A. P. Guthrie and M. J. Natan, *Journal of American Chemical Society*, 1996, **118**, 1148-1153.

25. N. H. Kim, J. Lee Seung and K. Kim, *Chemical communications*, 2003, 724-725.

26. X. Li, J. Zhang, W. Xu, H. Jia, X. Wang, B. Yang, B. Zhao, B. Li and Y. Ozaki, *Langmuir*, 2003, **19**, 4285-4290.

27. S.-W. Joo, W.-J. Kim, W. S. Yoon and I. S. Choi, *Journal of Raman Spectroscopy*, 2003, **34**, 271-275.

28. K. Kneipp, H. Kneipp, G. Deinum, I. Itzkan, R. R. Dasari and M. S. Feld, *Applied Spectroscopy*, 1998, **52**, 175-178.

29. S. De, A. Pal, N. R. Jana and T. Pal, *Journal of Photochemistry and Photobiology, A: Chemistry*, 2000, **131**, 111-123.

30. R. M. Bright, D. G. Walter, M. D. Musick, M. A. Jackson, K. J. Allison and M. J. Natan, *Langmuir*, 1996, **12**, 810-817.

31. J. Fang, Y. Huang, X. Li and X. Dou, *Raman Spectroscopy*, 2004, **35**, 914-920.

32. L. A. Lyon, C. D. Keating, A. P. Fox, B. E. Baker, L. He, S. R. Nicewarner, S. P. Mulvaney and M. J. Natan, *Analytical Chemistry*, 1998, **70**, 341R-361R.

33. R. F. Aroca, *Surface-Enhanced Vibrational Spectroscopy*, Wiley, 2006.

34. M. Fleischmann, P. J. Hendra and A. J. McQuillan, *Chemical Physics Letters*, 1974, **26**, 163-166.

35. M. Moskovits, *Reviews of Modern Physics*, 1985, **57**, 783-826.

36. M. G. Albrecht and J. A. Creighton, *Journal of the American Chemical Society*, 1977, **99**, 5215-5217.

37. M. Moskovits, *Solid State Communications*, 1979, **32**, 59-62.

38. E. Wentrup-Byrne, S. Sarinas and P. M. Fredericks, *Applied Spectroscopy*, 1993, **47**, 1192-1197.

39. K. Kneipp, H. Kneipp, I. Itzkan, R. R. Dasari and M. S. Feld, 99-US4167, Massachusetts Institute of Technology, USA, 1999, p. 57 pp.

40. K.-H. Cho, J. Choo and S.-W. Joo, *Spectrochimica Acta, Part A: Molecular and Biomolecular Spectroscopy*, 2005, **61A**, 1141-1145.

41. M. Moskovits, *Journal of Raman Spectroscopy*, 2005, **36**, 485-496.

42. A. Otto, *Journal of Raman Spectroscopy*, 2005, **36**, 497-509.

43. C. F. Bohren and D. R. Huffman, *Absorption and Scattering of Light by Small Particles*, John Wiley & Sons, New York, **1983**.

44. C. Chin, *Journal of Young Investigators*, 2008, **16**.

45. N. G. Tognalli, A. Fainstein, C. Vericat, M. E. Vela and R. C. Salvarezza, *Journal of Physical Chemistry B*, 2006, **110**, 354-360.

46. E. C. Le Ru, M. Meyer and P. G. Etchegoin, *Journal of Physical Chemistry B*, 2006, **110**, 1944-1948.

47. K. Kneipp, Y. Wang, H. Kneipp, L. T. Perelman, I. Itzkan, R. R. Dasari and M. S. Feld, *Physical Review Letters*, 1997, **78**, 1667-1670.

48. S. Nie and S. R. Emory, *Science* 1997, **275**, 1102-1106.

49. A. Otto, *Journal of Raman Spectroscopy*, 2002, **33**, 593-598.

50. K. Kneipp, H. Kneipp, I. Itzkan, R. R. Dasari and M. S. Feld, *Chemical Reviews*, 1999, **99**, 2957-2975.

51. M. Sackmann and A. Materny, *Journal of Raman Spectroscopy*, 2006, **37**, 35-310.

52. S. E. J. Bell and S. J. Spence, *Analyst (Cambridge, United Kingdom)*, 2001, **126**, 1-3.

53. http://www.nanoplextech.com/html/technology.html, Nanoplex SERS nanotags, http://www.nanoplextech.com/html/technology.html.

54. S. Nie and W. Doering, 2004-US26786, Emory University, US, 2005, p. 29.

55. T. Gu, J. K. Whitesell and M. A. Fox, *Chemistry of Materials*, 2003, **15**, 1358-1366.

56. P. Johansson, H. Xu and M. Kall, *Physical Review B: Condensed Matter and Materials Physics*, 2005, **72**, 1-17.

57. G. Schneider, G. Decher, N. Nerambourg, R. Praho, M. H. V. Werts and M. Blanchard-Desce, *Nano Letters*, 2006, **6**, 530-536.

58. W. R. Premasiri, D. T. Moir, M. S. Klempner, N. Krieger, G. Jones and L. D. Ziegler, *The Journal of Physical Chemistry B*, 2004, **109**, 312-320.

59. G. Frens, *Nature, Physical Science*, 1973, **241**, 20-22.

60. L. Lu, A. Kobayashi, K. Tawa and Y. Ozaki, *Chem. Mater.*, 2006, **18**, 4894-4901.

61. L. G. Olson, Y.-S. Lo, T. P. Beebe Jr. and J. M. Harris, *Analytical Chemistry*, 2001, **73**, 4268.

62. A. M. Schwartzberg, C. D. Grant, A. Wolcott, C. E. Talley, T. R. Huser, R. Bogomolni and J. Z. Zhang, *Journal of Physical Chemistry B*, 2004, **108**, 19191-19197.

63. H. Bengter, C. Tengroth and S. P. Jacobsson, *Journal of Raman Spectroscopy*, 2005, **36**, 1015-1022.

64. W. S. Sutherland and J. D. Winefordner, *Colloids and Interface Science*, 1992, **148**, 129-141.

65. S. E. J. Bell and N. M. S. Sirimuthu, *Journal of Physical Chemistry A*, 2005, **109**, 7405-7410.

66. R. Wen and Y. Fang, *Journal of Colloid and Interface Science*, 2005, **292**, 469-475.

67. H. Zhu, C. Tao, S. Zheng, S. Wu and J. Li, *Colloids and Surfaces, A: Physicochemical and Engineering Aspects*, 2005, **256**, 17-20.

68. S. Sanchez-Cortes and J. V. Garcia-Ramos, *Surface Science*, 2001, **473**, 133-142.

69. R. M. Bright, Fundamental properties of metal nanoparticle assemblies, The Pennsylvania State University, Pennsylvania, United States 1997.

70. R. M. Bright, M. D. Musick and M. J. Natan, *Langmuir*, 1998, **14**, 5695-5701.

71. M.-C. Daniel and D. Astruc, *Chemical Reviews*, 2004, **104**, 293-346.

72. C. L. Haynes and R. P. Van Duyne, *Abstracts of Papers, 225th ACS National Meeting, New Orleans, LA, United States, March 23-27, 2003*, 2003, COLL-073.

73. Z. S. Pillai and K. P. V, *Journal of Physical Chemistry B*, 2004, **108**, 945-951.

74. R. Woods and G. A. Hope, *Colloids and Surfaces, A: Physicochemical and Engineering Aspects*, 1999, **146**, 63-74.

75. P. C. Lee and D. Meisel, *Journal of Physical Chemistry*, 1982, **86**, 3391-3395.

76. C. L. Haynes, A. D. McFarland and R. P. Van Duyne, *Analytical Chemistry*, 2005, **77**, 338A-346A.

77. K. Kneipp, H. Kneipp, R. R. Dasari and M. S. Feld, *Indian Journal of Physics, B*, 2003, **77B**, 39-47.

78. K. Kneipp, G. Hinzmann and D. Fassler, *Chemical Physics Letters*, 1983, **99**, 503-506.

79. W. R. Glomm, *Journal of Dispersion Science and Technology*, 2005, **26**, 389-414.

80. M. Suzuki, Y. Niidome, Y. Kuwahara, N. Terasaki, K. Inoue and S. Yamada, *Journal of Physical Chemistry B*, 2004, **108**, 11660-11665.

81. S. W. Joo, T. D. Chung, W. C. Jang, M.-s. Gong, N. Geum and K. Kim, *Langmuir*, 2002, **18**, 8813-8816.

82. F. Manea, F. B. Houillon, L. Pasquato and P. Scrimin, *Angewandte Chemie, International Edition*, 2004, **43**, 6165-6169.

83. L. Pasquato, F. Rancan, P. Scrimin, F. Mancin and C. Frigeri, *Chemical Communications*, 2000, 2253-2254.

84. S. Eustis and M. A. El-Sayed, *Chemical Society Reviews*, 2006, **35**, 209-217.

85. K. G. Thomas and P. V. Kamat, *Accounts of Chemical Research*, 2003, **36**, 888-898.

86. S. I. Stoeva, V. Zaikovski, B. L. V. Prasad, P. K. Stoimenov, C. M. Sorensen and K. J. Klabunde, *Langmuir*, 2005, **21**, 10280-10283.

87. C. E. Talley, J. B. Jackson, C. Oubre, N. K. Grady, C. W. Hollars, S. M. Lane, T. R. Huser, P. Nordlander and N. J. Halas, *Nano Letters*, 2005, **5**, 1569-1574.

88. P. V. Kamat, *Journal of Physical Chemistry B*, 2002, **106**, 7729-7744.

89. H. C. van de Hulst, *Light Scattering by Small Particles*, Dover Publications, Inc., New York, 1981.

90. E. Mine, A. Yamada, Y. Kobayashi, M. Konno and L. Liz-Martin, *Colloid and Interface Science*, 2003, **264**, 385-390.

91. J. W. Slot and H. J. Gueuze, *European Journal of Cell Biology*, 1985, **38**, 87-93.

92. T. J. Norman, Jr., C. D. Grant, D. Magana, J. Z. Zhang, J. Liu, D. Cao, F. Bridges and A. Van Buuren, *Journal of Physical Chemistry B*, 2002, **106**, 7005-7012.

93. S. W. Joo, S. W. Han and K. Kim, *Journal of Physical Chemistry B*, 2000, **104**, 6218-6224.

94. S. W. Han and K. Kim, *Colloid and Interface Science*, 2001, **240**, 492-497.

95. A. Ihs, K. Uvdal and B. Liedberg, *Langmuir*, 1993, **9**, 733-739.

96. A. Ulman, *Chemical Review*, 1996, **96**, 1533-1554.

97. A. Lorén, J. Engelbrektsson, C. Eliasson, M. Josefson, J. Abrahamsson, M. Johansson and K. Abrahamsson, in *Anal. Chem.*, 2004, pp. 7391-7395.

98. J.-W. Hu, Y. Zhang, J.-F. Li, Z. Liu, B. Ren, S.-G. Sun, Z.-Q. Tian and T. Lian, *Chemical Physics Letters*, 2005, **408**, 354-359.

99. X.-H. Ji, L.-Y. Wang, X.-T. Zhang, Y.-B. Bai, T.-J. Li, Z.-Z. Zhi, X.-G. Kong and Y.-C. Liu, *Gaodeng Xuexiao Huaxue Xuebao*, 2002, **23**, 2357-2359.

100. C. J. Murphy, T. K. Sau, C. J. Orendorff and A. M. Gole, 2006065762, University of South Carolina, USA, 2006, p. 50.

101. D. S. dos Santos, Jr., R. A. Alvarez-Puebla, O. N. Oliveira, Jr. and R. F. Aroca, *Journal of Materials Chemistry*, 2005, **15**, 3045-3049.

102. C. L. Haynes, A. J. Haes and R. P. Van Duyne, *Materials Research Society Symposium Proceedings*, 2001, **635**, C6.3/1-C6.3/6.

103. Y. C. Cao, R. Jin, J.-M. Nam, C. S. Thaxton and C. A. Mirkin, *Journal of the Americal Chemical Society*, 2003, **125**, 14676-14677.

104. Z. Wang, J. Lee, A. R. Cossins and M. Brust, *Analytical Chemistry*, 2005, **77**, 5770-5774.

105. C. S. Levin, S. W. Bishnoi, N. K. Grady and N. J. Halas, *Analytical Chemistry*, 2006, **78**, 3277-3281.

106. K. Faulds, R. E. Littleford, D. Graham, G. Dent and W. E. Smith, *Analytical Chemistry*, 2004, **76**, 592-598.

107. J.-B. Kim, M. L. Bruening and G. L. Baker, *Journal of American Chemical Society*, 2000, **122**, 7616-7617.

108. S. Luo, J. Xu, Y. Zhang, S. Liu and C. Wu, *Journal of Physical Chemistry B*, 2005, **109**, 22159-22166.

109. M. Larsson, J. Lu and J. Lindgren, *Journal of Raman Spectroscopy*, 2004, **35**, 826-834.

110. K. Kimura, H. Yao and S. Sato, *Synthesis and Reactivity in Inorganic, Metal-Organic, and Nano-Metal Chemistry*, 2006, **36**, 237-264.

111. J. W. Hotchkiss, A. B. Lowe and S. G. Boyes, *Chemistry of Materials*, 2007, **19**, 6-13.

112. J. Shan, M. Nuopponen, H. Jiang, E. Kauppinen and H. Tenhu, *Macromolecules*, 2003, **36**, 4526-4533.

113. A.-S. Duwez, P. Guillet, C. Colard, J.-F. Gohy and C.-A. Fustin, *Macromolecules*, 2006, **39**, 2729-2731.

114. K. Matsumoto, R. Tsuji, Y. Yonemushi and T. Yoshida, 2004, **6**, 649-659.

115. M. Zheng, Z. Li and X. Huang, *Langmuir*, 2004, **20**, 4226-4235.

116. R. G. Shimmin, A. B. Schoch and P. V. Braun, *Langmuir*, 2004, **20**, 5613-5620.

117. R. Jordan, N. West, A. Ulman, Y.-M. Chou and O. Nuyken, *Macromolecules*, 2001, **34**, 1606-1611.

118. S. Nuss, H. Bottcher, H. Wurm and M. L. Hallensleben, *Angewandte Chemie, International Edition*, 2001, **40**, 4016-4018.

119. K. Ohno, K. Koh, Y. Tsujii and T. Fukuda, *Angewandte Chemie, International Edition*, 2003, **42**, 2751-2754.

120. K. Ohno, K.-m. Koh, Y. Tsujii and T. Fukuda, *Macromolecules*, 2002, **35**, 8989-8993.

121. J. Raula, J. Shan, M. Nuopponen, A. Niskanen, H. Jiang, E. I. Kauppinen and H. Tenhu, *Langmuir*, 2003, **19**, 3499-3504.

122. W. Huang, G. Skanth, G. L. Baker and M. L. Bruening, *Langmuir*, 2001, **17**, 1731-1736.

123. W. Huang, S. Ganesan, M. L. Bruening and G. L. Baker, *Abstracts of Papers - American Chemical Society*, 2000, **220th**, POLY-157.

124. G. Moad, E. Rizzardo and S. H. Thang, *Accounts of Chemical Research*, 2008, **41**, 1133-1142.

125. C. Barner-Kowollik, T. P. Davis, J. P. A. Heuts, M. H. Stenzel, P. Vana and M. Whittaker, *Polymer Science, Part A.*, 2003, **41**, 365-375.

126. G. Moad, Y. K. Chong, A. Postma, E. Rizzardo and S. H. Thang, *Polymer*, 2005, **46**, 8458-8468.

127. S. Perrier and P. Takolpuckdee, *Polymer Science, Part A.*, 2005, **43**, 5347-5393.

128. T. Tang, V. Castelletto, P. Parras, I. W. Hamley, S. M. King, D. Roy, S. Perrier, R. Hoogenboom and U. S. Schubert, *Macromolecular Chemistry and Physics*, 2006, **207**, 1718-1726.

129. G. Liu, X. Yan, Z. Lu, S. A. Curda and J. Lal, *Chemistry of Materials*, 2005, **17**, 4985-4991.

130. G. K. Such, R. A. Evans and T. P. Davis, *Macromolecules*, 2006, **39**, 9562-9570.

131. D. Quemener, T. P. Davis, C. Barner-Kowollik and M. H. Stenzel, *Chemical Communications*, 2006, 5051-5053.

132. R. Plummer, D. J. T. Hill and A. K. Whittaker, *Macromolecules*, 2006, **39**, 8379-8388.

133. H. Chaffey-Millar, M. H. Stenzel, T. P. Davis, M. L. Coote and C. Barner-Kowollik, *Macromolecules*, 2006, **39**, 6406-6419.

134. J. Bernard, X. Hao, T. P. Davis, C. Barner-Kowollik and M. H. Stenzel, *Biomacromolecules*, 2006, **7**, 232-238.

135. R. Venkatesh, B. B. P. Staal, B. Klumperman and M. J. Monteiro, *Macromolecules*, 2004, **37**, 7906-7917.

136. V. Darcos, A. Dureault, D. Taton, Y. Gnanou, P. Marchand, A.-M. Caminade, J.-P. Majoral, M. Destarac and F. Leising, *Chemical Communications*, 2004, 2110-2111.

137. S. Carter, B. Hunt and S. Rimmer, *Macromolecules*, 2005, **38**, 4595-4603.

138. Z. Wang, J. He, Y. Tao, L. Yang, H. Jiang and Y. Yang, *Macromolecules*, 2003, **36**, 7446-7452.

139. J. Ni, R. J. Lipert, G. B. Dawson and M. D. Porter, *Analytical Chemistry*, 1999, **71**, 4903.

140. R. G. Freeman, W. E. Doering, I. D. Walton, S. G. Penn, G. Davis, F. Wong and M. J. Natan, in *2005 SPIE Nanobiophotonics & Biomedical Applications II*, eds. A. N. Cartwright and M. Osinski, Bellingham, WA, 2005.

141. T. Vo-Dinh and D. L. Stokes, *Biomedical Photonics Handbook*, 2003, **64**, 1-39.

142. S. P. Mulvaney, M. D. Musick and M. Natan, *Abstracts of Papers - American Chemical Society*, 2000, **220th**, COLL-162.

143. X. Dou, Y. Yamaguchi, H. Yamamoto, S. Doi and Y. Ozaki, *Raman Spectroscopy*, 1998, **29**, 739-742.

144. G. Frens, *Nature (London, U. K.)*, 1973, **241**, 20-22.

145. W. S. Sutherland, Winefordner, J D, *Colloid Interface Science*, 1992, **148**, 129-141.

146. L. Liz-Martin, *Langmuir*, 2006, **22**, 32-41.

147. J. Kneipp, H. Kneipp, M. McLaughlin, D. Brown and K. Kneipp, *Nano Letters*, 2006, **6**, 2225-2231.

148. H. Kneipp and K. Kneipp, *Raman Spectroscopy*, 2005, **36**, 551-554.

149. J.-M. Nam, C. S. Thaxton and C. A. Mirkin, *Science*, 2003, **301**, 1884-1886.

150. C. Wang, S. X. Wang and Q. Li, 2005158877, US, 2005, p. 6.

151. A. Kudelski and J. Bukowska, *Chemical Physics Letters*, 1996, **253**, 246-250.

152. K. C. Grabar, R. G. Freeman, M. B. Hommer and M. J. Natan, *Analytical Chemistry*, 1995, **67**, 735-743.

153. T. Pal, N. R. Jana, A. Pal, J. A. Creighton and A. E. Beezer, *Journal of the Indian Chemical Society*, 2000, **77**, 34-35.

154. Y. Yang, S. Matsubara, M. Nogami and J. Shi, *Materials Science and Engineering B*, 2007.

155. P. K. Jain, K. S. Lee, I. H. El-Sayed and M. A. El-Sayed, *J. Phys. Chem. B*, 2006, **110**, 7238-7248.

156. Q.-H. Wei, K.-H. Su, X.-X. Zhang and X. Zhang, in *SPIE Conference 2003 - Plasmonics: Metallic Nanostructures and Their Optical Properties*, SPIE-The International Society for Optical Engineering, San Diego, CA, USA, 2003, pp. 92-99.

157. R. G. Freeman, R. M. Bright, M. B. Hommer and M. J. Natan, *Raman Spectroscopy*, 1999, **30**, 733-738.

158. C. Rodger, V. Rutherford, P. C. White and W. E. Smith, *Raman Spectroscopy*, 1998, **29**, 601-606.

159. C. McLaughlin, D. Graham and W. E. Smith, *Journal of Physical Chemistry B*, 2002, **106**, 5408-5412.

160. S. Sanchez-Cortes and J. V. Garcia-Ramos, *Raman Spectroscopy*, 1998, **29**, 365-371.

161. M. J. Natan, R. G. Freeman and W. Doering, *NSTI Nanotech 2007, Nanotechnology Conference and Trade Show, Santa Clara, CA, United States, May 20-24, 2007*, 2007, **2**, 449-452.

162. O. M. Bakr, B. H. Wunsch and F. Stellacci, *Chemistry of Materials*, 2006.

163. P. C. Lee and D. Meisel, *Chemical Physics Letters*, 1983, **99**, 262-265.

164. P. R. Selvakannan, S. Mandal, S. Phadtare, R. Pasricha and M. Sastry, *Langmuir*, 2003, **19**, 3545-3549.

165. B. Liu and S. Perrier, *Journal Polymer Science, Part A*, 2005, **43**, 3643-3654.

166. J. Chiefari, Y. K. Chong, F. Ercole, J. Krstina, J. Jeffery, T. P. T. Le, R. T. A. Mayadunne, G. F. Meijs, C. L. Moad, G. Moad, E. Rizzardo and S. H. Thang, *Macromolecules*, 1998, **31**, 5559-5562.

167. D. H. Solomon, E. Rizzardo and P. Cacioli, in *Eur. Pat. Appl.*, (CSIRO, Australia). Ep, 1985, p. 63 pp.

168. F. Lecolley, C. Waterson, A. J. Carmichael, G. Mantovani, S. Harrisson, H. Chappell, A. Limer, P. Williams, K. Ohno and D. M. Haddleton, *Journal of Materials Chemistry*, 2003, **13**, 2689-2695.

169. R. K. O'Reilly, M. J. Joralemon, W. Lui, C. J. Hawker and K. L. Wooley, *Polymer Preprints (American Chemical Society, Division of Polymer Chemistry)*, 2005, **46**, 183-184.

170. R. Thibault, M. Malkoch, E. Drockenmuller, M. Messerschmidt, B. Voit and C. J. Hawker, *Abstracts of Papers, 229th ACS National Meeting, San Diego, CA, United States, March 13-17, 2005*, 2005, POLY-222.

171. E. R. Zubarev, J. Xu, A. Sayyad and J. D. Gibson, *Journal of the American Chemical Society*, 2006, **128**, 4958-4959.

172. Z. Merican, T. L. Schiller, C. J. Hawker, P. M. Fredericks and I. Blakey, *Langmuir*, 2007, **23**, 10539-10545.

173. C. Schilli, M. G. Lanzendorfer and A. H. E. Muller, *Macromolecules*, 2002, **35**, 6819-6827.

174. C. Barner-Kowollik, J. F. Quinn, U. L. Nguyen, J. P. A. Heuts and T. P. Davis, *Macromolecules*, 2001, **34**, 7849-7857.

175. K. B. Sharpless and H. C. Kolb, *Book of Abstracts, 217th ACS National Meeting, Anaheim, CA, USA, March 21-25*, 1999, ORGN-105.

176. V. r. J. Gandubert and R. B. Lennox, *Langmuir*, 2005, **21**, 6532-6539.

177. N. Z. Clarke, C. Waters, K. A. Johnson, J. Satherley and D. J. Schiffrin, *Langmuir*, 2001, **17**, 6048-6050.

178. K. U. Von Raben, Yale University, Connecticut United States, 1982.

179. X. Qian, X.-H. Peng, D. O. Ansari, Q. Yin-Goen, G. Z. Chen, D. M. Shin, L. Yang, A. N. Young, M. D. Wang and S. Nie, *Nature Biotechnology*, 2008, **26**, 83-90.

180. O. Seitz, M. M. Chehimi, E. Cabet-Deliry, S. Truong, N. Felidj, C. Perruchot, S. J. Greaves and J. F. Watts, *Colloids and Surfaces, A: Physicochemical and Engineering Aspects*, 2003, **218**, 225-239.

181. J.-H. Kim and T. R. Lee, *Abstracts of Papers, 225th ACS National Meeting, New Orleans, LA, United States, March 23-27, 2003*, 2003, COLL-261.

182. M. K. Corbierre, N. S. Cameron, M. Sutton, K. Laaziri and R. B. Lennox, *Langmuir*, 2005, **21**, 6063-6072.

183. J. Shan, M. Nuopponen, H. Jiang, T. Viitala, E. Kauppinen, K. Kontturi and H. Tenhu, *Macromolecules*, 2005, **38**, 2918-2926.

184. M. Valentini, A. Vaccaro, A. Rehor, A. Napoli, J. A. Hubbell and N. Tirelli, *Journal of the Americal Chemical Society*,, 2004, **126**, 2142-2147.

185. M. K. Corbierre, N. S. Cameron and R. B. Lennox, *Langmuir*, 2004, **20**, 2867-2873.

186. M. Q. Zhu, L. Q. Wang, G. J. Exarhos and A. D. Q. Li, *Journal of the Americal Chemical Society*, 2004, **126**, 2656-2657.

187. K. Matsumoto, R. Tsuji, Y. Yonemushi and T. Yoshida, *Nanoparticle Research*, 2004, **6**, 649-659.

188. S. P. Mulvaney, M. D. Musick, C. D. Keating and M. J. Natan, *Langmuir*, 2003, **19**, 4784-4790.

189. W. E. Doering and S. Nie, *Anal. Chem.*, 2003, **75**, 6171-6176.

190. C. S. Levin, S. W. Bishnoi, N. K. Grady and N. J. Halas, *Analytical Chemistry*, 2006, **78**, 3277-3281.

191. N. H. Kim, S. J. Lee and K. Kim, *Chemical Communications*, 2003, 724-725.

192. D. S. Grubisha, R. J. Lipert, H.-Y. Park, J. Driskell and M. D. Porter, *Analytical Chemistry*, 2003, **75**, 5936-5943.

193. D. Bethell, D. J. Schiffrin, C. Kiely, M. Brust and J. Fink, *Hyper-Structured Molecules II: Chemistry Physics and Application, [International Forum on Hyper-Structured Molecules], 2nd, Sapporo, Japan, May 30-June 1, 1997*, 2001, 179-195.

194. J. L. Meier, A. C. Mercer, H. Rivera, Jr. and M. D. Burkart, *Journal of the American Chemical Society*, 2006, **128**, 12174-12184.

195. H. Flaster and H. Kohn, *Journal of Heterocyclic Chemistry*, 1981, **18**, 1425-1436.

196. P. J. DeLaLuz, M. Golinski, D. S. Watt and T. C. Vanaman, *Bioconjugate Chemistry*, 1995, **6**, 558-566.

197. C. Corona, B. K. Bryant and J. B. Arterburn, *Organic Letters*, 2006, **8**, 1883-1886.

198. J. Xu, A. J. DeGraw, B. P. Duckworth, S. Lenevich, C.-M. Tann, E. C. Jenson, S. J. Gruber, G. Barany and M. D. Distefano, *Chemical Biology & Drug Design*, 2006, **68**, 85-96.

199. I. Islam, K. Y. Ng, K. T. Chong, T. J. McQuade, J. O. Hui, K. F. Wilkinson, B. D. Rush, M. J. Ruwart, R. T. Borchardt and J. F. Fisher, *Journal of Medicinal Chemistry*, 2002, **37**, 293-304.

200. R. Huisgen, *Angewandte Chemie, InternationalEdition*, 1963, **2**, 633-645.

201. H. C. Kolb, M. G. Finn and K. B. Sharpless, *Angewandte Chemie, International Edition*, 2001, **40**, 2004-2021.

202. R. Ranjan and W. J. Brittain, *Macromolecules*, 2007, **40**, 6217-6223.

203. R. K. O'Reilly, M. J. Joralemon, C. J. Hawker and K. L. Wooley, *New Journal of Chemistry*, 2007, **31**, 718-724.

204. R. K. O'Reilly, M. J. Joralemon, K. L. Wooley and C. J. Hawker, *Chemistry of Materials*, 2005, **17**, 5976-5988.

205. M. J. Joralemon, R. K. O'Reilly, C. J. Hawker and K. L. Wooley, *Journal of the American Chemical Society*, 2005, **127**, 16892-16899.

206. W. H. Binder, R. Sachsenhofer, C. J. Straif and R. Zirbs, *Journal of Materials Chemistry*, 2007, **17**, 2125-2132.

207. Q. Zeng, T. Li, B. Cash, S. Li, F. Xie and Q. Wang, *Chemical Communications* , 2007, 1453-1455.

208. R. K. O'Reilly, M. J. Joralemon, C. J. Hawker and K. L. Wooley, *Polymer Preprints (American Chemical Society, Division of Polymer Chemistry)*, 2005, **46**, 92-93.

209. Y. Zhou, S. Wang, K. Zhang and X. Jiang, *Angewandte Chemie, International Edition*, 2008, **47**, 7454-7456.

210. T. Zhang, Z. Zheng, X. Ding and Y. Peng, *Macromolecular Rapid Communications*, 2008, **29**, 1716-1720.

211. M. Fischler, A. Sologubenko, J. Mayer, G. Clever, G. Burley, J. Gierlich, T. Carell and U. Simon, *Chemical Communications*, 2008, 169-171.

212. E. Boisselier, L. Salmon, J. Ruiz and D. Astruc, *Chemical Communications*, 2008, 5788-5790.

213. E. Boisselier, A. K. Diallo, L. Salmon, J. Ruiz and D. Astruc, *Chemical Communications*, 2008, 4819-4821.

214. J. L. Brennan, N. S. Hatzakis, T. R. Tshikhudo, N. Dirvianskyte, V. Razumas, S. Patkar, J. Vind, A. Svendsen, R. J. M. Nolte, A. E. Rowan and M. Brust, *Bioconjugate Chemistry*, 2006, **17**, 1373-1375.

215. A. Palm, *The Journal of Physical Chemistry*, 1951, **55**, 1320-1324.